Paleomagnetic study of the Central Andes with special reference to the Bolivian orocline

by

Kosuke Heki

Geophysical Institute, Faculty of Science, University of Tokyo

December 1983

Abstract Paleomagnetic studies were done on more than 600 oriented rock samples collected from the Central Andes between northern Peru and the northernmost Chile. Samples are composed of both volcanic and sedimentary rocks and range in their ages from Jurassic to Quaternary. Paleomagnetic studies of these rock formations revealed post-Cretaceous counterclockwise rotation of the Peruvian Andes and the northernmost Chile with respect to the South American platform. A significant correlation was noted between the rotation angles and the strike of the Andean structural trend and is interpreted as the consequence of the coherent rotation of the whole Peruvian Andes as a block. On the other hand, paleomagnetic results of Chilean and Argentine Andes are compatible with platform data. These results confirm that the Central Andes were oroclinally bent giving rise to the Arica-Santa Cruz deflection at the Peru-Chile border. One Neogene dike swarm in central Peru showed about a half of the rotation of the Cretaceous rocks. If this counterclockwise rotation is the result of the large area rotation as suggested from the Mesozoic data, it gives constraints to the timing of this oroclinal bending, that is, a half amount of the bending still occurred after Late Miocene time. Such recent rapid bending of the Central Andes is considered to give rise to various tectonic features not only in the Andean Cordillera itself but also in the surrounding area such as South American foreland and the subducting Nazca plate. As the possible cause of the bending, it is speculated that the collision of some unsubductable mass to South America stopped the receding oceanic trench and formed the bending axis.

Acknowledgement This work was financially supported as the grant-in-aid for overseas scientific researches by Ministry of Education (Science and Culture, Grant Nos. 504204 and 56041015). The mission is composed of Masaru Kono (chief scientist, Tokyo Institute of Technology), Yoshio Onuki (University of Tokyo), Tadahide Ui (Kobe University), Hajimu Kinoshita (Chiba University), Yoshio Fukao (Nagoya University), Yozo Hamano (University of Tokyo), Asahiko Taira (Kochi University) and Kosuke Heki (University of Tokyo, the present author). I am very grateful to each of the members for valuable criticisms and discussions about my work. Paleomagnetic studies were especially helped by Masaru Kono and Yozo Hamano. For the measurement of weak magnetic remanences, I used a cryogenic magnetometer of University of California, Santa Barbara by courtesy of Michael D. Fuller. Also I received help from Richard Dodson and John R. Dunn in UCSB in using the magnetometer. In Peru, this work was done in collaboration with Instituto Geofisico del Peru (IGP) in Lima, where we received much logistic help from Mateo Casaverde, Leonidas Ocola and Mutsumi Ishizuka. I especially acknowledge the generosity of Mutsumi Ishizuka who lent us his Land-Cruiser for the field trip to the northern Peru. This field trip was participated and helped by Jose Machare (geologist) and Julio Melgar (chauffeur) in IGP. In the field trip to the central Peru (Ocros dike swarm), Felix Monge (geologist) and Flanklin Moreno (chauffeur) participated and helped us. In the Chilean Altiplano, field trips were done in collaboration with Hugo Moreno, Universidad de Chile (Santiago). I thank also Konosuke Sawamura, Universidad de Norte (Antofagasta) for the help in the

field works in the Arica region. When we cut the rock samples to make the specimens available to magnetometers, Hugo Tsuda kindly lent us his garage. Measurements of Cuya dike samples were executed by Naoaki Morikawa and Kazushige Nomura as the bachelor thesis of Chiba University. Supplementary measurements of weak remanences of limestones in Japan were done at National Institute of Polar Reseach with help from Minoru Funaki. Radiometric age informations were provided by Yutaka Takigami, University of Tokyo. I also thank Akira Hayashida, Doshisha University for sending me some unpublished Bolivian paleomagnetic data. I received much valuable criticisms and encouragements from Minoru Ozima, Ichiro Kaneoka, Hideo Tsunakawa and Toshiyuki Tosha, Geophysical Institute, University of Tokyo.

Contents

(to be continued)

(continued)

Chapter 1.General introduction - Paleomagnetism in orogenic belts

Paleomagnetic studies have mostly been carried out in the stable continental interiors mainly because such paleomagnetic results are expected to represent the movement of the whole continent. Systematic paleomagnetic studies over these continents established Phanerozoic apparent polar wonder paths and substantiated continental drift hypothesis proposed by Wegener. This urged the construction of completely new earth science system and during the later half of 1960's, newly developed concepts such as ocean floor spreading hypothesis (Hess, 1962), oceanic magnetic lineation (Vine and Matthews, 1963), transform fault (Wilson, 1965) were synthesized into a new global tectonic model known as plate tectonics that rigid spherical caps cover the whole earth and present day tectonics is generally interpreted in terms of relative motions of these rigid plates (McKenzie and Parker, 1967; Morgan, 1968; Le Pichon, 1968). The establishment of the movement history of the continent yielded, in turn, another large future potential of paleomagnetism in investigating smaller deformations on sub-continental scale to understand the complex evolutional history in orogenic belts and to elucidate various tectonic phenomena at plate margins.

As a basic assumption, it is widely accepted that the geomagnetic field, when averaged over sufficient time span, coincide with that of an axial and almost geocentric dipole. This assumption enables time-averaged paleomagnetic data to be interpreted in terms of apparent paleopole positions (hereafter

referred to as "paleomagnetic pole"), in other words, paleolatitude of the sampling sites and their original orientations with respect to the paleomeridians. Comparison of paleomagnetic results from tectonic area with those from some reference area (usually, adjacent cratonic region is used) provides an information on the deformation history in terms of latitudinal movement and/or tectonic rotation about a vertical axis and yields important keys to the understandings of the tectonic evolution of the orogenic belts.

There are several problems in studying paleomagnetism in the region of active tectonics. For example, it has long been emphasized that one should be careful with the applicability of the results of the studied tectonic unit over surrounding region, that is to say, it is sometimes dangerous to simply extrapolate the data from single locality over wider area in the active region such as orogenic belts. More cautious investigations should be done than the conventional paleomagnetic study in stable area. In practice, the most important point is that rocks are widely sampled from a number of localities to ascertain paleomagnetic consistency. It is also important that informations of surface geological structure are carefully investigated so as to recognize the regions detached from the surroundings in a quite local scale. The extent of the region of coherent paleomagnetic results determines the concept of tectonic unit of movements/deformations such as area, province, block, continent, plate. The western edge of North America is a good example where a region lacks overall paleomagnetic coherency and is composed of

several discrete blocks, from which a new concept of displaced terranes has been developed.

The objective of the present work is to contribute to the understandings of the evolution of the Central Andes by paleomagnetic approach. It is the most fundamental problem whether the Central Andes is a coherent block as believed in conventional geology or is composed of various accreted terranes in a similar manner with North American Cordillera. From geological observations, there are suggestions that the Andes is made up of several tectonically and stratigraphically distinct geological assemblages which have been welded together over a wide range of geological time (e.g., Zeil, 1979). Nur and Ben-Avraham (1982) and Jones et al. (1983) invoke the possibility that the orogenic history of the Andes may have involved accretion tectonics. Another important aim is to detect the rotational movements in connection with the sudden change of the Andean structural trend at the Peru-Chile border which was interpreted as a secondary feature impressed by the bending of originally rectilinear trend (orocline hypothesis; Carey, 1955). The problems in the Andes are fully discussed in the next chapter. Here, I briefly review several European and North American examples where paleomagnetism is playing an important role in investigations of the evolutional history and the mechanism of formation of orogenic belts.

Alpine mountain system in Europe has a complex history resulting from the collision of European and African plates. Paleomagnetism has been studied by many workers to detect rotational motion especially in the Periadoriatic belts which

contain many arcuate features (Sicily, Apennines, Southern Alps, Dinarides and Hellenides). Extensive studies of deformed Periadoriatic belt revealed large amount of clockwise rotation of Sicily and counterclockwise rotation of southern Apennines (e.g., Channel et al., 1980; Channel and Tarling, 1975). These results are explained by an extension of Tyrrhenian Sea and consequent occurrence of curvature of the Calabrian Arc which had been much less arched in Mesozoic time. The Umbrian Apennines have also smaller scale arcuate structural curvature and paleomagnetism showed systematic declination change along the trend (Channel et al., 1978), which was interpreted as a differential horizontal transport (decollement) along the fold belt (Van der Voo and Channel, 1980).

Appalachian mountain belt in eastern North America is known to have several "recesses" and "salients" resulting in a sinuous shape of the belt. Carey (1958) proposed a hypothesis of oroclinal bending that the changes in the angular trend are secondary features caused by the bending. However, paleomagnetic survey proved the inexistence of any supportive evidences such as sinusoidal declination trace along the belt (Irving and Opdyke, 1965; Roy et al., 1967; Van der Voo and French, 1977; Schvartz and Van der Voo, 1983). Instead of the orocline concept, inherent irregularities of early rifted and passive margin are considered to be the precursors of curves in the afterwards developed orogenic belts (Rankin, 1976; Thomas, 1983).

The western edge of North America is the place where paleomagnetism provided the most important clue to the understandings

of the evolution. It has long been recognized that paleomagnetic results of western North America ranging from Alaska to California are discordant with those of craton but are characterized by diverse clockwise declination shift and/or flattening of the inclination (e.g., Cox, 1957; Beck, 1962). After years of controversy, current interpretations are mostly based on the concept of accretion tectonics that this region consists of various exotic terranes which were carried by oceanic plate generally from southern region and were accreted to the western boundary of North American plate (Irving, 1979; Beck, 1980). Clockwise rotation and shallow inclination are thought to be the consequences of dextral shear at the plate boundary accompanied by northward transport (Jones et al., 1983). Several investigators propose that such collision and accretion of small terranes such as oceanic plateaus or aseismic ridges work as the most essential forces of "Andean" type orogeny which was originally thought to be a result of the subduction of normal oceanic crust beneath a continent. Nur and Ben-Avraham (1982) invoke the applicability of this concept over the whole Pacific type orogeny involving the Andes itself.

In Japan, the post-Mesozoic bending of the main island at the so-called Fossa Magna was hypothesized from counterclockwise rotation of the Northeast Japan and clockwise rotation of the Southwest Japan (Kawai et al., 1961, 1971). Its mechanism has been discussed in connection with the back-arc opening of the Japan Sea (Uyeda and Miyashiro, 1974). Recent works of Otofuji and Matsuda (1983) revealed that substantial part of the clockwise rotation of the Southwest Japan occurred at much more

recent times than postulated by early workers, viz: between 28Ma and 12Ma ago. On the other hand, in Northeast Japan, not only the timing of the rotation but even the existence of the rotation itself has been open to question until present. It is because paleomagnetic data from the Northeast Japan are strongly dependent on plutonic rocks. The intrinsic ambiguity of their original attitude makes the results rather disputable (e.g., Ito and Tokieda, 1974). The scarcity of Tertiary paleomagnetic data is also a serious problem. In the last few years, several paleomagnetists have been starting the determination of paleomagnetic poles using rock units other than plutonic rocks. For example, very recent and rapid counterclockwise rotation (20° rotation after 8Ma ago) is reported at Miocene dikes of the Northeast Japan (Heki and Tsunakawa, 1983) and such recent rotation has been becoming well established by paleomagnetic works in Oga Peninsula by Tosha (1983).

There are also recent paleomagnetic topics that considerable portions of Japanese Islands are of allochthonous origin and were carried from equatorical zone on an oceanic plate and were accreted to Japan (Hattori and Hirooka, 1979; Kodama et al., 1983; Shibuya et al., 1983). Such results would be of much importance in discussing the tectonic evolution history of Japanese islands and more intensive studies would be necessary from both geophysical and geological aspects.

Chapter 2. Review of paleomagnetic study in South America

a) Introduction

South American continent is roughly divided into four parts (after Harrington, 1962); i.e., 1)cratons and nesocratons, 2)intracratonic basins, 3)pericratonic basins and 4)Andean orogenic belt. Category 1) involves two major Precambrian cratons, that is, Guiana shield and Brazilian shield. Smaller scale Precambrian massifs in Argentina (the Pampean Massif, Patagonian Massif and Deseado Massif) are also included. 2) consists of three major paleozoic sedimentary basins, i.e., the Amazon Basin, Parnaiba Basin and Parana Basin. These basins are characterized by thick marine and continental sedimentary rocks of Paleozoic age and Mesozoic basic igneous activities which occurred at the time of the break-up of the Gondwana continent. The basements of these sedimentary rocks are still little known. 3) corresponds to what we call Subandes thrust-fold belt running in parallel with the Andean orogenic belt. 4) can be divided into three parts at latitudes of about 5°S and 47°S from geophysical and geological viewpoints, i.e., the Northern Andes, the Central Andes and the Southern Andes. General descriptions of South American geology are given in several texts such as Harrington (1962), Jenks (1979), and those for the Andes are given in Gansser (1973), Zeil (1979) and others.

Paleomagnetic works in this continent are scanty in comparison with other continents such as North America and Europe. Paleomagnetic data reported before 1972 and 1980 are listed and summerized in McElhinny (1973) and Vilas (1981),

respectively. Studies reported prior to 1970 are mainly carried out to establish apparent polar wonder path of South American continent and the rocks of stable South American platform were preferentially used. These works are described in detail by Creer (1970). The most important event of South America in Phanerozoic time would be the separation from Africa as a consequence of the fragmentation of Gondwana continent. Paleomagnetic works in the earlier half of 1970's were focused upon the determination of the timing of this break-up. For this purpose, Mesozoic igneous rocks in the intracratonic basins (e.g., Creer et al., 1972) and Permo-Triassic continental clastic sediments (e.g., MacDonald and Opdyke, 1974) were widely investigated and were compared with contemporaneous African data. During the latter half of 1970's, much older rocks began to be intensively studied. Since oceanic magnetic anomalies do not give informations on the relative movements of continents before Jurassic time, paleomagnetism is especially important. The region of northwestern Argentina was most frequently studied for this purpose (e.g., Valencio et al., 1980).

On the other hand, since Andean region is thought to have undergone much local deformations, paleomagnetic study in such a region was considered to be not suitable for the problem of continental drift. Consequently, the Andean paleomagnetic study has been neglected until relatively recent time. This was also due to the paucity of the reference data from stable South America which should be compared with those of Andean region. It is not until about 1980 that a number of paleomagnetic studies

began to be reported in the region of Andean mountain belt. Some of these studies are intended to detect rotational movements proposed by the oroclinal bending hypothesis of the Andes (e.g., Palmer et al., 1980a; Burns et al., 1980) invoked by Carey (1958).

Apart from these studies of tectonic interest, paleomagnetic study of South America is important from purely geomagnetic interest. It is because the site distribution of basic paleomagnetic data of geomagnetic phenomena such as secular variation, paleointensity, polarity transition and time-averaged non-dipole field is heavily biased to the northern hemisphere. Most paleomagnetists are aware of that more data accumulation from the southern hemisphere is necessary to construct any global model about these geomagnetic problems. In the last few years several data were reported from South America on these problems such as recent secular variation recorded in lake sediments (Creer et al., 1983) and archeointensity (Gunn and Murray, 1980).

b) Stable platform

Apparent polar wonder path of South America since Cambrian time is illustrated in Fig. 2-1 (After McElhinny, 1973). This is mainly based on the pioneer works carried out in 1960's by Kenneth M. Creer (summerized in Creer (1970)). According to this polar wonder path, the paleomagnetic pole is in the equatorial zone a little eastward of South America in Cambro-Ordovician time, and it starts rapid southward movement until they reach the vicinity of the present geographic pole in Permian time. The paleomagnetic pole from Mesozoic time up to present keeps nearly

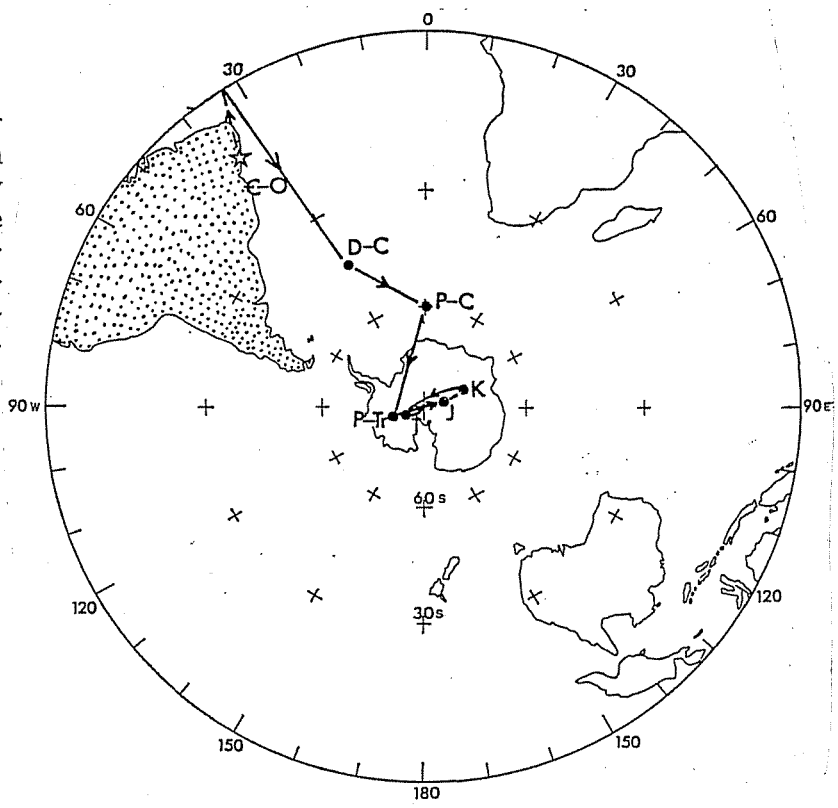

Fig.2-1 Apparent polar wonder path for South America after McElhinny (1973). Abbreviations are as follows; Є-O:Cambro-Ordovician, D-C:Devonian-Carboniferous, P-C:Permo-Carboniferous,P-Tr:Permo-Triassic, J:Jurassic, K: Cretaceous, T:Tertiary.

coincident with the today's pole. Generally speaking, paleomagnetic data after Permian time are relatively abundant in this continent with poles obtained from several sampling sites distributed over the continent. In contrast, poles for older ages are usually based on one or two localities and their positions are therefore tentative.

The comparison of these apparent polar wonder paths between continents enables us to discuss the relative motion of the continents. For example, we can determine the timing of the fragmentation of the Western Gondwana (Africa and South America) from the coherency of apparent polar wonder paths of these continents plotted on the pre-fragmentation disposition map deduced from the computational fitting of the continents (e.g., Bullard et al., 1965; Smith and Hallam, 1970). The time when

these apparent polar wonder paths separate is the Early Cretaceous time (e.g., Valencio and Vilas, 1976), which is consistent with the timing determined by identifying oceanic magnetic anomalies of the South Atlantic (e.g., Larson and Ladd, 1973).

The rocks of the Central Andes measured in this work are younger than Middle Jurassic. The reference poles from the stable region of South America in these ages are defined below using appropriate paleomagnetic data so far reported. In order to discuss the deformation of orogenic belt, reference paleomagnetic poles should be determined using only platform paleomagnetic data. However, currently available standard South American poles (such as those in Creer (1970) and Vilas (1981)) are based on the averages of paleomagnetic poles from both platform and orogen and are not suitable for comparing with the results of the Central Andes in the present study. Since small scale deformations are to be discussed, reference poles themselves need to be determined precisely by rather strict criteria. I emphasize the following three points; 1) only data within the area of stable South American platform are treated, 2) paleosecular variation is canceled out by averaging many independent volcanic units or measuring a lot of sedimentary samples, 3) appropriate stability tests are performed on natural remanent magnetization (NRM) such as stepwise demagnetization by alternating field (AF) or by thermal treatment. There are some examples where one rock formation is reported in several different papers such as Serra Geral Formation (Creer, 1962a; Pacca and Hiodo, 1976) and Chon Aike Formation (Valencio and Vilas, 1970; Creer et al., 1972;

Vilas, 1974). So as to prevent the reference pole from being biased by the data of limited area, such paleomagnetic poles were combined by recalculating the mean pole position.

As Middle Jurassic paleomagnetic poles, two poles were selected as reliable references, viz., Maranhâo volcanics in northeast Brazil (Schult and Guerreiro, 1979) and Chon Aike Formation in southern Argentina (Valencio and Vilas, 1970; Creer et al., 1972; Vilas, 1974). Paleomagnetic poles of Chon Aike Formation are reported from three different sites, that is, Camarones Bay (Creer et al., 1972), Puerto Deseado (Valencio and Vilas, 1970) and Estancia La Reconquista (Vilas, 1974). However, these localities are relatively close and need not to be treated separately. The mean pole was calculated by averaging 54 virtual geomagnetic poles (VGP) which are considered to cancel out paleo-secular variation satisfactorily and define Middle Jurassic paleomagnetic pole. Maranhâo volcanics pole comprises 15 VGPs which are derived from large number of samples per site and also meets the standard. The ages are both around 160Ma (Middle Jurassic). Two pole positions are well coincident with one another despite of the large distance between these two sites (Fig. 2-2). Actual pole positions and their confidence limits are listed in table 2-1.

Cretaceous paleomagnetic data are a little more abundant. In Vilas (1981), minor-scale but very complicated Cretaceous polar motion is proposed, i.e., South American paleomagnetic pole underwent early Early Cretaceous hairpin motion along Greenwich meridian as far as 78°S latitude. Valencio et al. (1983) present

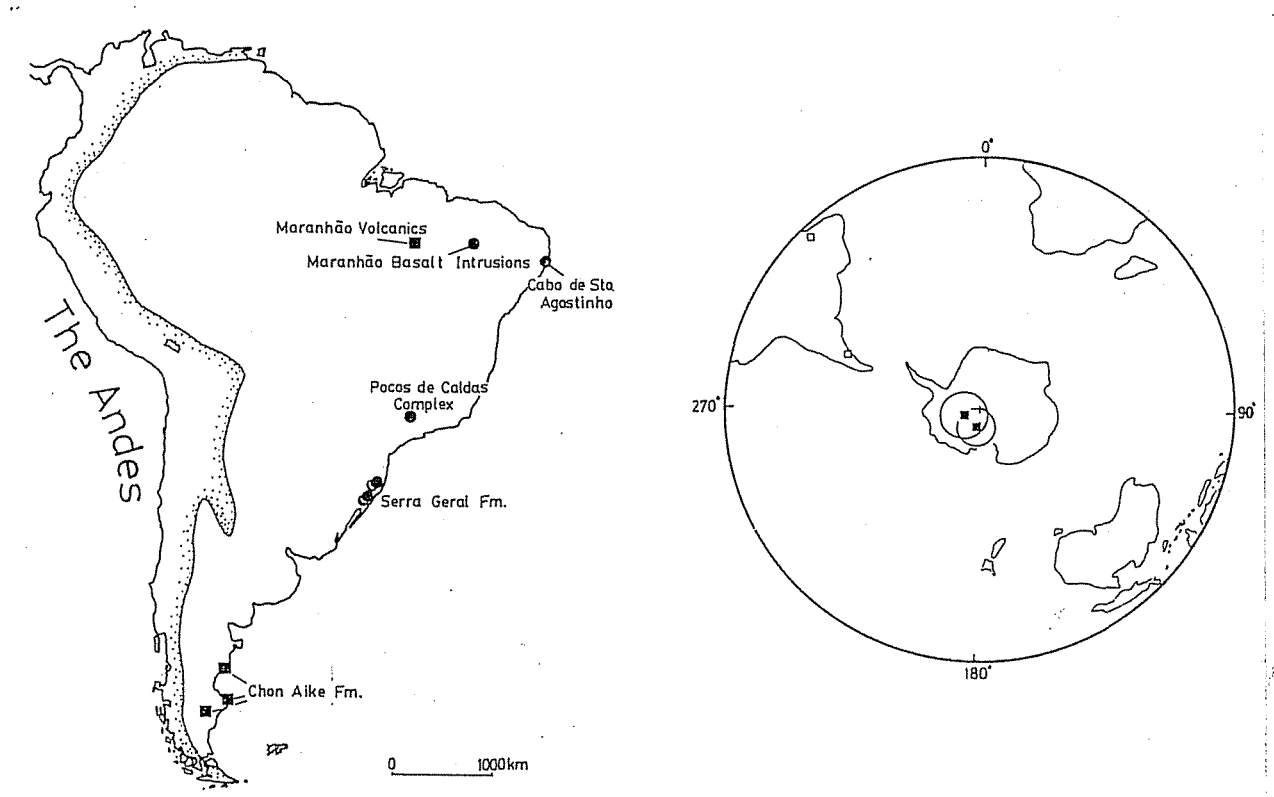

Fig.2-2 Mesozoic sampling localities for paleomagnetic study in the South American platform (left) and corresponding Jurassic paleopoles (right). 95% confidence circles are also illustrated for the poles. In the map, circles indicate Cretaceous sampling sites and squares indicate Jurassic sampling sites. See Table 2-1.

still more complicated Cretaceous polar motion which demonstrates another similar hairpin at the Cretaceous-Tertiary boundary. However, their individual positions of "South American" pole are not based on sufficient paleomagnetic data covering wide area but are no more than the averages of a few number of poles derived both from the platform and the orogenic belt. Such a confusion of platform poles and orogenic belt poles makes the results unnecessarily complex. In particular, the first hairpin peak is defined by poles derived solely from single locality, viz., Vulcanitas Cerro Colorado Formation (Valencio, 1972), Almafuerte

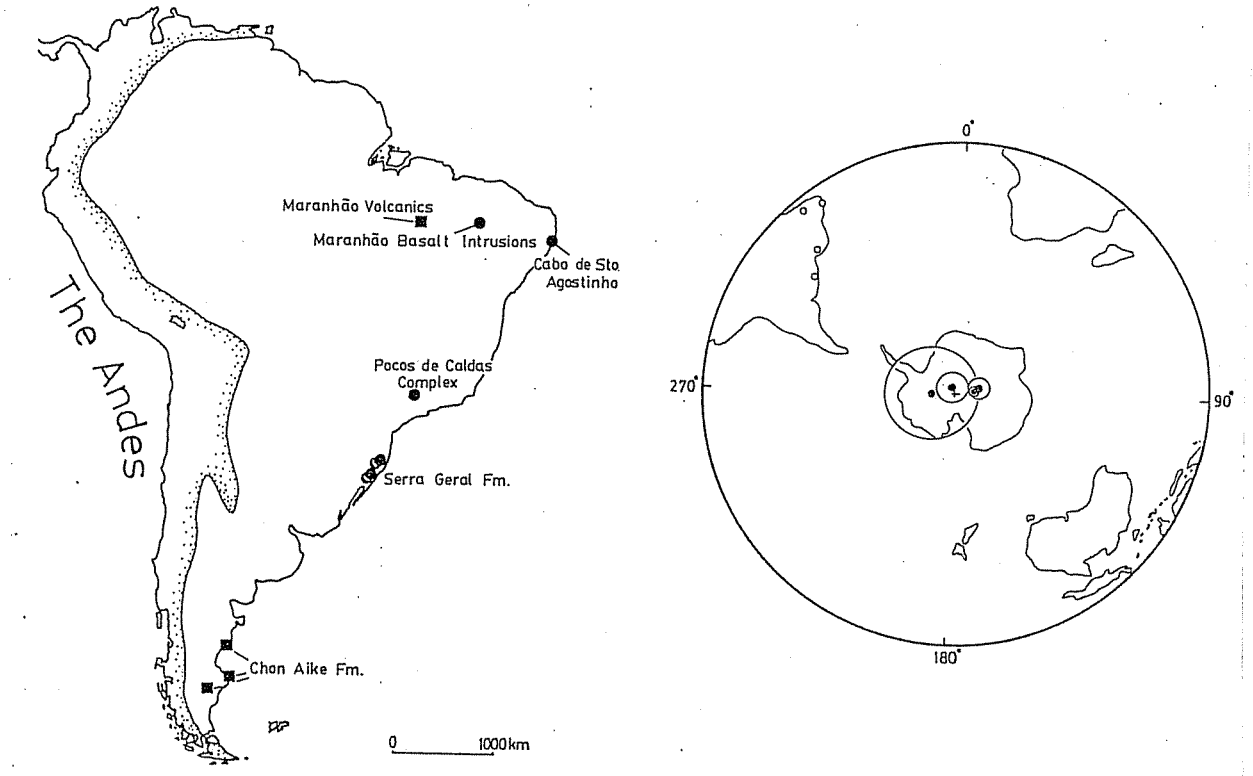

Fig.2-3 Sampling localities for paleomagnetic study in the South American plarform (left) and corresponding Cretaceous paleopoles and their 95% confidence circles (right). See Table 2-1.

lava flows (Mendia, 1978) and Rio de los Molinos dikes (Linares and Valencio, 1975). These rocks are not considered to be suitable as platform pole calculation since these rocks are considered to have suffered considerable tectonic disturbances in response to the Andean orogeny.

From the considerations above, I adopted four paleomagnetic poles as representing the reliable poles of the platform. Data from Serra Geral Formation covering the wide region from Uruguay to Southern Brazil is reported in two different papers, namely Creer (1962a) and Pacca and Hiodo (1976). These are based on the rocks of similar ages and localities and their results were combined to calculate an overall mean. In northeast Brazil,

Table 2-1 Jurassic and Cretaceous paleomagnetic poles of South American platform

Rock unit (Ref.)	Site Lat. (°S)	Site Long. (°W)	Age (Ma)	N. of sites (samples)	Pole Lat. (°S)	Pole Long. (°E)	A_{95} (°)
			--Middle Jurassic--				
Chon Aike Fm. (1,2,3)	44-48	65-69	166±5	54(165)	85	197	6
Maranhâo volcanics (4)	6.4	47.4	158±12	15(121)	85	263	7
Mean position (85.8°S, 230.0°E) N=2, R=1.9977, A_{95}=11.9°							
			--Cretaceous--				
Serra Geral Fm. (5,6)	20-30	46-56	115±15	67(230)	83	76	3
Maranhâo basalt intrusion(4)	6.5	42	118	21(190)	84	81	2
Cabo de Sto. Agostinho(7)	8.4	35.0	99-85	9(100)	88	315	5
Pocos de Caldas comlex(8)	21.9	46.6	75	7(42)	82	268	14
Mean position (88.7°S, 42.6°E) N=4, R=3.9771, A_{95}=8.0°							

References, 1;Valencio and Vilas (1970), 2;Creer et al.(1972), 3;Vilas (1974), 4;Schult and Guerreiro (1979), 5;Pacca and Hiodo (1976), 6;Creer (1962a), 7;Schult and Guerreiro (1980), 8;Opdyke and MacDonald (1973).

A_{95}:radius of 95% confidence cone of a pole.

there are paleomagnetic reports on Cabo de Sto. Agostinho volcanic rocks (Schult and Guerreiro, 1980) and Maranhâo basalt intrusions (Schult and Guerreiro, 1979) which consist of sufficient number of independent volcanic units and are satisfactory as reference paleomagnetic poles. Pocos de Caldas complex (Opdyke and MacDonald, 1973) also contains a number of volcanic units and their mean pole was recalculated by averaging seven VGPs (in the original paper, averaging is performed on site-mean field directions). These sites/poles are illustrated in Fig.2-3 and listed in Table 2-1.

These Cretaceous paleomagnetic poles are nearly coincident within their 95% confidence levels in spite of the large distances of the site localities and diversity of ages (140-100Ma for Serra Geral Formation and about 75Ma for Pocos de Caldas complex). Hence, there is no reason to consider temporal shift of paleopole during Cretaceous time as invoked by paleomagnetists of Buenos Aires group (Vilas, 1981; Valencio et al., 1983). The mean position of these four poles is used hereafter as the reference Cretaceous pole of South American platform.

Tertiary paleomagnetic poles are not reported in the region of stable platform of South America. Paleomagnetic data since Miocene mainly derived from volcanics in western Argentina (Creer and Valencio, 1969; Valoncio et al., 1975) demonstrate that the pole of these ages are coincident with the present pole. Tertiary polar wonder of other continents (Irving, 1977) together with the movement record of South America suggested from oceanic magnetic anomalies (Ladd, 1976) or hot spot traces (Duncan, 1981) do not suggest substantial apparent polar shift from the present

pole in South America for Tertiary time.

c) Orogenic belt

Prior to the review of regional paleomagnetic results, notation of the relative movements of the studied area with respect to the reference region must be defined. Once the position of the paleomagnetic pole of the reference region (in this case, stable platform) of a certain age is determined, one can deduce the paleomagnetic field direction which should be observed at the sampling site within a orogenic belt. This direction is referred to as "expected" direction hereafter. If the "observed" paleomagnetic direction of the sampling site in an orogenic belt differs significantly from the expected direction, the discrepancy is defined by two parameters, namely, inclination anomaly and declination anomaly. If we assume the inexistence of undetected tilt of strata, the former implies latitudinal displacements and the latter corresponds to rotational movements. The notations follow those of Beck (1980) which deals with the anomalous paleomagnetic results of the exotic terranes discovered at the western North America. Although the deviatory poles derived from various exotic terranes are quite divergent, the tendency of the deviation from the pole of North American craton was found to be fairly uniform, namely, rotation is predominatly clockwise and inclination is predominantly flattened suggesting the occurrence of dextral shear together with northward transport. These are defined as R and F which stand for rotation and flattening respectively (Fig. 2-4). R and F and their 95%

confidence intervals can be obtained as follows:

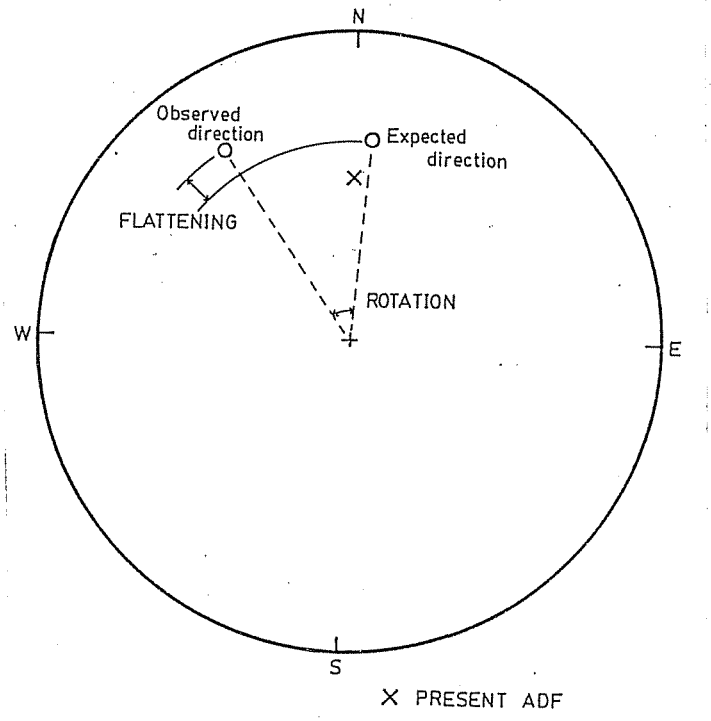

Fig.2-4 Definitions of Rotation (R) and Flattening (F) after Beck (1980). ADF:axial dipole field.

$$R = D_o - D_x \qquad (1)$$

$$F = I_x - I_o \qquad (2)$$

$$\Delta R = (\Delta D_o^{\,2} + \Delta D_x^{\,2})^{1/2} \qquad (3)$$

$$\Delta F = (\Delta I_x^{\,2} + \Delta I_o^{\,2})^{1/2} \qquad (4)$$

$$\Delta D_o = \arcsin (\sin \alpha_{95} / \cos I_o) \qquad (5)$$

$$\Delta D_x = \arcsin (\sin A_{95} / \sin p) \qquad (6)$$

$$\Delta I_o = \alpha_{95} \qquad (7)$$

$$\Delta I_x = \frac{2A_{95}}{1 + 3\cos^2 p} \qquad (8),$$

where suffixes o and x represent "observed" and "expected"

respectively. A_{95} and α_{95} are the 95% confidence semiangles (Fisher, 1953) around the pole and field direction respectively. p is the colatitude, or the angular distance between the site and the reference pole. When the studied area is in the southern hemisphere, we use reversed polarity directions in calculating the flattening. By using such anomaly notations we will review the paleomagnetic data of Andean orogenic belt as three separate regions: the Northern Andes, the Southern Andes and the Central Andes.

The Northern Andes The Northern Andes or Colombian-Venezuelan Andes generally indicates the part of the Andes north of Huancabamba deflection at the Peru-Ecuador border, where the northwest striking Central Andes (Peruvian Andes) suddenly deflects into the north-northeast striking Northern Andes showing several different geological aspects, e.g., the existence of active volcanoes and ophiolites. The Northern Andes has the most complete set of the coastal, western, central and eastern Cordilleras in the whole Andean chain, and the various structural elements are strikingly displayed in the very marked virgation from the Panama branch to the Cordillera de la Costa in northern Venezuela. A part of this northern virgation seems to lead into the Caribbean Sea. An analogy of this part with the Southern (Patagonian) Andes has long been suggested, that is, Caribbean Sea and the Northern Andes are of similar tectonic setting but are at more mature stage of the Scotia Sea and Patagonian Andes. According to the senario of Malfait and Dinkelman (1972), formerly continuous Caribbean plate was decoupled from Pacific

oceanic plate in early Eocene and has been moving eastward with respect to South America. Sykes et al. (1982) suggested that the total eastward displacement amounts to 1,400km. It is therefore envisaged that the northern and southern margins of the present Caribbean plate have possibly incorporated some preexisting peninsulas which were oroclinally bent just like the Patagonian Andes and the Antarctic Peninsula and later deformed by east-west shear and/or north-south compression. Therefore these deformed peninsulas, if any, would be found today, for example, in the coast of northern Venezuela and Colombia.

Anomalous paleomagnetic directions were first recognized by Hargraves and Shagam (1969) for the Triassic-Jurassic La Quinta Formation, south of Lake Maracaibo, northern Venezuela. In similar regions, also anomalous paleomagnetic data are reported for Permo-Carboniferous redbeds (Shagam and Hargraves, 1970) and Cretaceous lavas and diorites in Guajira Peninsula, northern Colombia (MacDonald and Opdyke, 1972). Recent reports of Caribbean Andes (Skerlec and Hargraves, 1980) and Netherland Antilles (Sterns et al., 1982) also show Cretaceous anomalous paleomagnetic directions. These paleomagnetic data are characterized by nearly horizontal and east-west trending direction, that is, 90° horizontally rotated direction from the expected one. However, shallow inclination due to the closeness to the equator makes the distinction between normal and reversed polarity quite difficult. In other words, it is difficult to determine whether the 90° rotation is counterclockwise or clockwise. Such 90° rotation is also known at the northern

boundary of Caribbean plate in Greater Antilles such as Jamaica, Hispaniora, etc. (e.g., Vincenz and Dasgupta, 1978). For the explanation of these large amount declination anomalies, Skerlec and Hargraves (1980) proposed large couterclockwise rotation for the northern margin of Caribbean plate and equally large clockwise rotations for the southern margin along the Venezuelan coast as a consequence of the shear between Caribbean plate and surrounding North and South American plates. This region of anomalous declination in the Northern Andes is confined within the coastal region and the region farther inland does not show such anomalous directions (MacDonald and Opdyke, 1974).

In the Colombian Andes south of 10°N, post-Mesozoic paleomagnetic data are less-well investigated. Creer (1970) reported reversed NRM direction of Cretaceous sandstone of Aptraxa Formation which is not far from the present axial dipole field and is consistent with cratonic reference direction. However, the reliability of this data is not high due to the absence of the demagnetization treatments. For Tertiary system of this region, two Neogene paleomagnetic data are available, viz, MacDonald (1980) and Hayashida (1983). The former reports counterclockwisely rotated declination with highly scattered inclination from Upper Miocene andesitic intrusions in Cauca depression between the Western Cordillera and the Central Cordillera. Yet the latter reported from Middle Miocene Honda Formation between the Central Cordillera and the Eastern Cordillera the mixed polarity directions almost concordant with the present axial dipole field. This implies that the anomalous direction by MacDonald (1980) may be quite local and would be interpreted as

the complicated combination of regional shear, fold and thrusting.

The Southern Andes The name the Southern Andes (Patagonian Andes) is applied to the part ranging from the Gulf of Peñas in Chile (the intersection with Chile Rise) to Tierra del Fuego at the southernmost Andes. Geological similarity between the Southern Andes and the Antarctic Peninsula and the fact that north-south structural trends of the Andes and the Antarctandes tend to become more east-west at the margins of the Scotia Sea have led to the suggestion that the Andean-Antarctandean Cordillera was originally straight and that this orogenic belt has been bent and disrupted by the formation of the intervening Scotia Sea (Deuser, 1970; Dalziel and Elliot, 1973). Paleomagnetic studies of the Southern Andes are very few; the currently available data are only those by Dalziel et al. (1973) and Burns et al. (1980). These two papers report paleomagnetic results of similar sampling sites in the Patagonian Andes but the former covers also the Antarctandean side. Owing to the small horizontal component of paleomagnetic field due to the relatively high latitude, rotations are difficult to detect in comparison with low latitude regions. However, the Mesozoic paleomagnetic results present systematic declination deflection along the arcuate trend of the Patagonian Andes demonstrating the oroclinal bending as Carey (1958) suggested with the name "Magellanes orocline". Paleomagnetism in the Antarctandes (Kellog and Reynolds, 1978), however, provided no definite evidences for or against oroclinal bending of Antarctic Peninsula due to the ambiguity of declina-

tion. The data from the Patagonian Andes are also considered to be insufficient in several aspects such as the number of sampling sites and further paleomagnetic study of both the Andean and Antarctandean sites will be meaningful.

The Central Andes The Central, or the Chilean-Peruvian Andes corresponds to the part of the Andes, ranging from Peru through Bolivia to northern Chile, and are characterized by many features typical of the subduction zones such as trenchs deeper than 5km, deep focus earthquakes occurring at depth greater than 300km and existence of numerous active/Quaternary volcanoes. As noticed immediately, an abrupt change in the structural trend is observed at the Peru-Chile border as shown by the sudden break of the coastline trend. This feature is generally referred to as Arica deflection or Santa Cruz deflection and is interpreted as an oroclinal bend by Carey (1955). Another minor deflection also exists around 12°S-14°S and is usually called Pisco-Abancay deflection.

Paleomagnetic studies of the Central Andes have been carried out mainly in the southern half, especially in western Argentina, where the most complete Phanerozoic paleomagnetic records are available. Cretaceous data are especially abundant in the foreland basins to the east of the Andes (Subandes zone) such as Pirgua Subgroup (Valencio et al., 1977), Vulcanitas Cerro Rumipalla Formation (Vilas, 1976), Almafuerte lava flows (Mendia, 1978) and so on. In the Chilean side, there are two Mesozoic paleomagnetic reports, i.e., Cretaceous strata in the central Chile (Palmer et al., 1980b) and Jurassic Camaraca Formation at the northernmost Chile (Palmer et al., 1980a). Paleomagnetic

reports, on the other hand, at the northern side (Peruvian side) of Arica-Santa Cruz deflection are very scanty. In Peru, since the early reconnaissance works summerized in Creer (1970), there are no recent studies except rather special one dealing with the Arequipa Massif (Shackleton et al., 1979). As for Bolivia, several Paleozoic data are presented in Creer (1970) but these are not suitable for discussing the deformation of orogenic belt since Paleozoic reference poles of South American platform are not well established. In this autumn, new Bolivian paleomagnetic data were reported for Eocene sediment in the Altiplano by Hayashida et al. (1983). Here I review post-Jurassic paleomagnetic data of the Central Andes dividing them into three regions: southern part (region south of Arica-Santa Cruz deflection, or Chilean and Argentine Andes), northern part (region north of the deflection, namely, Peruvian Andes) and Arica region, northernmost Chile, the very point of the deflection. One might take the sharp bend of the coastline at 18°30'S for the hinge of the deflection, but the actual deflection macroscopically viewed is more diffuse and lies as a zone between 18°S and 20°S (this corresponds to the coast between Arica and Pisagua). This is clear especially in the bathymetric and topographic map (Fig.2-5 after Prince (1980)).

Paleomagnetic data of the southern part do not yield any systematic trends of rotation/flattening although minor scale rotation is observed in both clockwise and counterclockwise senses. Most poles are concordant with reference poles, suggesting the inexistence of systematic tectonic rotations/lati-

tudinal movements of this part in spite of the strongly deformed geological structures formed in times of the Andean orogeny.

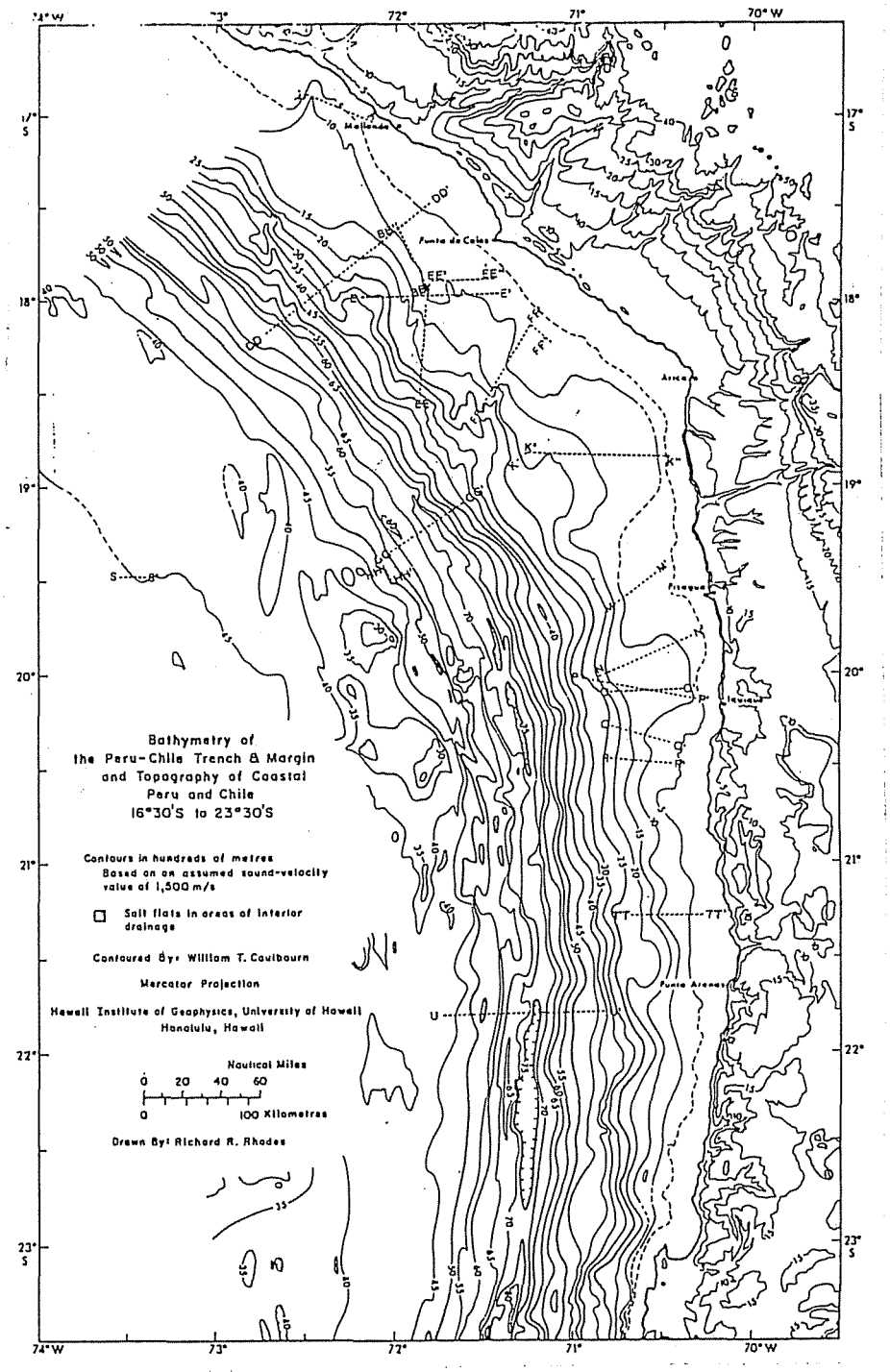

Fig.2-5 Bathymetric and topographic map of the region around Arica-Santa Cruz deflection zone after Prince (1980).

In the Peruvian Andes, Creer (1970) reports paleomagnetic results from Paleozoic, Cretaceous and Tertiary rocks, among which Paleozoic rock (Carboniferous Ambo Group) is not discussed here with the same reason as Bolivian data. Cretaceous data comprise two sedimentary rocks (Vinchos and Moracoche strata) and two dikes (Herradura dikes) of different bedding planes. Reported data are NRM measurements and no demagnetization are carried out on the samples. Four site-mean field directions show considerably good in situ grouping but after bedding corrections these directions get highly scattered and are not considered to maintain the direction of the original magnetization. These Cretaceous data suggest 30° counterclockwise rotation but their reliablity is quite poor. Tertiary rocks are heavily folded red sediments with almost vertical bedding plane. The actual timing of the magnetization together with the age of the rock itself are quite ambiguous and these data are also not discussed here.

In the Arica region, paleomagnetic results are reported by Palmer et al. (1980a). This study reports the data of 33 lava flows of Middle Jurassic Camaraca Formation which are based on modern rock magnetic and paleomagnetic techniques as well as K-Ar dating. About 25° counterclockwise rotation was observed from these rocks. The sampling site of early Eocene sediments in Boilivian Altiplano reported by Hayashida et al. (1983) is thought to correspond to the inland extension of this region. His results indicate both normal and reversed polarity direction with declination counterclockwisely deviated by about 25° from north-south axis and appear quite similar to those by Palmer et al. (1980a). The whole data of the Andes reviewed in this

section are listed in Table 2-2 and their rotations are illustrated in Fig. 2-6.

Fig.2-6 Mesozoic sampling localities for paleomagnetic studies in the Andean region (left, Table 2-2). Corresponding rotations and their 95% confidences are illustrated as the angles from the south (right). Circles and squares on the map indicate Cretaceous and Jurassic sampling sites respectively.

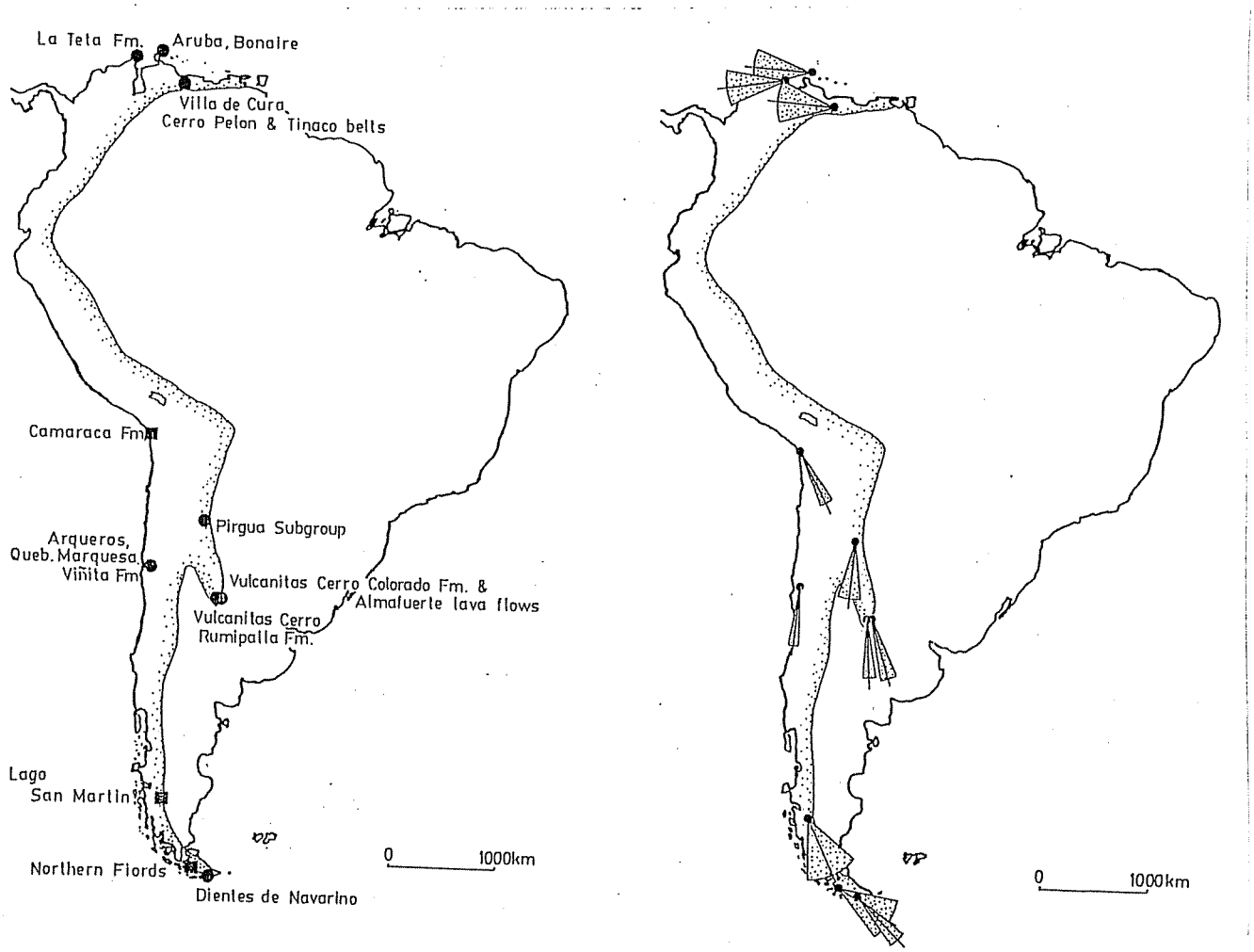

Table 2-2 Jurassic and Cretaceous paleomagnetic poles for the Andean orogenic belt.

Rock unit (Ref.)	Site Lat. (°S)	Site Long. (°W)	Age (Ma)	N. of sites (samples)	Pole Lat. (°S)	Pole Long. (°E)	A_{95} dp (°)	A_{95} dm (°)
--Northern Andes--								
Guajira Pen. Colombia(1)	-12	72	120-95	9(49)	-9.2	22.2	9.0	18.0
Villa de Cura, Cerro Pelon, Tinaco belts(2)	-10	68	K	15(68)	2.5	16.6	9.5	18.9
Bonaire and Aruba(3)	-12	68-70	K	10(92)	-0.1	25.6		13.1
--Southern Andes--								
Lago San Martin(4)	72.2	49.0	J	3?(11)	77	283	13.7	18.8
Northern Fiords(4)	70.0	54.4	J	3(7)	61	20	13.2	16.6
Dientes de Navarino(4)	67.6	53.0	115	3?(13)	54	43	4.9	7.1
--Central Andes--								
Central Chile(5)	29.9	70.9	125-85	30(110)	81	-151	4.4	
Camaraca Fm. northern Chile (6)	18.6	70.3	157±4	33(106)	71	10	6	
Pirgua Subgroup(7)	25.7	65.8	114-77	14(81)	85	222	7	10
Vulcanitas Cerro Rumipalla Fm.(8)	32.2	64.1	<121	6(61)	83	95	5.9	
Vulcanitas Cerro Colorado Fm. and Almafuerte lava flows(9,10,11)	32.2	64.2	127-119	23(150)	76	23	5.5	

References, 1;MacDonald and Opdyke (1972), 2;Skerlec and Hargraves (1980), 3;Sterns et al.(1982), 4;Burns et al.(1980), 5;Palmer et al. (1980b), 6;Palmer et al. (1980a), 7;Valencio et al. (1977), 8;Vilas (1976), 9;Valencio (1972), 10;Mendia (1978),11;Vilas (1976).

dp:radius of confidence oval measured in the direction from site toward pole, dm:radius of confidence oval measured perpendicular to dp. For other legends, see Table 2-1.

Chapter 3. Paleomagnetic studies in the Peruvian Andes

a) Introduction

As noted in Chapter 2, the Peruvian Andes occupies the northern half of the Central Andes and just corresponds to the range between Arica-Santa Cruz deflection (Peru-Ecuador border) and Huancabamba deflection (Peru-Chile border) and in this part, the Andes is running approximately northwest-southeast with a minor deflection around 14°S (Pisco-Abancay deflection). Field works comprising of paleomagnetic sampling, geological survey and gravity measurements were carried out in 1980 and 1981 in collaboration with Instituto Geofisico del Peru (IGP) along the route as indicated in the index map of Fig. 3-1. Paleomagnetic samples were taken both from sedimentary rocks and igneous rocks so as to check mutual consistency of their paleomagnetic results. Although the original sampling plan was to cover the whole Phanerozoic rocks existing in Peru, the ages of acutually sampled rocks are strongly biased by their natural abundances in the Peruvian Andes, and the whole ages are not equally covered as intended prior to the field trips. For example, Mesozoic rocks sampled in this work are composed mostly of Cretaceous rocks which are especially abundant in the Andean Peru and occupy approximately three fourths of the whole Mesozoic rocks distributed in Peru. Accordingly, although sampled rocks range in their ages from the Precambrian to the Quaternary, the meaningful paleomagnetic results cannot satisfactorily be derived from all these ages. As mentioned in chapter 1, any definite paleomagnetic results in such an orogenic region should be based on rocks

widely sampled throughout the region and so we present only Cretaceous results and Neogene results as conclusive ones. Other data (e.g., those of Quaternary age) are given in the Appendix B as reference data.

Sampling was done preferably at the outcrops where information of the original attitudes was available and we avoided plutonic rocks whose bedding planes are essentially impossible to know. For the rocks whose bedding planes are available, bedding corrections were made assuming the single tilting about a horizontal axis. In case of dikes, there are two independent informations of their original attitudes: the bedding plane, if observable, of their host rocks and the plunges of their contacts (dikes are considered to intrude vertically in general; see Matsuda et al., 1979). Structural corrections were performed on remanent magnetizations of dikes in principle but no structural corrections were performed if the in situ dike contacts are nearly vertical and the bedding correction makes these contacts plunge systematically toward a certain direction (in this case, the dikes are thought to have intruded after the tilting of the country rocks). Rock types, precise latitudes and longitudes of sites and dips/strikes of the bedding planes and dike contacts are listed in the Appendix A.

Samples were always taken as blocks by hammers and were oriented by using clinometers. Specimens for the measurements were afterwards cut from these samples as one inch cores. Gasoline-powered drills were not used in this study.

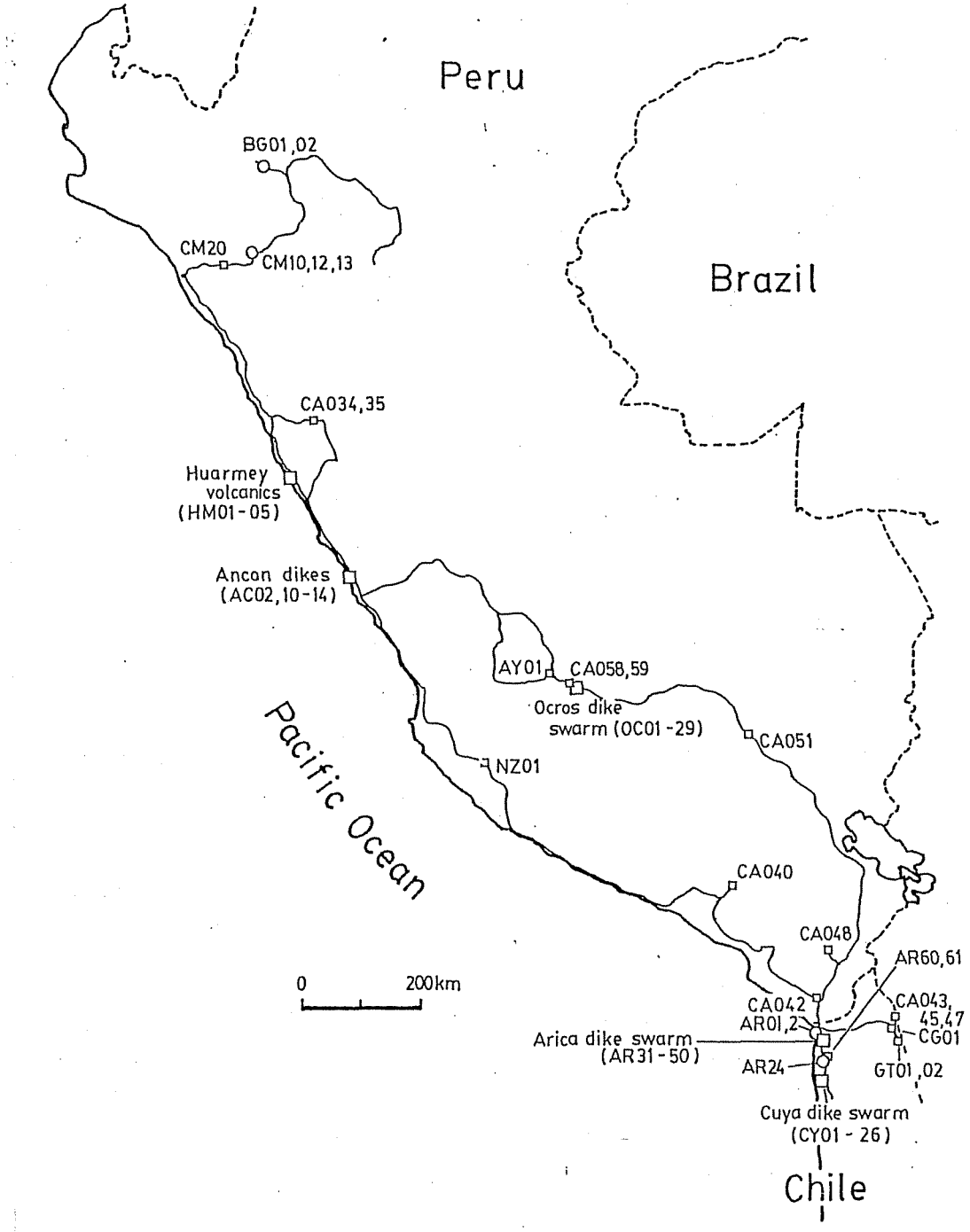

Fig.3-1 Sampling route and sites in the present study. Squares indicate volcanic samples and circles indicate sedimentary samples. Blue:Plio-Quaternary, brown:Tertiary, green:Cretaceous, red:Jurassic.

b) Cretaceous sedimentary and volcanic rocks in Peru

1) Geology

The distribution of Cretaceous rocks can be divided into three major belts: western volcano-plutonic belt, central marine sedimentary belt and eastern marine-continental sedimentary belt (Fig. 3-2). Along the coast of Peru, Cretaceous marine volcanic and sedimentary rocks are exposed forming a relatively narrow belt. To the east of this belt, Cretaceous to early Tertiary granitic plutons are distributed forming the Andean batholith belt which runs throughout the whole Andes with considerable linearity. To the east of this, Tertiary (partly Cretaceous) volcanics and volcanic sediments form the Western Cordillera. The western belt as a whole can be regarded as a Cretaceous-early Tertiary volcanic arc of Andean orogenic belt, which has been usually described as eugeosyncline (Cobbing, 1976). In the central belt, sedimentary sequences of Paleozoic to Cretaceous age compose a thrust-fold belt showing a westward vergence. The Cretaceous system in this belt can be divided into two major lithologic units: clastic dominated Neocomian to Aptian sequence and carbonate dominated Albian to Turonian sequence. This belt is described as miogeosyncline in Cobbing (1976). The eastern belt which forms Subandean thrust-fold belt shows an intensive eastward vergent structural style. The lithofacies are dominated by more clastic materials than carbonates.

From the coastal belt, igneous rocks such as lava flows or dikes were collected at the outcrops along the coastal highway (Carretera Panamericana; Panamerican Highway) between 7°S and

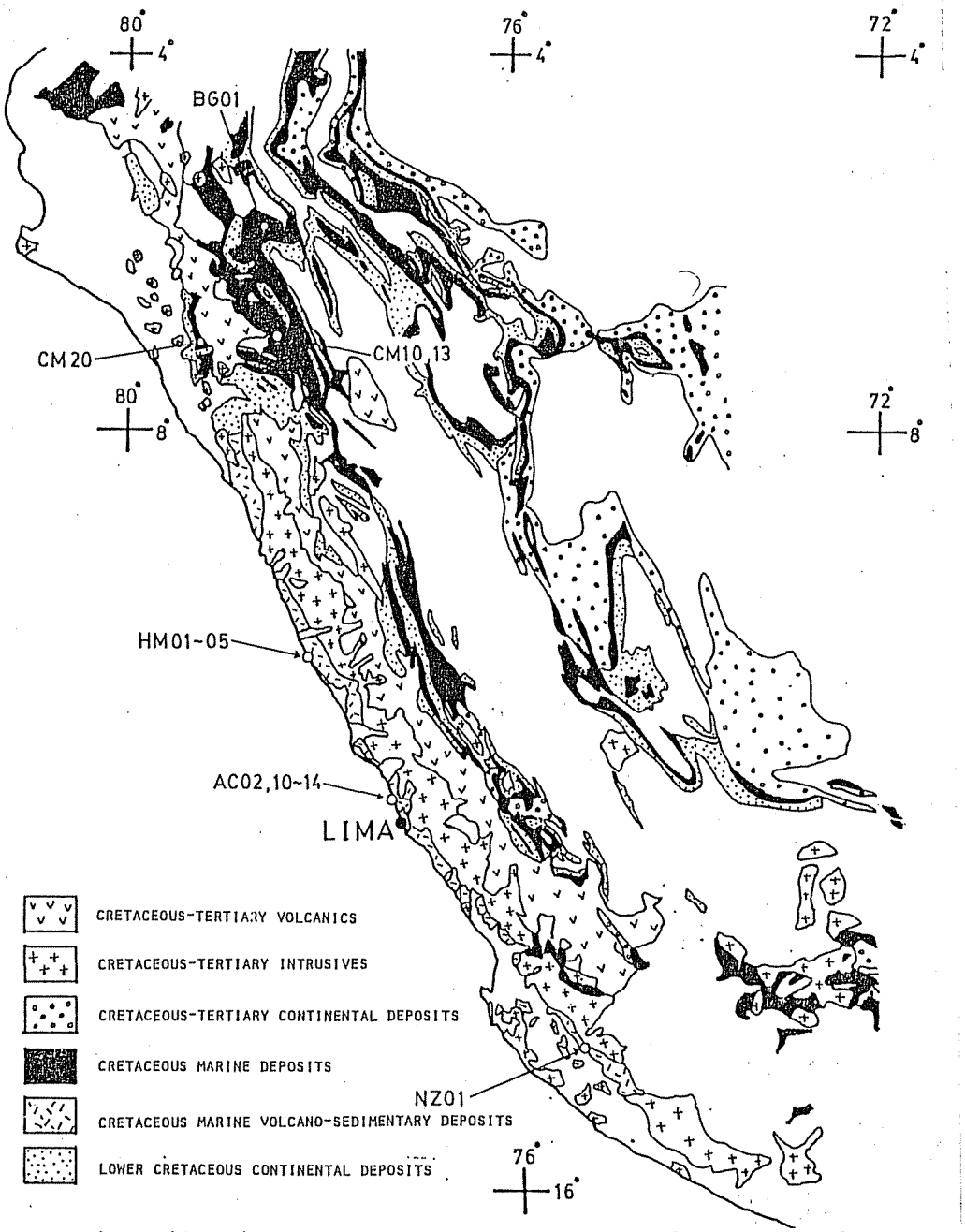

Fig.3-2 Distribution of Cretaceous rock formations in the Peruvian Andes. Sampling sites for paleomagnetic studies are also shown as hollow circles. Redrawn after Bellido (1979) and Taira (1983).

14°S. Detailed descriptions are given in the following section in the following order; Huarmey area (HM), Ancon area (AC) and other areas (NZ01, CM20). From the central belt, carbonate dominated Albian to Cenomanian formations in Cajamarca region (CM10,12,13) and Bagua region (BG01,02) were sampled. These

sampling sites are illustrated in Fig. 3-2. The eastern belt is not covered by the present sampling route. From 5 to 10 oriented hand samples were taken at each site except at BG01,02.

Huarmey area (HM series) In this region, paleomagnetic samples were taken at five sites (HM01-05) from outcrops along the Panamerican Highway. Detailed geological informations are available in Myers (1974). Sampled rocks belong to Punta Gramadal Formation and La Zorra Formation of Casma Group, which was defined for widespread Cretaceous volcanics and sediments in the coastal Peru (Trottereau and Ortiz, 1963). Punta Gramadal Formation is composed of a 600m sequence of pillow lava interbedded with tuff, tuffaceous graywacke and tuffaceous/

Fig.3-3 Geologic map and sampling sites in Huarmey region (HM01-05). Geologic map is after Myers (1974).

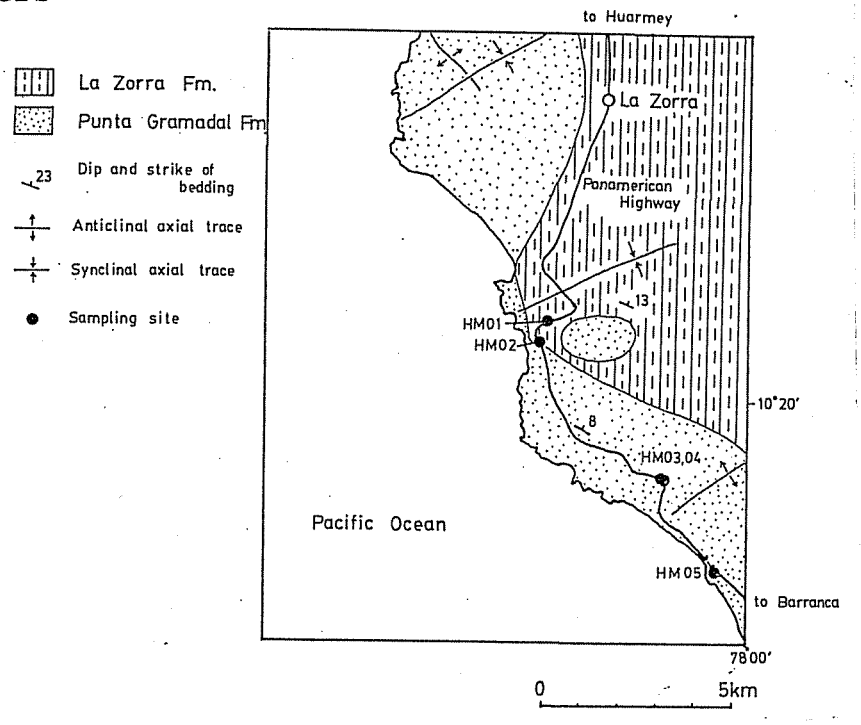

bituminous limestone. One pillow lava (HM03), one dike (HM04) and one basalt lava flow (HM05) were sampled for paleomagnetic study. The age of late middle Albian obtained from fossils in the sediment layer suggest that this formation is almost synchronous with Pariatambo Formation in the central sedimentary belt (Myers, 1974). La Zorra Formation conformably overlies Punta Gramadal Formation and is composed of 1,800m sequence of andesite lava flows, both andesite and dacite ignimbrite, tuff, submarine pyroclastic flow, etc. One andesite lava (HM01) and one andesite dike (HM02) were sampled at the points near the border between Punta Gramadal Formation and La Zorra Formation. Fossil age is also suggested to be late middle Albian from thin bedded bituminous and tuffaceous limestones in this region. Sampling sites in this area are illustrated on the geologic map (Fig. 3-3).

Ancon area (AC series) Five andesite dikes (AC10-14) and one andesite lava flow (AC02) were sampled at the seashore outcrops near the lighthouse of Ancon Peninsula some 30km north of Lima (Fig.3-4). Dikes vertically cut the alternation of tuffs, volcanic sandstones and autobrecciated

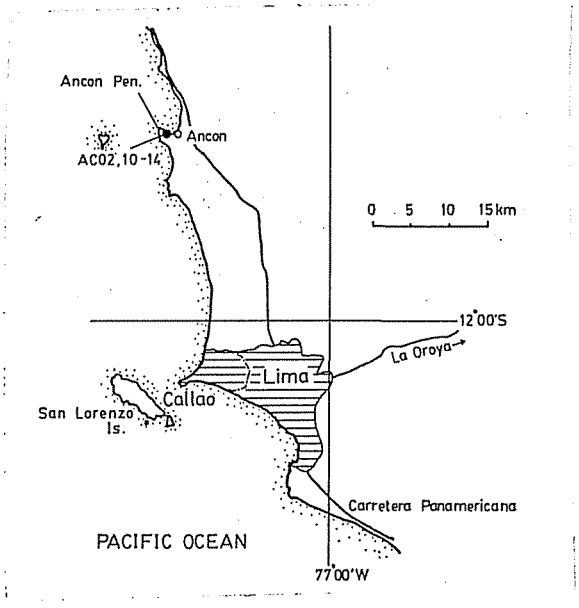

Fig.3-4 Sampling sites of Ancon dikes (AC02, AC10-14).

lava flows and are overlain by a massive lava flow. The dikes range in their width from 50 cm to 1 m and trend approximately north-south which is perpendicular to the present maximum horizontal stress (σ_{Hmax}) direction obtained from focal mechanism solution of earthquakes (Stauder, 1975). These rocks are also considered to belong to Casma Group (Bellido, 1979).

Other Cretaceous volcanics (CM20 and NZ01) Rocks were sampled from one porphyry dike (CM20) which cuts Cretaceous limestone strata near Tembradera, northern Peru. One pyroxene andesite dike (NZ01) was sampled near Nazca at the outcrop along the Panamerican Highway. The dike cuts thin bedded fine tuff of Cretaceous age. The ages of these dikes themselves are not known but we tentatively classified them into Cretaceous age.

Cretaceous sediments of northern Peru (CM10,12,13,BG01,02) In the Western Cordillera of Peru, Cretaceous marine and continental sediments are widely distributed. Late Early to early Late Cretaceous marine carbonate dominated sediments are especially abundant in the region of northern Peru near Cajamarca (Reyes, 1980). Paleomagnetic samples were taken at road cut exposures along the road between Encañada and Celendin (CM10,12,13) and at a stream cut valley of Rio Utcubamba near Bagua Grande (BG01,02). Lower Albian Chulec Formation conformably covers fluvial deposits of Neocomian-Aptian Goyllarisquizga Group. This formation consists of white-grey psammitic limestone-marl and is considered to be cyclic shelf carbonates (Taira, 1983). Paleomagnetic samples

were collected from bedded micritic limestone layer exposed some 10km northeast of Encañada (CM13). Upper Albian Pariatambo Formation lies conformably over Chulec Formation and is composed of dark bituminous limestone-dolomitic limestone and is characterized by O_2 minima depositional environment suggesting maximum transgression in this time which may correlate with the worldwide ocean anoxic event. Sampling was done at marl and bituminous shale layer exposed near Encañada (CM10). Pariatambo Formation is overlain by Cenomanian Yumagual Formation, which consists of limestone and dolomite. Samples were taken at the site some 5km northeast of Encañada (CM12) from calcareous shale layer interbedded by coquina sandstones and ostrea beds. Localities of CM13, CM10 and CM12 are illustrated on the geologic map of Fig. 3-5.

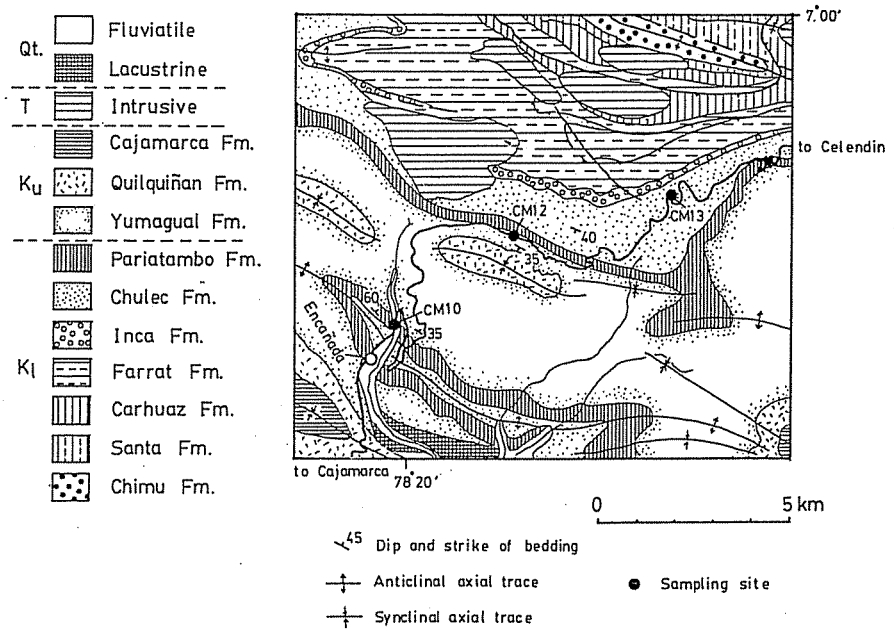

Fig.3-5 Geologic map and sampling sites along the route between Encañada and Celendin near Cajamarca (CM10,12,13). Geologic map is after Reyes (1980).

Paleomagnetic samples of Yumagual Formation were also taken in the outcrop along Rio Utcubamba some 40km east-southeast of Bagua Grande (BG01,02). This outcrop consists of two separate units: lower marl unit and upper limestone unit. The lower marl unit consists of massive and faintly laminated grey marl with intercalation of minor shell beds including the fossils suggesting Cenomanian age (Taira, 1983). The upper bedded micritic limestone unit is composed of two lithofacies: unfossiliferous dolomitic micrite and fossiliferous biomicrite. In the former facies, dolomite rhombs are abundant with a minor amount of benthic foraminifera. Authigenic quartz crystals occur locally. Biomicrite facies contains gastropods, cepharopods, echinoids and ostracods. Hematitic pigments are often associated

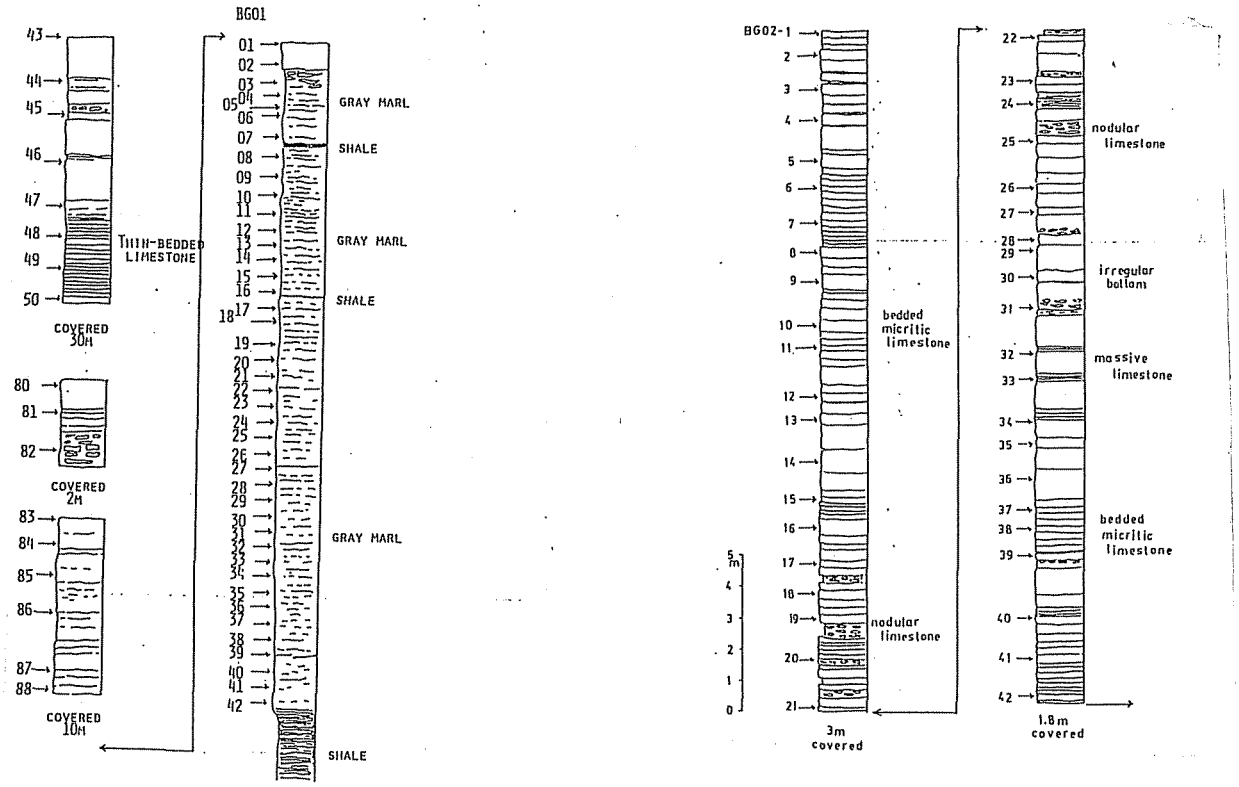

Fig.3-6 Columnar section of Bagua Grande cliff section of Yumagual Formation (BG01,02). The upper part (BG02) was sampled in each 1 m and the lower part (BG01) was sampled in each 50 cm. Sample numbers are attached to the left and lithological descriptions are given to the right of the column.

with bioclasts. Thin section analysis indicates that marly and thinnly bedded parts are often less fossiliferous and more dolomitic. Occurrence of dolomitic micrite with very limited fauna suggests rather restricted and evaporitic condition. Thus, environment of deposition of this sequence can be inferred as a stable, but rather restricted carbonate shelf with occasional occurrence of open circulation or storm condition which is responsible for the supply of bioclastics (Taira, 1983). Samples were taken for paleomagnetic study from each 1 m in upper limestone section (BG02) and 50 cm apart in lower marl section (BG01) (Fig. 3-6).

2) Experimental procedure and paleomagnetic results

Volcanic rocks NRMs of the volcanic rocks were measured using a Schonstedt spinner magnetometer in University of Tokyo, and stepwise AF demagnetization was performed upon all specimens. The samples showed relatively weak NRM intensities (10^{-5} - $10^{-6}Am^2/kg$) in comparison with those of typical igneous rocks but sufficient stabilities were found against AF-demagnetization. Median destructive fields (MDF) were generally higher than 30mT (Fig.3-7a,b). Paleomagnetic field direction was obtained from the gradient of the linear portion of the Zijderveld diagram (Zijderveld, 1967; Dunlop, 1979) by least square fitting (LSF) and when sufficient length of the linear portion was not obtained, certain optimum steps were determined by minimum dispersion criterion. HM05 data were discarded because of their large directional scatter and unstable behaviors against demagne-

tization.

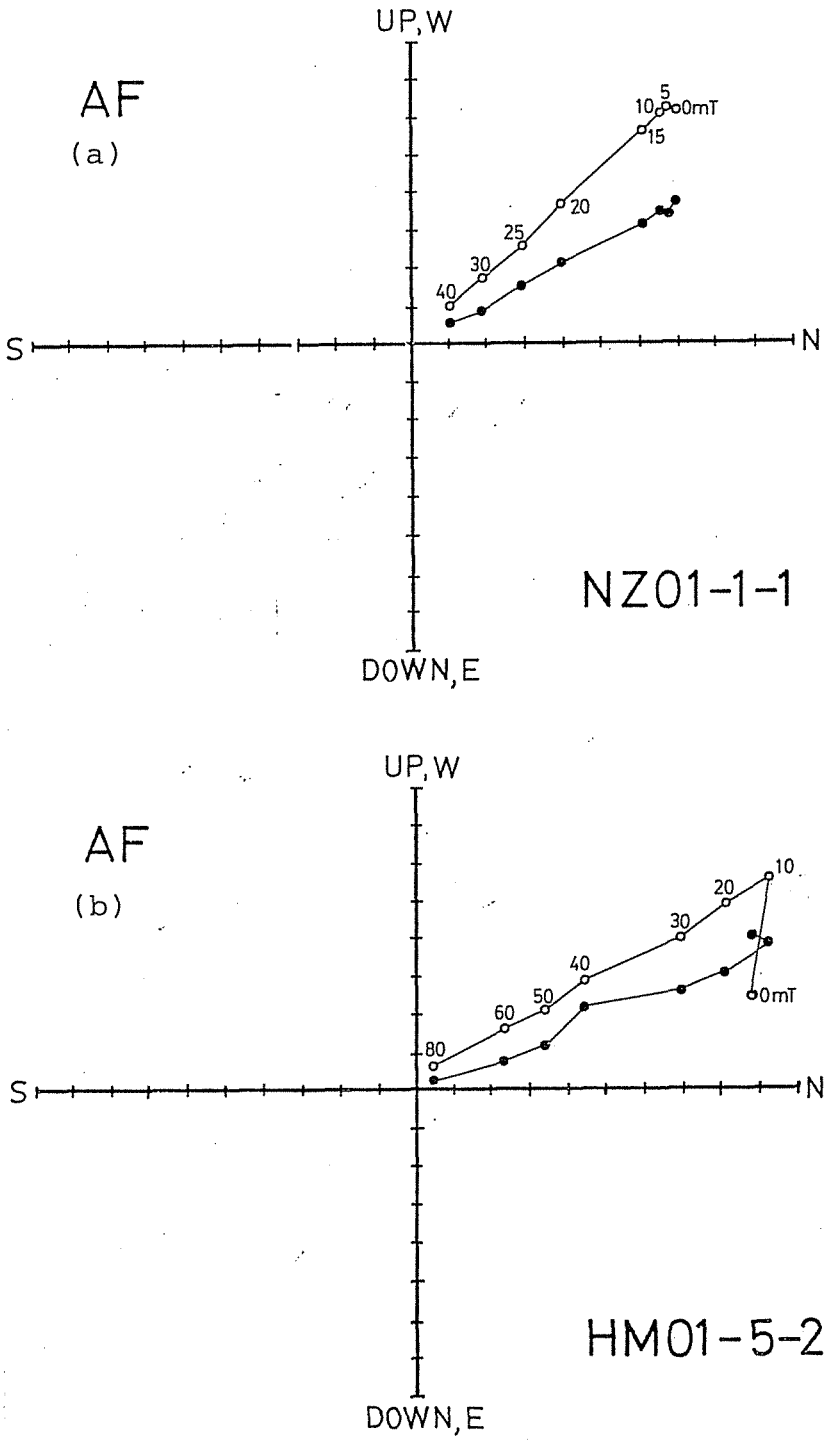

Fig.3-7a,b Zijderveld vector diagram (Zijderveld, 1967) in AF demagnetization of Cretaceous volcanic rocks in coastal Peru. Scales are arbitrarily taken. Open and solid symbols denote projections on vertical and horizontal planes respectively. Demagnetizing field strength (in peak intensity) is also given.

The country rock of Ancon dikes have westward dip of about 15° but almost vertical dike contacts demonstrate that the intrusions are post-folding and so no bedding corrections were made on the paleomagnetic field directions of dikes. In Huarmey area, foldings are very gentle as shown in Fig.3-3 and ascertained by the field observations of the pillow structure (HM03), so that no structural corrections were made on HM series samples, either. For NZ01 and CM20, bedding corrections were made using the bedding angles of the host rocks.

Paleomagnetic field directions were mostly of normal polarity but two reversed polarity directions were obtained from

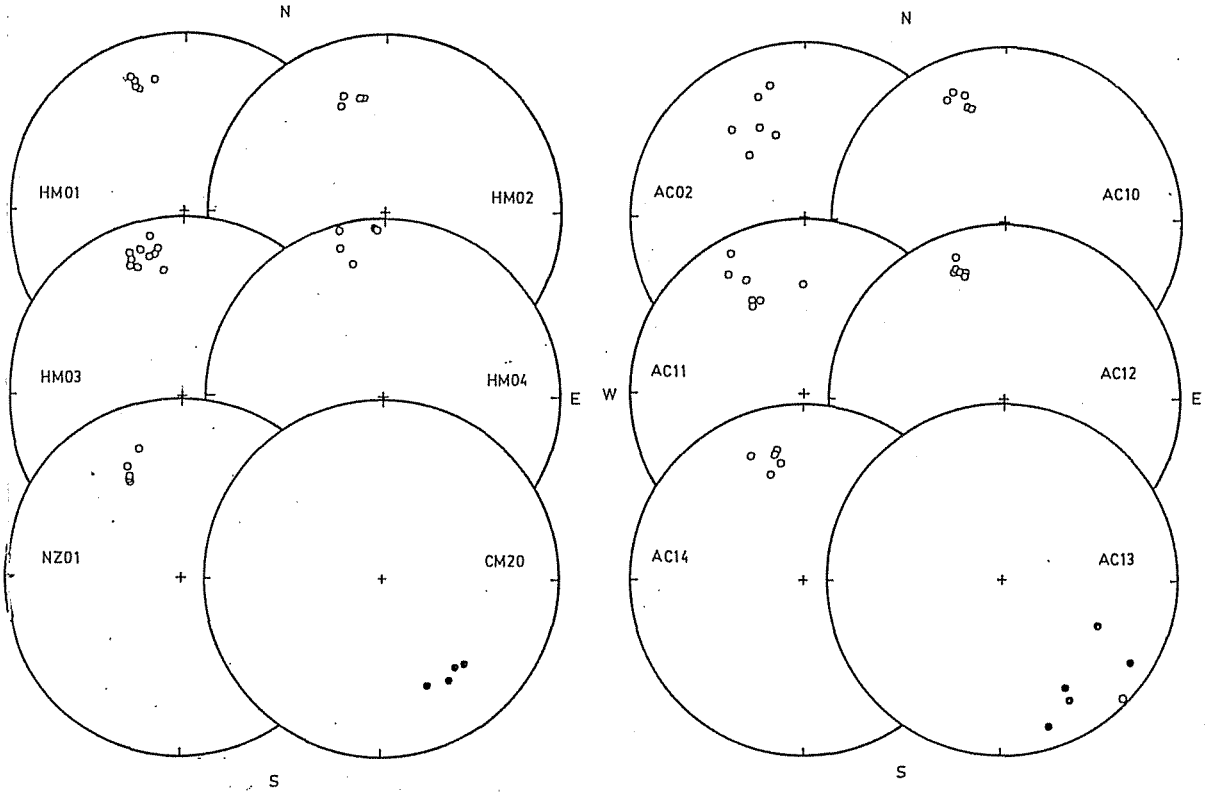

Fig.3-8 Lambert equal-area projection of the directions of the remanent magnetization of twelve Cretaceous volcanics of Peruvian coast. Open symbols denote negative (upward) inclination and solid symbols denote positive (downward) inclination.

AC13 and CM20. They showed 20°-30° counterclockwise declination shifts from present axial dipole field. Paleomagnetic results are illustrated in Fig.3-8 and site mean directions and statistical results (Fisher, 1953) are summarized in Table 3-1.

Sedimentary rocks An SCT cryogenic magnetometer in University of California, Santa Barbara was used in the measurements of the remanences of sedimentary rocks. Some of the samples had NRM of the order of $10^{-7}Am^2/kg$, but typical NRM intensity was of the order of $10^{-8}Am^2/kg$ (Fig.3-9). Stepwise AF demagnetization was performed usually up to 80mT in peak intensity on each specimen and soft secondary components were removed.

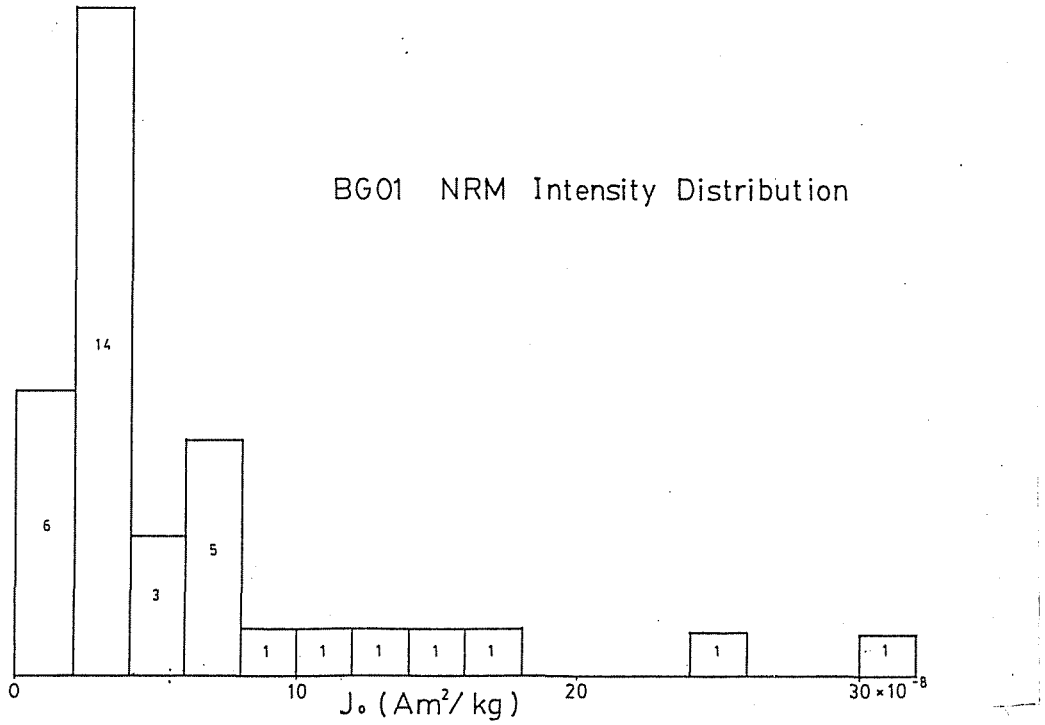

Fig.3-9 Histogram showing NRM intensity distribution of 35 BG01 limestone samples.

The developments of high sensitivity magnetometers such as cryogenic magnetometers made the measurements of quite weak magnetic remanences possible so that rocks such as limestones

which were hitherto not measurable by conventional magnetometers can be used in paleomagnetism. Nevertheless, rock magnetic investigations of marine limestones have been very difficult owing to quite low concentration of magnetic minerals. Lowrie and Heller (1982) compiled current knowledge about the magnetic properties of marine limestone and showed that both magnetite and hematite are the most popular carriers of the NRM. Magnetite is generally of depositional origin while hematite is considered to grow during the diagenesis (see also Channel et al., 1982). Importance of these two magnetic components is controlled by their relative contributions to the total NRM. Limestone whose NRM is carried mainly by hematite can be distinguished by its pinkish color and higher coercivity and blocking temperature than the one whose NRM is carried by magnetite.

Peruvian limestones studied here range in its color from grey to pinkish grey. Purely grey specimens are easily demagnetized during stepwise AF demagnetization as far as 80mT while those with pinkish hue hardly change their direction nor intensity throughout the AF demagnetization, which suggests the existence of bimodal remanences carried by magnetite and hematite. Hematite contribution is especially large for the fossiliferous limestones in BG02, which is consistent with the hematitic pigment concentration in bioclasts observed in thin sections (Taira, 1983). This implies that there are some differences in the condition of diagenetic hematite growth between bioclasts and their matrix. In this study, I preferred magnetization component carried by magnetite since hematite of

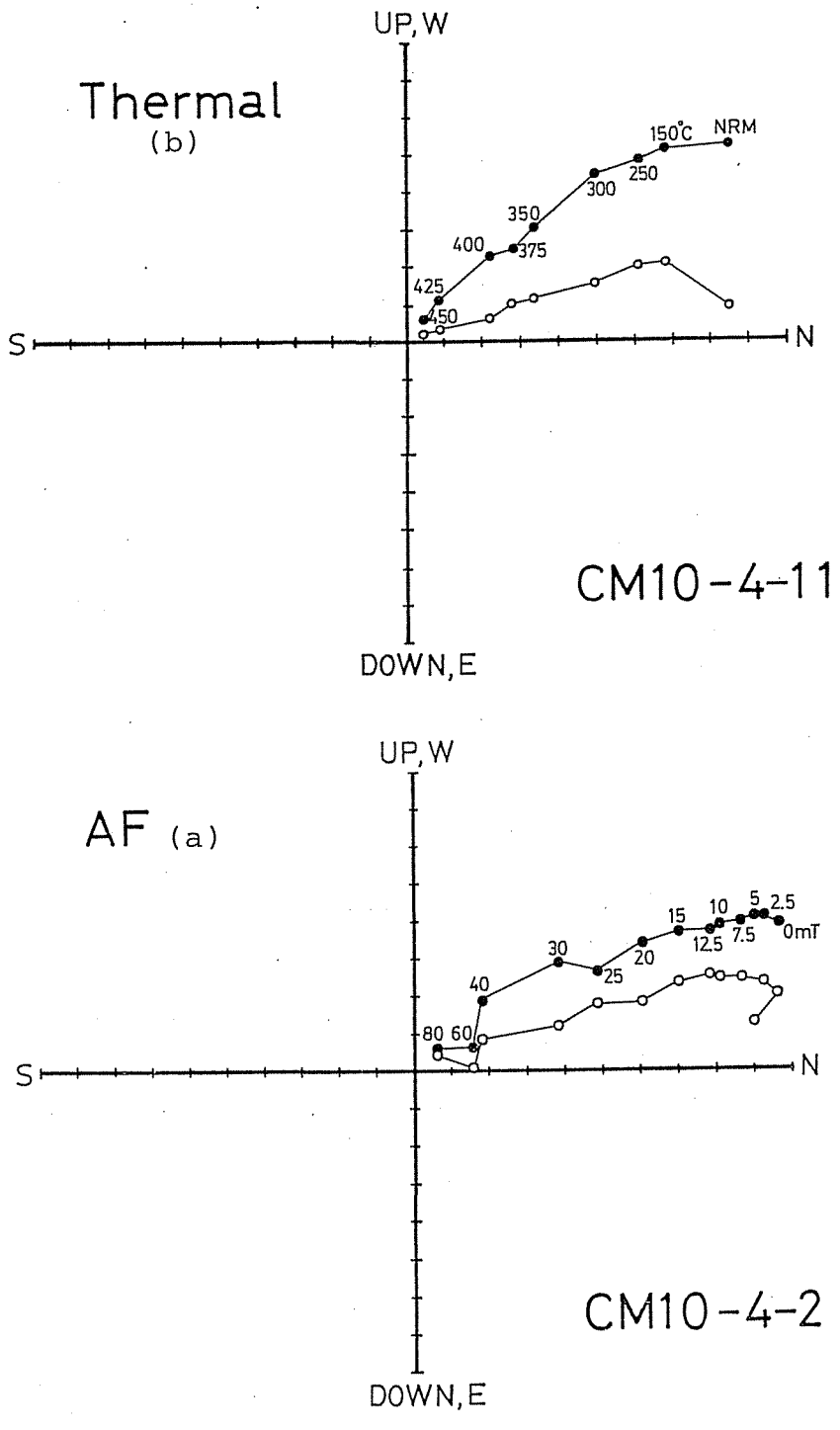

Fig.3-10a,b Zijderveld diagram of limestone specimens of CM10 in progressive AF (a) and thermal (b) demagnetization. Open and solid symbols correspond to the projection onto vertical and horizontal planes respectively.

diagenetic growth possibly delay in its acquisition of remanence. From these viewpoints, only samples with their Zijderveld vector diagrams converging to the origin in the process of AF demagnetization were used for paleomagnetic discussions (Fig.3-10a). Specimens whose NRMs are considered to be carried to some extent by hematite were discarded. For BG01,02 section, only samples taken from the lowest marl layers met this standard (BG01; 30-42). Thermal demagnetization performed on several of these samples showed that their maximum blocking temperatures do not exceed the Curie temperature of magnetite (Fig.3-10b). CM12 samples were discarded because they were heavily overprinted by secondary remanences and stable endpoints could not be obtained by demagnetization.

Obtained field directions are structurally corrected using the bedding planes of the strata and plotted on equal area projections in Fig.3-11. Observed field directions are solely of

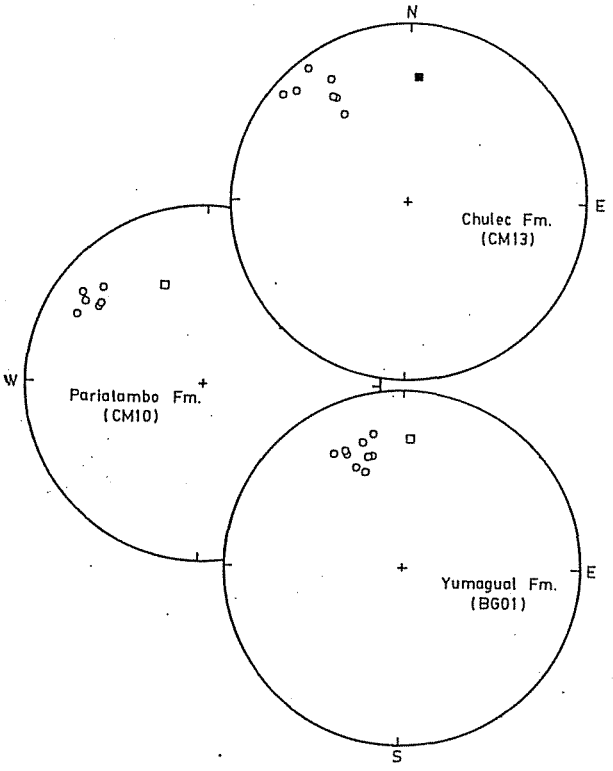

Fig.3-11 Equal-area projection of remanent magnetization direction of Cretaceous sedimentary rocks in northern Peru. Squares indicate present axial dipole field directions viewed from the individual paleohorizons. Open and solid symbols indicate negative and positive inclinations respectively.

normal polarity which perhaps corresponds to Cretaceous long normal polarity interval and is consistent with the assigned fossil ages (Albian to Cenomanian) of the rocks. Inclinations are nearly concordant with present axial dipole field but counterclockwise declination shifts by 20°-50° from north were observed. This is also consistent with the results from volcanic rocks. Statistical parameters and site-mean field directions are also listed in Table 3-1.

3) Discussion

Paleomagnetic directions derived from Peruvian Cretaceous rocks showed notable feature that their declination deviates counterclockwisely by 20°-50° from north-south axis (Fig. 3-12). Virtual geomagnetic poles (VGPs) given by twelve Peruvian Cretaceous volcanics are all converted to southern hemisphere poles and are averaged. Angular dispersion of these VGPs is interpreted as the results of geomagnetic secular variation. The mean position (68.0°S, 0.5°W, A_{95}=5.3°) is considered to be a paleomagnetic pole. Poles derived from Pariatambo Formation (CM10), Chulec Formation (CM13) and Yumagual Formation (BG01) are also calculated and listed together in Table 3-2. Following the convention, paleomagnetic poles are hereafter expressed using southern hemisphere poles irrespectively of the actual polarities of the remanent magnetization. These four Peruvian Cretaceous poles and Cretaceous platform poles (Table 2-1) are illustrated together in Fig.3-13. Peruvian poles show significant systematic difference from South American reference poles suggesting considerable amount of relative movements with respect to the

Table 3-1 Paleomagnetic directional data of Peruvian Cretaceous rocks

Site	N	Incl. (°)	Decl. (°)	R	k	α_{95} (°)	ODF (mT)	Pole Lat. (°N)	Pole Long. (°E)
				(volcanic rocks)					
HM01	5	-26.2	-20.0	4.9892	371	4.0	LSF	70.1	179.7
HM02	4	-34.2	-16.7	3.9886	262	5.7	LSF	71.8	162.4
HM03	10	-20.5	-14.7	9.9014	115	4.5	LSF	75.5	-170.3
HM04	5	-8.9	-9.8	4.8854	35	13.1	LSF	78.6	-137.6
AC02	6	-38.8	-26.8	5.8504	33	11.8	5	62.5	167.7
AC10	5	-28.4	-20.4	4.9729	147	6.3	10	69.9	-179.0
AC11	7	-33.1	-23.8	6.8011	30	11.2	LSF	66.2	174.7
AC12	6	-24.4	-19.2	5.9867	376	3.5	LSF	71.2	-172.2
AC13	6	21.9	140.0	5.6136	13	19.3	LSF	-50.8	9.2
AC14	5	-31.1	-14.4	4.9715	140	6.5	40	75.2	171.5
CM20	4	34.6	145.0	3.9776	134	8.0	80	-54.0	-11.7
NZ01	5	-33.0	-26.4	4.9600	100	7.7	LSF	64.4	183.3
				(sedimentary rocks)					
CM10	6	-21.1	-52.5	5.9676	154	5.4	40	35.9	-179.2
CM13	7	-22.6	-38.3	6.8328	36	10.2	40	52.0	-178.4
BG01	9	-32.2	-20.6	8.9220	103	5.1	LSF	66.7	159.7

N:number of samples studied, R:length of the resultant vector, k:precision parameter, α_{95}:radius of 95% confidence circle, ODF:optimum demagnetizing field determined from minimum dispersion criterion (LSF means that field direction was determined by least square fit to the linear portion of the demagnetization diagram.).

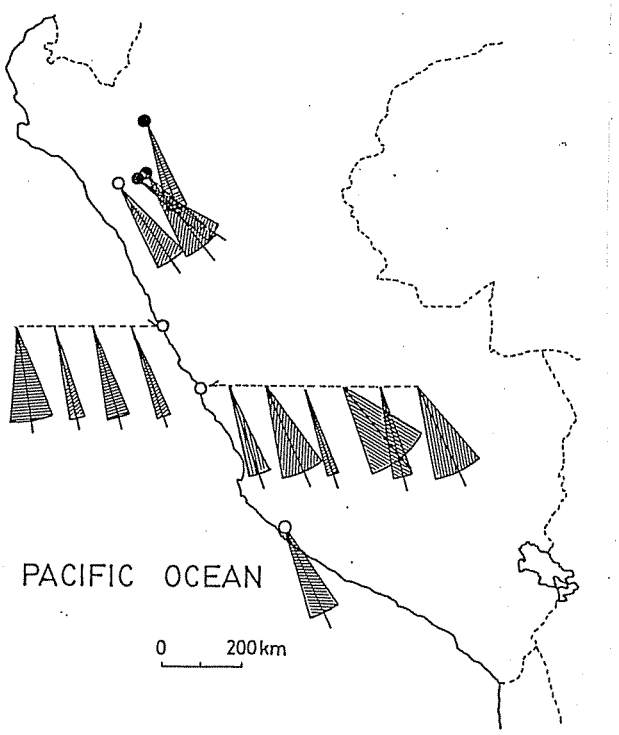

Fig.3-12 Site mean declinations and their 95% confidence intervals of Cretaceous rock samples in Peru. Open circles indicate volcanic rocks and solid circles indicate sedimentary rocks. For the sake of visual simplicity, polarities are taken as reversed one.

cratonic region. Peruvian Cretaceous poles are relatively well clustered in spite of their diverse sampled localities and rock units, suggesting rather coherent block movements of the Peruvian Andes than the independent movements of smaller tectonic units. This problem is fully discussed in chaper 5.

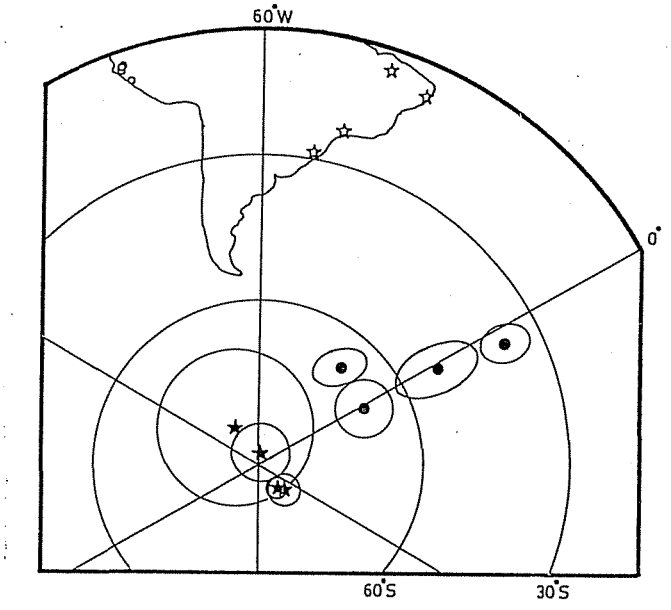

Fig.3-13 Equal-area projection of the paleomagnetic poles of Cretaceous rock formations in the Peruvian Andes (circles) and stable platform (stars). 95% confidence circles or ovals are also illustrated. Corresponding sampling sites are shown as small open symbols on the map.

Table 3-2 Peruvian Cretaceous poles.

Rock unit	Locality Lat. (°S)	Locality Long. (°W)	Age	Pole Lat. (°S)	Pole Long. (°E)	dp (°)	dm (°)	A_{95} (°)
Coastal volcanics	5-15	75-80	K	68.0	359.5			5.1
Chulec Fm.(CM13)	7.1	78.3	Al.	52.0	1.6	4.7	8.8	
Pariatambo Fm.(CM10)	7.1	78.3	Al.	38.1	3.4	3.1	5.8	
Yumagual Fm.(BG01)	5.9	78.2	Cen.	66.7	339.7	3.2	5.7	

All poles are converted to southern hemisphere poles.
dp:radius of confidence oval measured in the direction from site toward pole, dm:radius of confidence oval measured perpendicular to dp, A_{95}:radius of 95% confidence circle, K:Cretaceous, Al.:Albian, Cen.:Cenomanian.

c) Cenozoic volcanic rocks in Peru

1) Geology

Upper Cretaceous to Quaternary volcanic formations are widely distributed in Peru over the highland of the Cordillera Occidental (Western Cordillera). These formations are composed of lava flows, volcanic breccias, agglomerates and tuffs and their compositions are mostly andesitic but minor amount rocks of rhyolitic, dacitic, trachytic and basaltic composition exist. These are roughly divided into three stratigraphical groups from their degree of the influences of the Andean orogeny: Upper

Cretaceous to Lower Tertiary Toquepala Group (or Sacsaquero Volcanics, Calipuy Volcanics), Middle to Upper Tertiary Tacaza Volcanics (or Casapalca Volcanics, Castrovirreyna Volcanics) and Plio-Pleistocene Barroso Volcanics (or Sillapica Volcanics). The youngest Barosso Group consists of andesite, dacite, trachyte and rhyolite volcanics with total thickness up to about 1,500m and lies almost horizontally over older Maure Group or Tacaza Group suggesting the age of Barosso Group after the last compressive deformation in the Andean orogeny (Bellido, 1979). Generally, Plio-Pleistocene ages are assigned to these volcanics but radiometric age determination studies often revealed that even the volcanic rocks whose ages were assumed to be Quaternary show the age of Upper Miocene (e.g., Bellon and Lefévre, 1976; Kaneoka and Guevara, 1983). This implies the importance of radiometric age determinations on these rocks.

During the field survey in July 1981 from Lima to the Andean region of central Peru, a dike swarm was found within these "Plio-Pleistocene" (Instituto de Geologia y Mineria, 1975) volcanic formations near Ayacucho, about 200km inside from the coastline (Fig.3-14). It was named "Ocros dike swarm" after the name of the nearest town. Its original volcanic edifice was found to be extensively eroded by glaciation. The sampling route spans about 4km extending approximately north to south, along which we collected six oriented hand samples from each of 29 dikes intruding into the alternation of lavas and pyroclastics (Fig.3-14, OC01-29). At several sites (OC03,05,06) lava flows adjacent to the dikes were also sampled. General trend of the dikes is N80°E which is perpendicular to the trend of Cretaceous

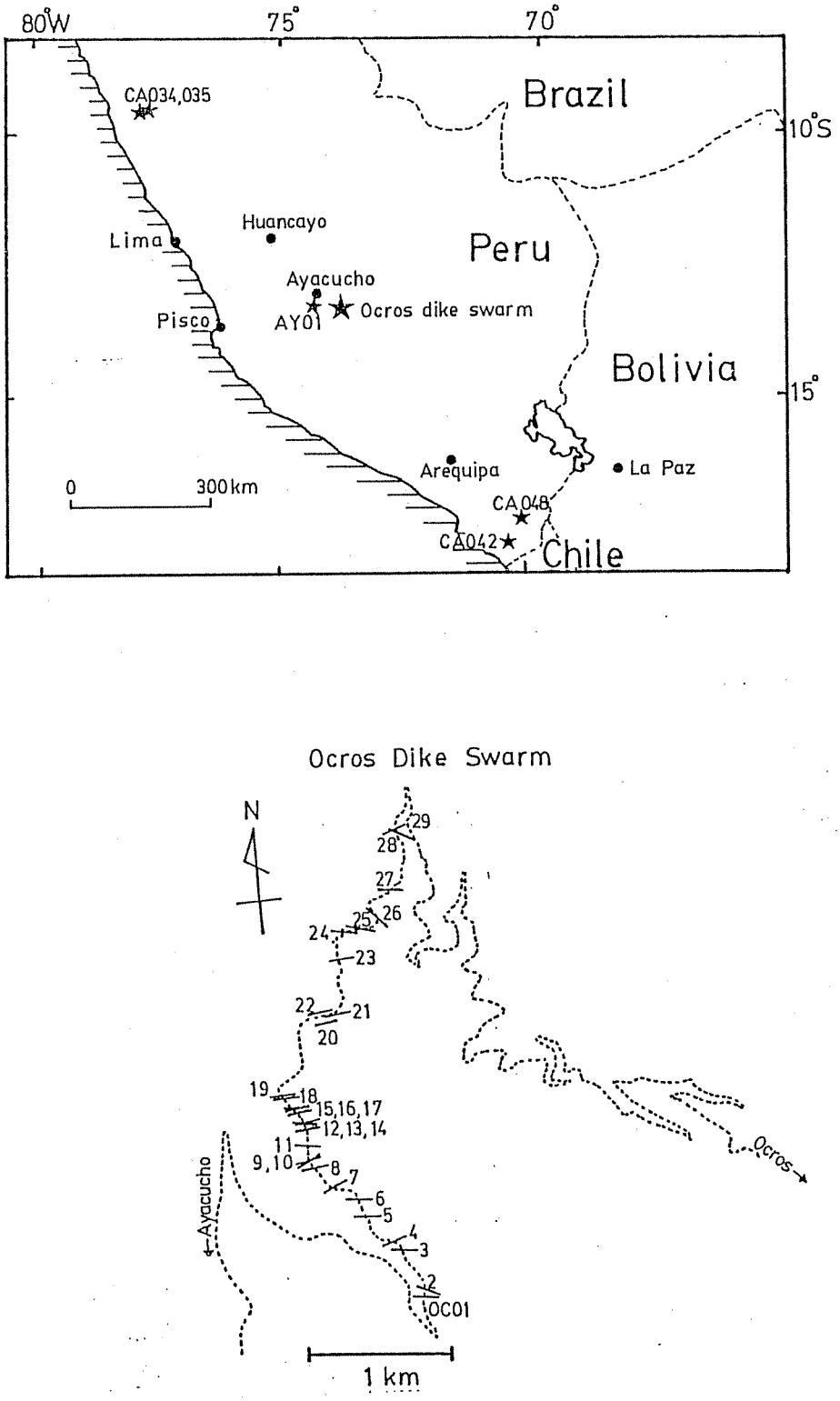

Fig.3-14 Sampling sites of Neogene volcanics in the Peruvian Andes (stars in the map). Close up of Ocros dike swarm is given below (OC01-29). The direction of the bar indicates the strike of the dike contact. Dotted line is the road between Ayacucho and Ocros.

dikes sampled in Ancon (chapter 3-b) but is in agreement with present σ_{Hmax} direction (Stauder, 1975). Thicknesses of the dikes range from 1.5 m to more than 50 m (see Appendix A) but are typically around 5-10 m. Diverse petrographic characteristics from olivine basalt, hornblende andesite through biotite trachyte were observed. Flow directions of the dikes were observed in situ using elongation of vesicles or alignment of long axes of phenocrysts (Ui et al., 1983). The results suggested that three magma sources were responsible for the formation of the dike swarm. Among these three groups, none of systematic variation of chemistry, petrography and dike orientation are detected and we can expect that these three groups are of similar geological ages. Although Peruvian geologic map (Instituto de Geologia y Mineria, 1975) indicates Plio-Pleistocene age of the formation, our preliminary K-Ar dating suggested slightly older age of Late Miocene (6-8Ma). Further confirmation of radiometric age would be an urgent problem.

In order to compare the data of Ocros dike swarm with those from other region, Neogene volcanics were sampled at five different sites in Peru (Fig. 3-14). CA034 and 035 locate near Huaraz and are both pyroxene andesite lava flows. CA042 and 048 locate at southernmost part of Peru and are both welded tuffs. AY01 locates near Ayacucho, central Peru and is an aphyric olivine basalt lava flow.

2) Experimental procedure and paleomagnetic results

A Schonstedt spinner magnetometer and an AF demagnetizer

were used for paleomagnetic analyses. NRM intensities ranged from 10^{-4} to 10^{-2} Am^2/kg. Many samples were considerably overprinted by soft and viscous magnetizations but these components were eliminated by AF demagnetization up to 15-20mT. Upon further treatment with higher AF, the direction of the decreasing remanence remained stable, showing that a single component was left. In Fig. 3-15a,b,c are shown Zijderveld demagnetization diagrams of typical specimens. Directions of the paleomagnetic field were determined from the gradient of the stable linear portion of the diagrams by LSF.

Fig.3-15a,b,c Typical Zijderveld diagrams of normal (OC16-2-1), intermediate (OC08-1-2) and reversed (OC04-5-1) polarity rock specimens in progressive AF demagnetization. Scales are arbitrarily taken.

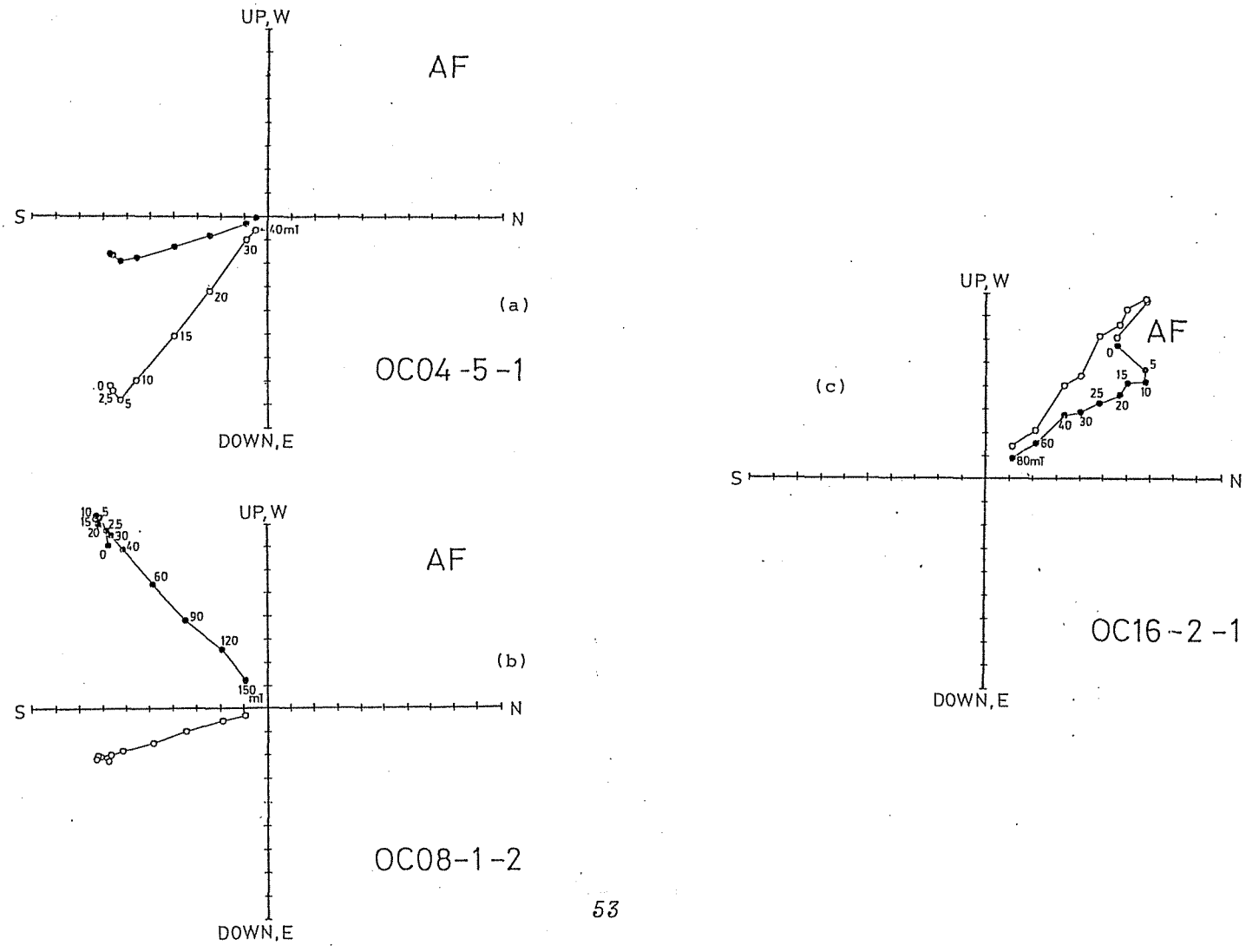

Thermomagnetic analyses were performed on several specimens using an automatic Curie balance and approximately reversible Js-T curves were obtained with Curie temperatures mainly of magnetite (580°C, Fig.3-16). Initial susceptibility was measured using Bison AC bridge and the Königsberger ratio (Qn ratio) ranged from 2 to more than 100. Susceptibility anisotropies measured by the spinner magnetometer were not so large as to affect the remanent magnetization directions. Experimental procedures for other samples (CA034,035,042,048, AY01) are the same as those for Ocros dike swarm samples.

Fig.3-16 Js-T curves of Ocros dike samples obtained by an automatic Curie balance.

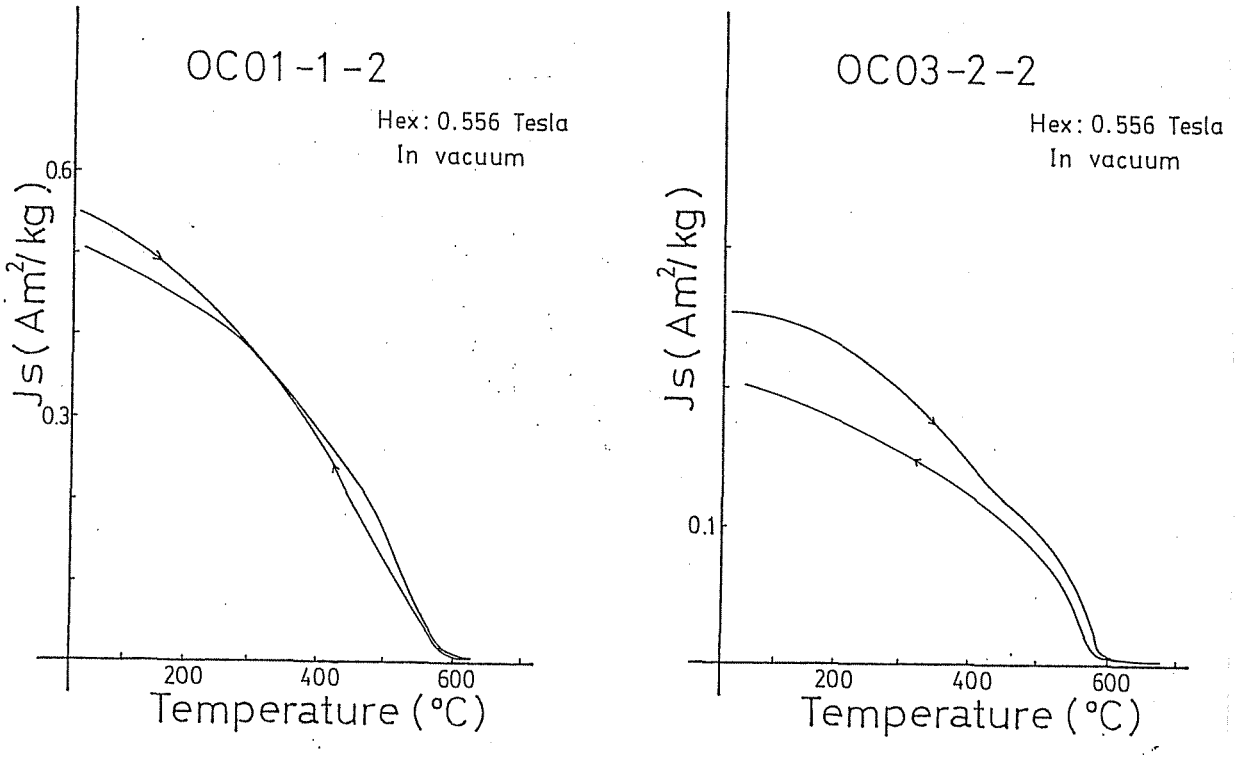

All paleomagnetic results are listed in Table 3-3. I obtained normal polarity directions from four dikes

(OC12,15,16,17) and reversed polarity directions from 21 dikes and lavas (OC01-07, 13,14,18,22-29) which are almost antipodal and deviate by about 15° counterclockwisely in their declinations from present axial geocentric dipole field. Seven dikes (OC08-11, 19-21) present directions which are not classified into normal nor reversed polarities and are interpreted as intermediate ones. These dike-mean directions are plotted by Lambert equal area projection on Fig.3-17.

Fig.3-17 Lambert equal-area projection of the dike mean field directions and their 95% confidence circles of Ocros dike swarm. Open and solid symbols indicate negative and positive inclinations respectively.

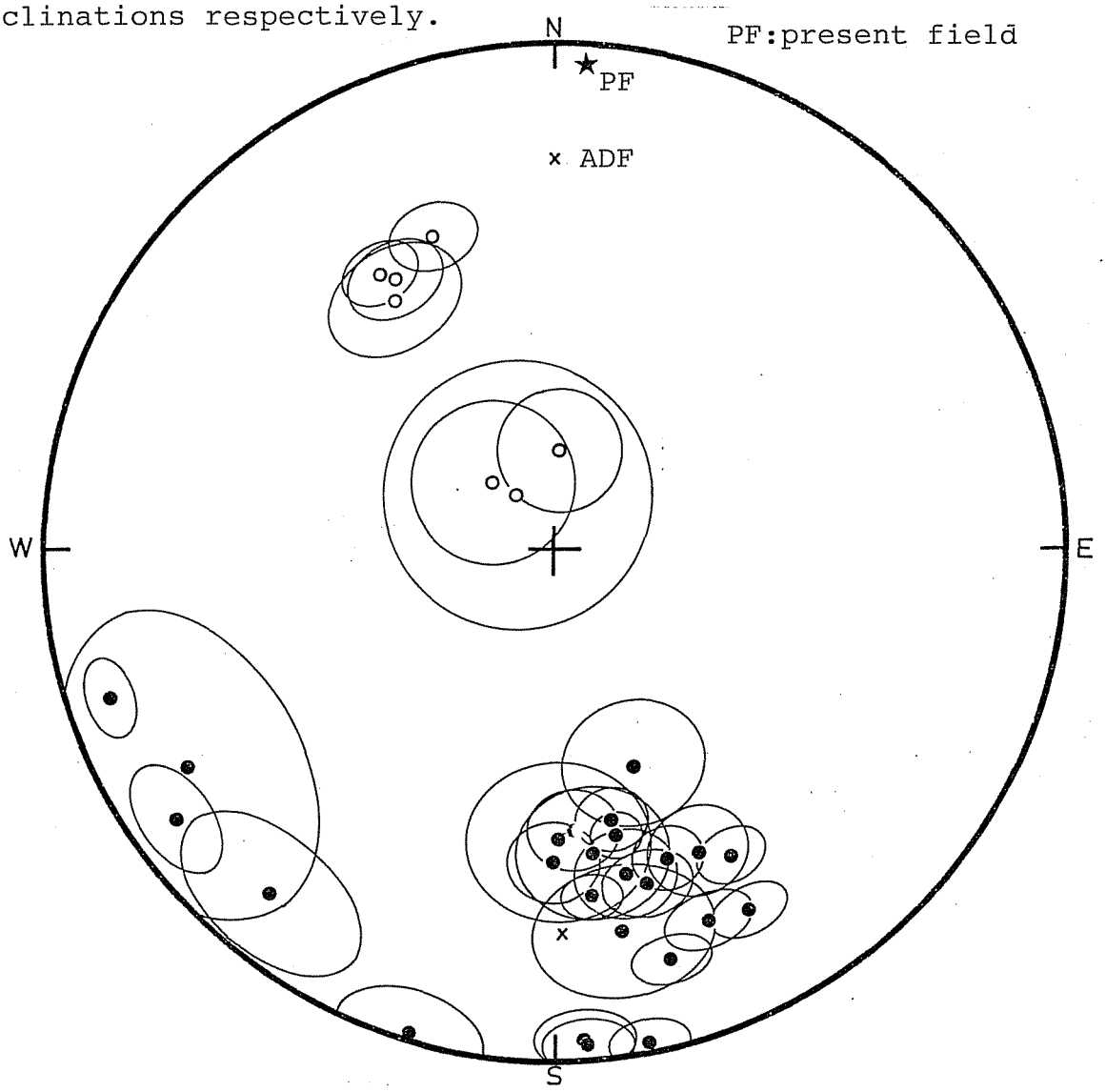

Table 3-3 Paleomagnetic directional data of Peruvian Cenozoic rocks

Site	N	Incl. (°)	Decl. (°)	R	k	α_{95} (°)	ODF (mT)	Pole Lat. (°N)	Pole Long. (°E)
OC01	4	3.9	176.5	3.9786	242	5.9	LSF	-78.0	88.9
OC02	6	0.8	-163.1	5.9209	63	8.5	LSF	-68.8	159.6
OC03	6	52.5	160.3	5.8739	40	10.8	LSF	-63.4	-34.9
OC03*	6	44.8	168.5	5.9649	142	5.6	LSF	-73.1	-36.0
OC04	5	42.4	179.3	4.8687	31	14.1	LSF	-78.8	-70.7
OC05	6	32.4	164.7	5.9578	118	6.2	LSF	-74.7	-1.8
OC05*	13	32.0	174.0	12.8808	101	4.2	LSF	-83.0	-18.6
OC06	6	24.7	170.2	5.8422	32	12.1	LSF	-80.5	17.6
OC06*	5	39.4	172.9	4.9244	53	10.6	LSF	-78.8	-37.9
OC07	6	17.5	164.4	5.9724	181	5.0	LSF	-74.1	30.6
OC08	5	17.2	-120.6	4.7201	14	20.9	LSF	-31.7	-161.8
OC09	6	13.1	-140.2	5.8151	27	13.1	LSF	-50.3	-169.7
OC10	6	9.5	-125.5	5.9375	80	7.5	LSF	-35.6	-167.7
OC11	6	8.8	-108.6	5.9755	204	4.7	LSF	-19.1	-163.9
OC12	6	-36.4	-32.5	5.9611	129	5.9	LSF	58.2	179.2
OC13	6	34.4	154.9	5.9335	75	7.8	LSF	-65.3	-0.1
OC14	6	34.6	167.7	5.9420	86	7.3	LSF	-76.9	-11.1
OC15	7	-34.6	-21.6	6.9315	88	6.5	LSF	68.5	178.0
OC16	6	-38.6	-30.7	5.9482	97	6.9	LSF	59.6	175.7
OC17	6	-41.6	-32.9	5.9043	52	9.4	LSF	57.2	172.5
OC18	7	38.4	-179.6	6.9192	74	7.1	LSF	-81.8	-76.6
OC19	4	-79.5	-37.0	3.8513	20	21.0	LSF	29.2	119.9
OC20	5	-75.4	-43.0	4.8872	36	13.0	LSF	32.3	127.9
OC21	6	-74.2	2.1	5.8976	49	9.7	LSF	42.9	104.6
OC22	6	31.2	150.5	5.9762	210	4.6	LSF	-61.3	5.4
OC23	6	43.8	176.1	5.9440	89	7.1	LSF	-77.2	-57.8
OC24	6	2.9	176.3	5.9655	145	5.6	LSF	-77.5	88.7
OC25	6	1.3	169.3	5.9709	172	5.1	LSF	-73.4	65.5
OC26	3	35.4	160.3	2.9963	545	5.3	LSF	-70.2	-4.7
OC27	5	41.9	168.1	4.9908	434	3.7	LSF	-74.4	-29.4
OC28	7	22.1	157.9	6.9487	117	5.6	LSF	-68.3	18.7
OC29	8	20.7	152.0	7.9520	146	4.6	LSF	-62.5	18.6
CA034	4	-29.3	-4.7	3.9588	73	10.8	LSF	82.3	138.5
CA035	3	-30.0	-16.0	2.9959	494	5.6	LSF	73.1	167.8
CA042	4	50.9	171.4	3.9947	570	3.9	LSF	-74.3	-42.2
CA048	5	-44.6	-15.0	4.9559	91	8.1	LSF	73.5	164.8
AY01	10	-7.7	37.3	9.8721	70	5.8	LSF	52.0	4.9

For legends, see Table 3-1.

*lava flows (rests are dikes).

3) Discussion

As stated in chaper 2, paleomagnetic results of such young volcanics are interesting in analysing of the geomagnetic field as well as tectonic point of view, and detailed geomagnetic discussions are given here on the problems such as paleosecular variation, polarity transitions. The declination shift and its tectonic implications are discussed in the last section.

Paleosecular variation The angular standard deviation (ASD) around their mean was calculated after Cox (1970) using 25 normal and reversed VGPs which are converted to a single polarity. Intermediate polarity VGPs are excluded from subsequent

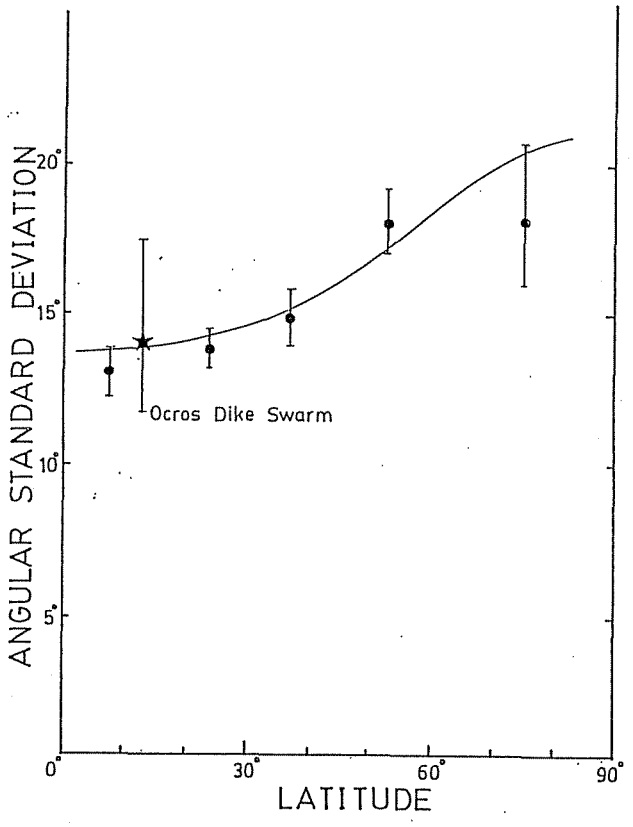

Fig.3-18a Angular standard deviation of Ocros dike swarm VGPs and the global trend of the last 5Ma summarized for each 15° latitude strips by McElhinny and Merrill (1975). Error bars indicate 95% confidence intervals.

discussions. The contribution of the within-site dispersion to the total ASD was corrected to isolate between-site ASD which is considered to represent true paleosecular variation. The 95% confidence limits of the ASD value were calculated from the table presented by Cox (1969). Obtained ASD value was 14.2° with the 95% confidence interval of 11.9°-17.7°. ASD values from VGPs covering sufficient time spans, say, more than a few tens of thousands of years (Heki, 1983) are expected to follow the worldwide trend of latitude dependence that the ASD value of equatorial sites of about 12° increases with latitude up to the value of about 20° in polar regions (McElhinny and Merrill, 1975). The ASD of Ocros dike swarm is in good agreement with this global trend (Fig. 3-18a) but seems slightly larger than several ASD data in the last 5Ma of similar southern latitude such as Southeast Africa (12.8°), New Guinea (10.8°), Fernando de Noronha (11.0°), Comoro Islands (11.8°) (Fig.3-18b). These differences, however, are not significant considering their large 95% confidence intervals. Present geomagnetic field has large assymmetry in its non-dipole field distribution between northern and southern hemispheres, namely, nondipole field component is significantly greater in southern hemisphere (Creer, 1962b; Cox, 1962). Such assymmetry is, however, not so clear in paleosecular variation data in southern hemisphere as shown in Fig.3-18c.

Fig.3-18b,c (next page) Angular standard deviation of VGPs of rock units for the Brunhes epoch and the last 5Ma in the southern hemisphere listed in McElhinny and Merrill (1975) (b) and those averaged in every 15° latitude strips in the southern hemisphere and the whole world (c). Error bars indicate 95% confidence intervals.

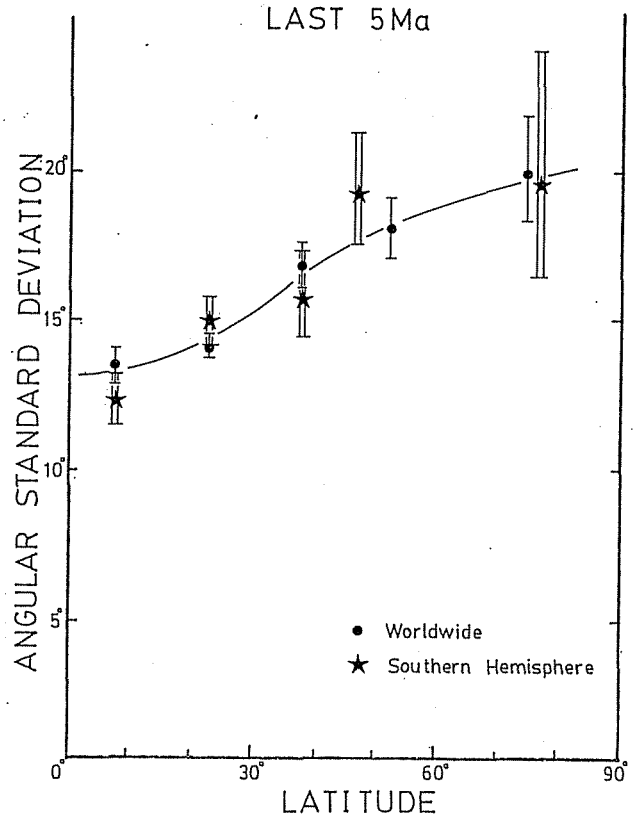

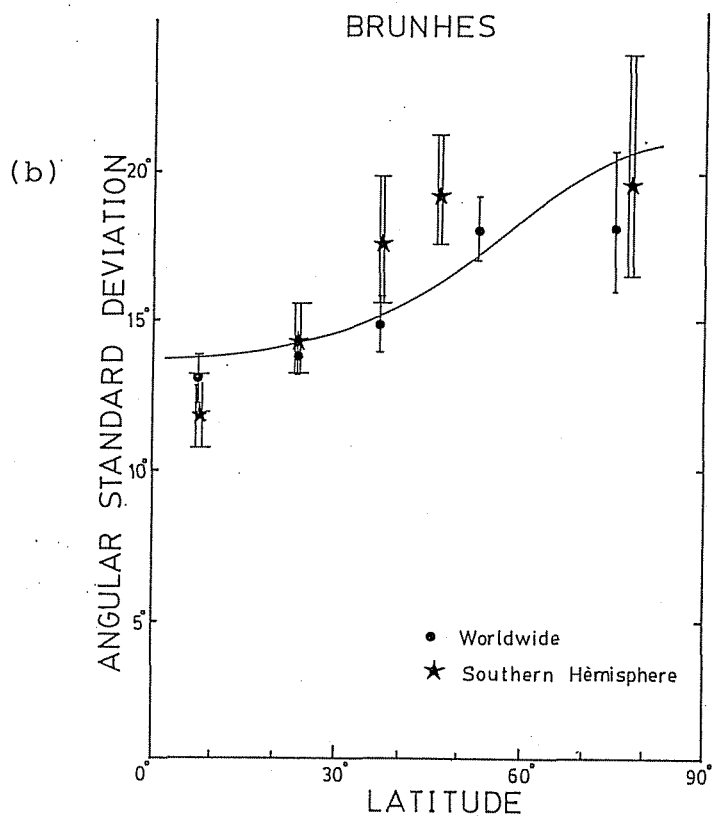

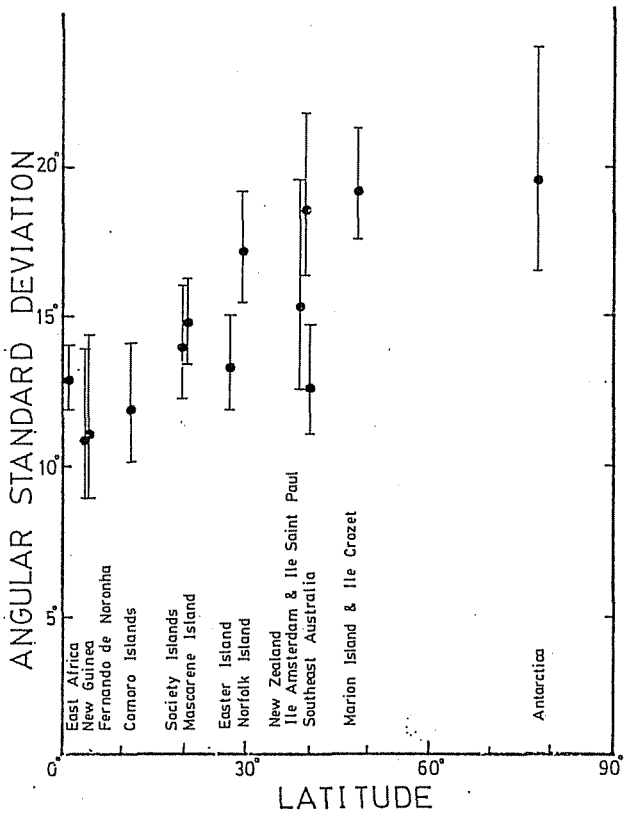

Southern Hemisphere [Last 5 Ma]

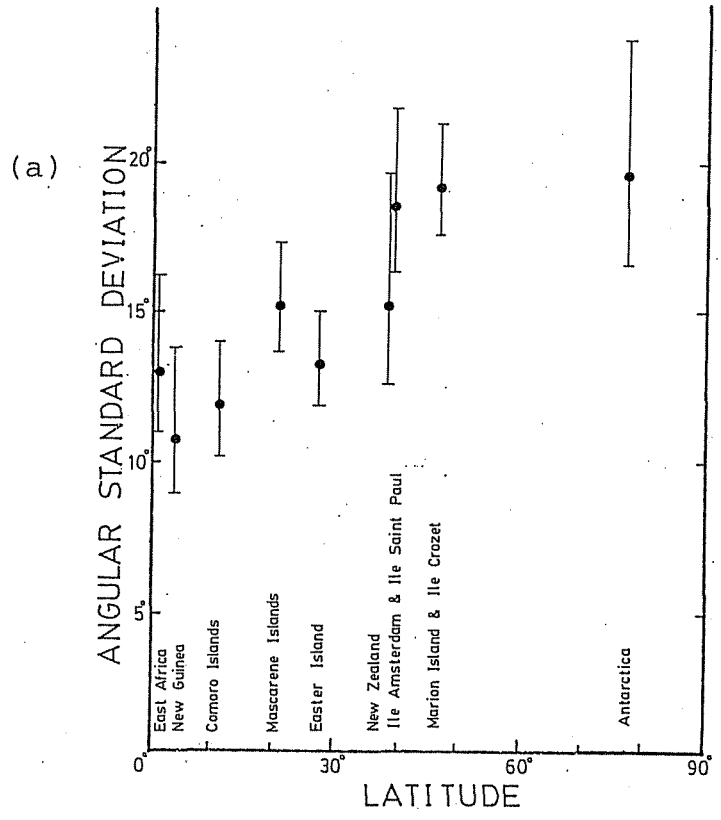

Southern Hemisphere [Brunhes]

VGP transition path In general, the time sequences of the dikes cannot be detected by field observations nor by laboratory experiments. A typical life length of a dike swarm is thought to be similar to that of a stratovolcano, say 10^4-10^5 years (see Heki and Tsunakawa, 1981) and it is difficult to detect the age differences between dikes in a dike swarm by radiometric age determinations (Feraud and Campredon, 1983). And so even when one derived normal and reversed polarity from a dike swarm, it is essentially impossible to know whether the normal polarity period predates or postdates the reversed polarity period and whether intermediate ones are of a polarity transition or of an excursion.

There are two groups in seven intermediate polarity dikes: almost horizontal and west-southwest seeking dikes (OC08,09,10,11) and almost vertical and upward seeking dikes (OC19,20,21). The former corresponds to VGPs to the west of the site about 90° apart and the latter corresponds to what they call far-sided VGPs (Fuller et al., 1979). With the present data only, it is ambiguous whether these two groups belong to a single polarity transition or represent two serial polarity transitions or no more than a geomagnetic excursion. Nevertheless, it is interesting as southern hemisphere data that definite far-sided intermediate VGPs were found which is usually observed in normal to reverse transitions at the zone of middle latitudes in the northern hemisphere (Fuller et al., 1979) and that new type intermediate VGPs of 90° apart from the site were found.

Deviation from axial geocentric dipole field The classical

dipole hypothesis predicts that geomagnetic field almost coincides with that of geocentric axial dipole when being averaged over a certain time span covering the whole periods of secular variation. A minor discrepancy from this hypothesis is found to be characterized by a systematic negative inclination anomaly in time averaged magnetic field (offset dipole; Wilson, 1971), which is expressed as zonal spherical harmonics, namely g_2^0 (and g_3^0) (Coupland and Van der Voo, 1980).

Field directions obtained from Ocros dike swarm show about 15° of counterclockwise declination shift although paleosecular variation seems large enough to cover the whole periods of secular variation (ASD=14.1°). Such a declination anomaly cannot be explained by g_2^0 and g_3^0 field, nor is it expected that paleomagnetic pole of such a young age show significantly different position from today's geographic pole as pointed out in chapter 2. It needs other interpretation.

One possibility is to assume some undetected tilt. In order to convert axial dipole field direction to Ocros mean field direction, about 30° westward tilt with a strike of N30°W is necessary if we assume a single horizontal tilting axis. Plio-Pleistocene tectonism shows clear contrast between the north and the south of Pisco-Abancay deflection zone (13°S-15°S) where Andean chain change its mean trend from N30°W to N50°W. Northern region (northern and central Peru) is characterized by the absence of volcanism and compressional tectonics while southern region is characterized by vigorous calc-alkaline volcanism and mostly extensional tectonics (Megard and Philip, 1976). However,

Ocros dike swarm lies just on the transition zone between these two regions and neotectonic data are not many in this zone. Determination of the timing of the defomation in neighboring region inferred from radiometric age determinations (McKee and Noble, 1982) demonstrates that major Late Cenozoic (Quechuan) compressive deformation took place between 19.5 and 17Ma ago and weak deformation after this time is observed only locally (see chapter 6-a and Fig.6-1). Observed dike contacts are almost vertical and such Plio-Pleistocene tilting by about 30° appears rather unlikely.

The other interpretation of the declination shift is a large-area counterclockwise rotation by about 15° around the vertical axis. In Fig.3-19 are illustrated additional paleomagnetic directions of Peruvian Neogene volcanics. Except AY01, four paleomagnetic directions of normal (CA034,035,048) and reversed (CA042) polarity deviate by 10°-15° counterclockwisely from the north-south axis. These data are no more than spot readings and counterclockwisely deviated directions might be foutuitous but this appears to support the interpretation of large-area tectonic rotation. Peruvian Cretaceous data reported already in this chapter also show rotations in the same sense but are about twice as large as that of Ocros dike swarm, which suggests the rotation lasted as late as the time of the Ocros dike intrusions. Paleomagnetic pole was calculated as the mean pole position of 25 normal and reversed VGPs converted to the southern hemisphere poles (Table 3-4).

Fig.3-19 Equal-area projection of site mean field directions and their 95% confidence circles for Miocene volcanic rocks in the Peruvian Andes.

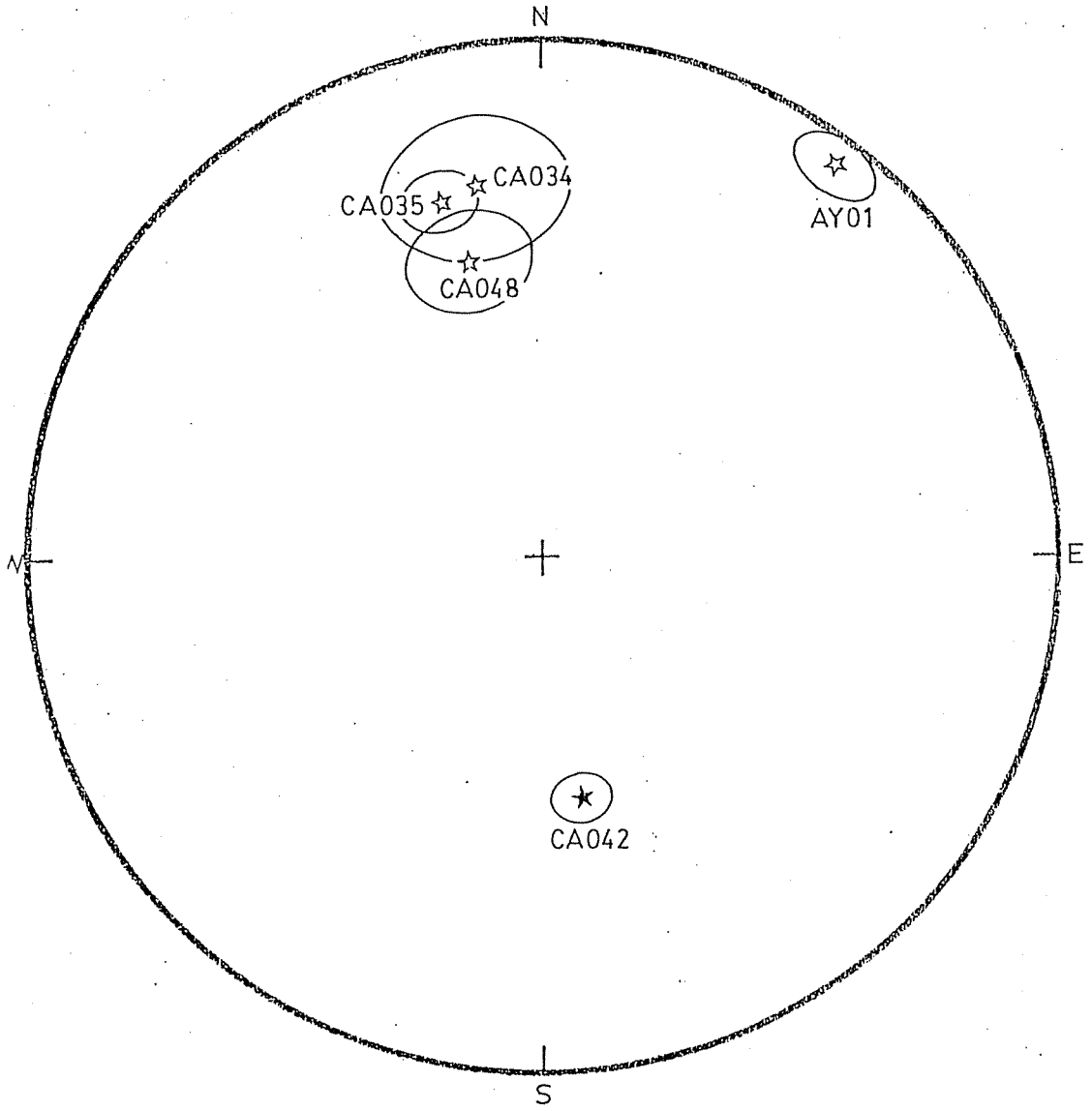

Table 3-4 Paleomagnetic pole from Ocros dike swarm.

Locality		Age	Pole			ASD		
Lat.	Long.		Lat.	Long.	A_{95}	S_b	S_u	S_l
(°S)	(°W)		(°S)	(°E)	(°)	(°)	(°)	(°)
13.4	74.0	Tm-p	75.8	358.8	5.3	14.2	17.7	11.9

ASD:angular standard deviation of VGPs, S_b:between-site angular standard deviation, S_u,S_l:upper and lower limits of S_b (95% level). For other legends, see Table 3-2.

Chapter 4. Paleomagnetic studies in Northern Chile

a) Introduction

In this chapter, paleomagnetic results are reported on Mesozoic volcanic and sedimentary rocks collected in the department of Arica and the department of Pisagua, northernmost Chile. As already noted in chapter 2, this region (18°S-20°S) just corresponds to the Arica-Santa Cruz deflection zone where Andean structural trend is deflecting making northwest-southeast striking Peruvian Andes into approximately north-south striking Chilean and Argentine Andes. Samplings were done in 1980 and 1981 in collaboration with Universidad de Chile at the sites shown in Fig.4-1a,b. It was also intended that both sedimentary and igneous rocks were sampled from the same ages. The oldest rocks studied in this region are of Middle Jurassic age and are composed of 26 dikes in Cuya dike swarm and shales of Camaraca Formation, Arica Group. Cretaceous samples are composed of 19 dikes in Arica dike swarm and red sandstones of Atajaña Formation, Vilacollo Group. Small number of Cenozoic rocks were sampled from ignimbrites of Oxaya Formation and from Quaternary volcanoes (Guallatiri volcano and Ajoya Caldera) in the Altiplano but the number of sites are not so many as to enable detailed discussions and these results are given in the Appendix B. Dips and strikes of the strata, precise localities, rock types, field observation data of dikes are all given in the Appendix A. Samples were also taken as oriented blocks with hammers and cut into one inch cores in the laboratory.

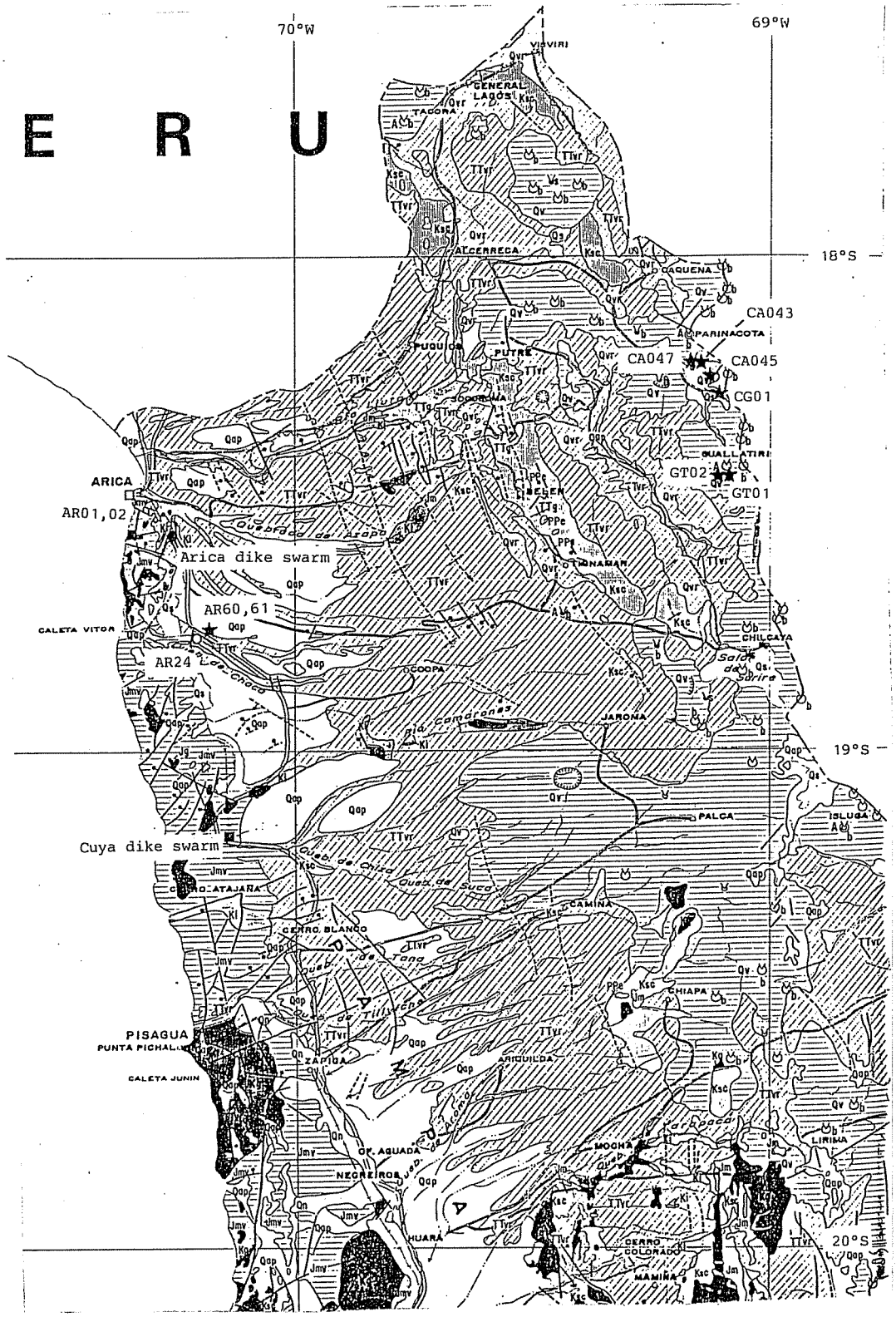

Fig.4-1a Geologic map and sampling sites in the northernmost Chile. Squares, circles and stars indicate Jurassic, Cretaceous and Plio-Quaternary sampling sites respectively. Open and solid symbols denote sedimentary and volcanic rocks respectively.

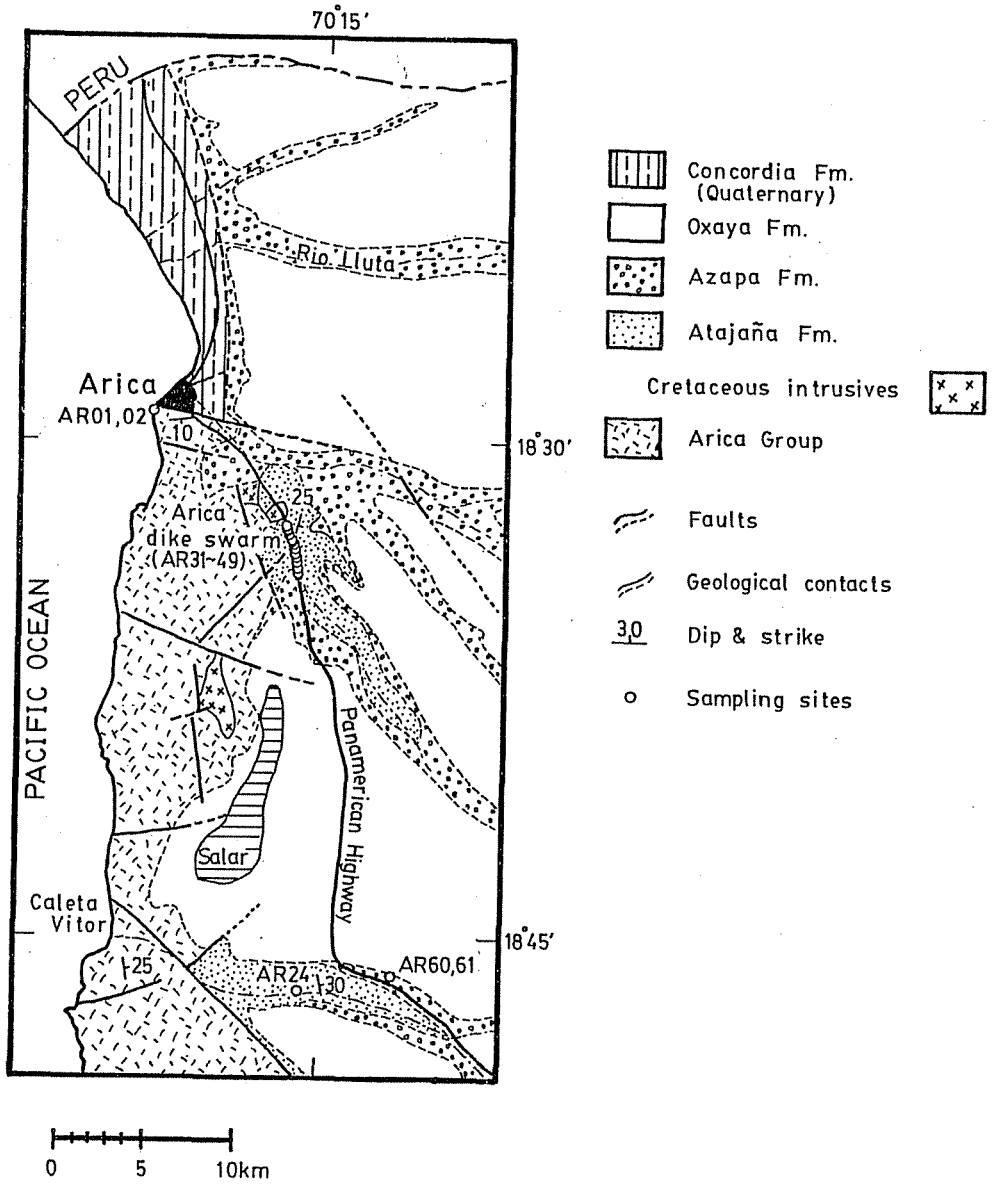

Fig.4-1b Close up of the region near the city of Arica. Geologic map is after Salas et al. (1966).

b)Jurassic sedimentary and volcanic rocks in the northern Chile

1) Geology

The department of Arica covered by the geologic map of Salas et al. (1966) is mostly occupied by Mesozoic and Cenozoic sedimentary and volcanic rocks with the total thickness up to

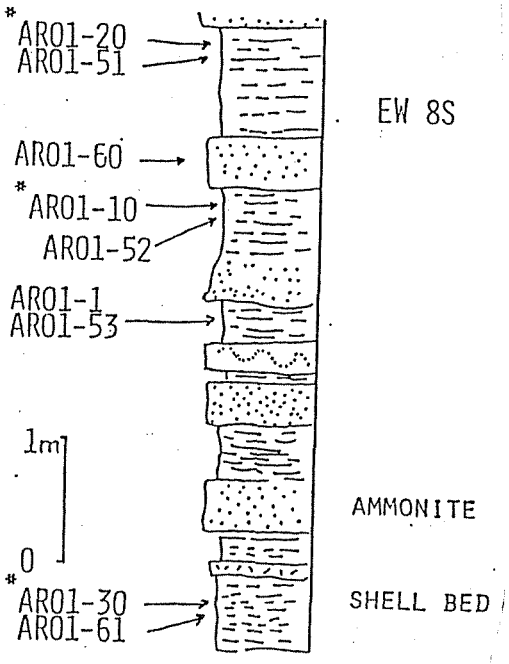

Fig.4-2 Columnar section of the sampling site of Jurassic shales in Camaraca Formation, Arica Group (AR01). Horizons sampled for paleomagnetic study are marked by stars.

8,000m. The oldest is Middle Jurassic Arica Group which consists of lower Camaraca Formation (upper Bajocian to Calovian) and upper Los Tarros Formation (Oxfordian). Camaraca Formation consists of dark color andesitic volcanics with some intercalations of marine sediments, and Los Tarros Formation is composed of the alternation of lutite, limestone, quartzite and minor amount of andesitic volcanic rocks. Paleomagnetic studies and K-Ar datings by Palmer et al. (1980a) are on the andesitic lava flows in this Camaraca Formation. Arica Group is uncomformably overlain by Neocomian Atajaña Formation, Vilacollo Group.

Sedimentary paleomagnetic samples were taken from the shale layer and an overlying pillow lava flow exposed at the northern face of the cliff called "Morro de Arica" which corresponds to the lower member of the Camaraca Formation. More than 20 samles were taken from four different horizons (AR01; 31-36, 11-15, 21-

25, 41-47&51, in ascending order, see Fig. 4-2). Their bedding plane dips by about 10° northward. The uppermost horizon (AR01;41-47&51) is just under the pillow lava layer. 10 samples were taken from comformably overlying andesite pillow lava (AR02) for comparison. In this pillow lava, one sample was taken from the center of each pillow block. This pillow lava corresponds to the site "AR-1" in the table 1 of Palmer et al. (1980a).

A dike swarm was found along the Panamerican Highway near Cuya, the boundary between the departments of Arica and Pisagua (named "Cuya dike swarm"). Dikes range in its thickness from 0.5 m to 7 m and generally trends north-south. Most dikes are made of porphyritic andesite and the country rocks (Los Tarros Formation) are made of calcareous sandstone and limestone dipping

Fig.4-3a Sketch of Cuya dike swarm (CY01-26) near the boundary between the departments of Arica and Pisagua. Numbers attatched to the dikes indicate serial numbers of dikes.

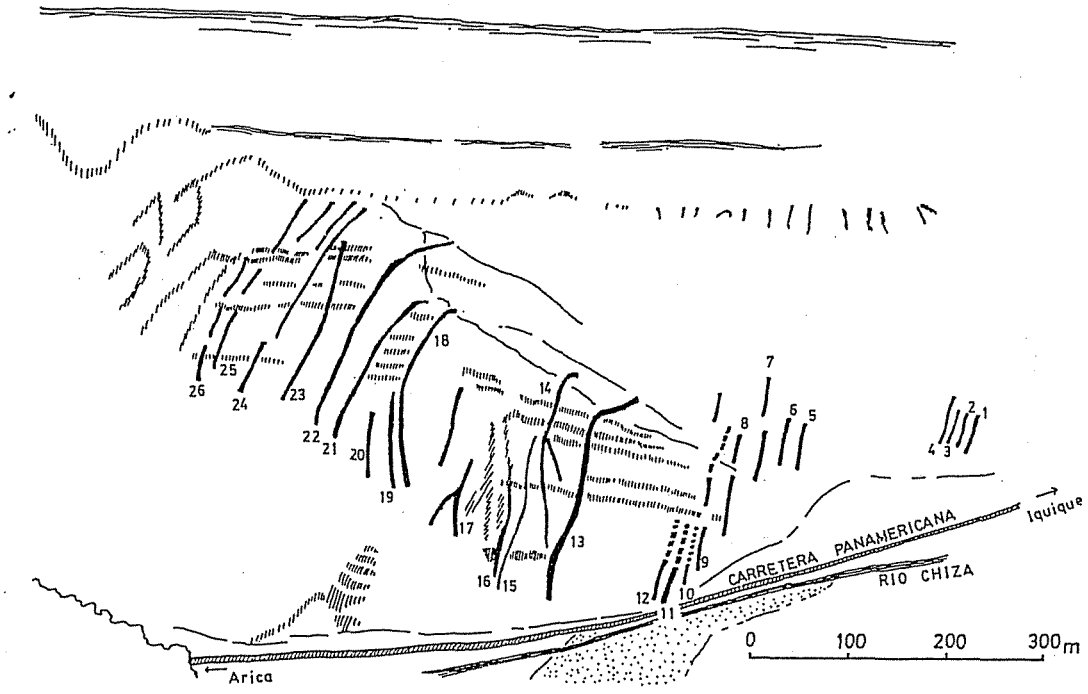

northeastward by about 30°-50°. Their top is eroded and is horizontally overlain directly by Tertiary ignimbrite of Oxaya Formation. Generally six hand samples were taken from each of 26 dikes (CY01-26, Fig.4-3a) and adjacent sedimentary rocks were also sampled at CY08 (CY08; 11-13, 21-23) and CY09 (CY09; 11-17, 21-27) with various distances from the contacts (Fig.4-3b) to carry out baked contact test (Irving, 1964).

Fig.4-3b Sketch of the positions of the samples used for baked contact test in Cuya dike swarm.

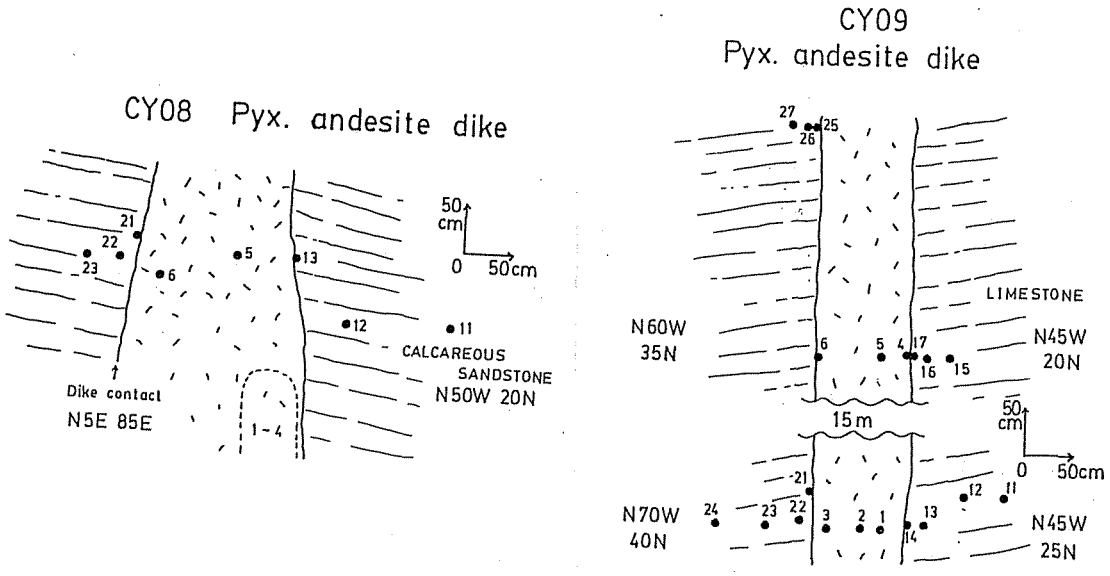

2)Experimental procedure and paleomagnetic results

Shale and pillow lava (AR01,02) NRM intensities of samples of AR01 and AR02 are generally of the order of 10^{-5}-$10^{-6}$$Am^2$/kg and were able to be measured with a Schonstedt spinner magnetometer. Stepwise AF demagnetization was carried out for each specimen as far as the original remanence was mostly destroyed. Thermal

Fig.4-4a,b Zijderveld diagrams of AR01 by AF demagnetization (a) and thermal demagnetization (b).

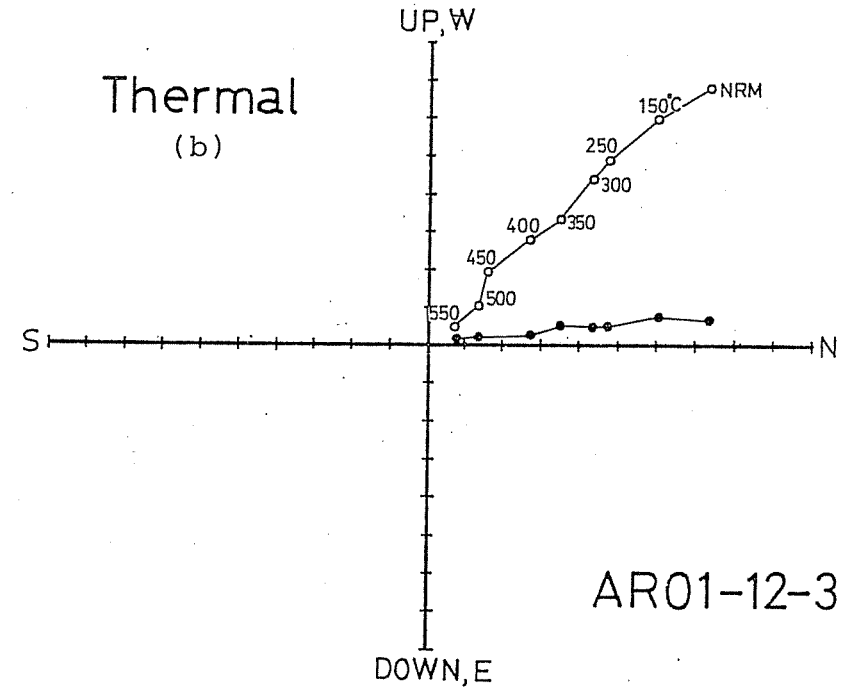

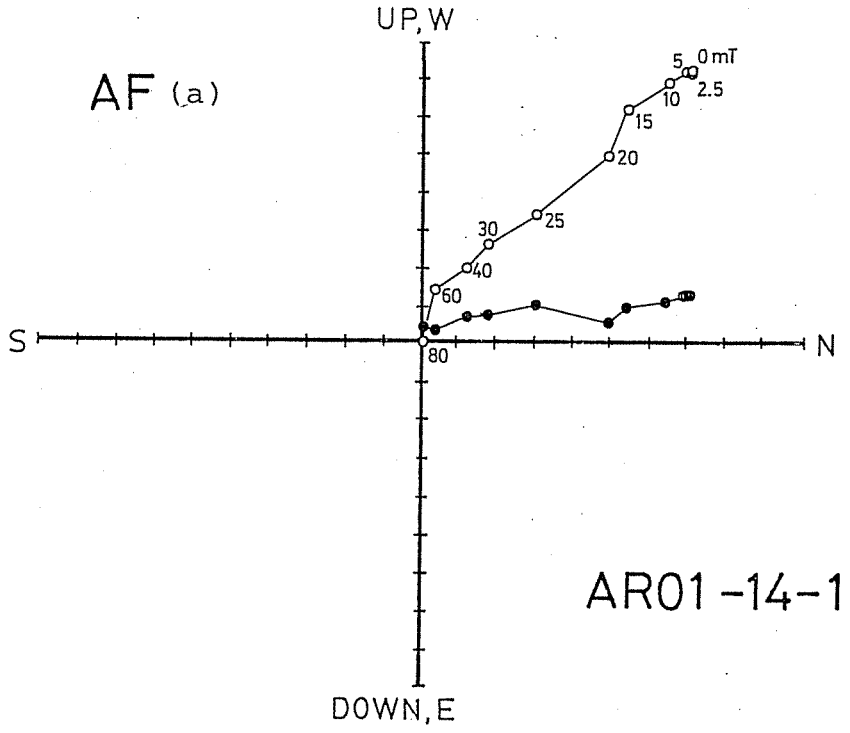

demagnetization was also performed on several specimens of AR01 and AR02 to infer the blocking temperature distribution. MDFs are usually between 20-25mT for AR01 and stable and single-component remanent magnetizations are suggested from Zijderveld diagrams (Fig.4-4a). Thermal demagnetization (Fig.4-4b) showed that the blocking temperatures distribute from less then 150°C continuously up to about 550°C and no blocking temperatures higher than the Curie temperature of magnetite were observed suggesting the inexistence of hematite. Paleofield directions were determined from the LSF to the linear portion of the diagram. Several samples were broken during the trip and coring

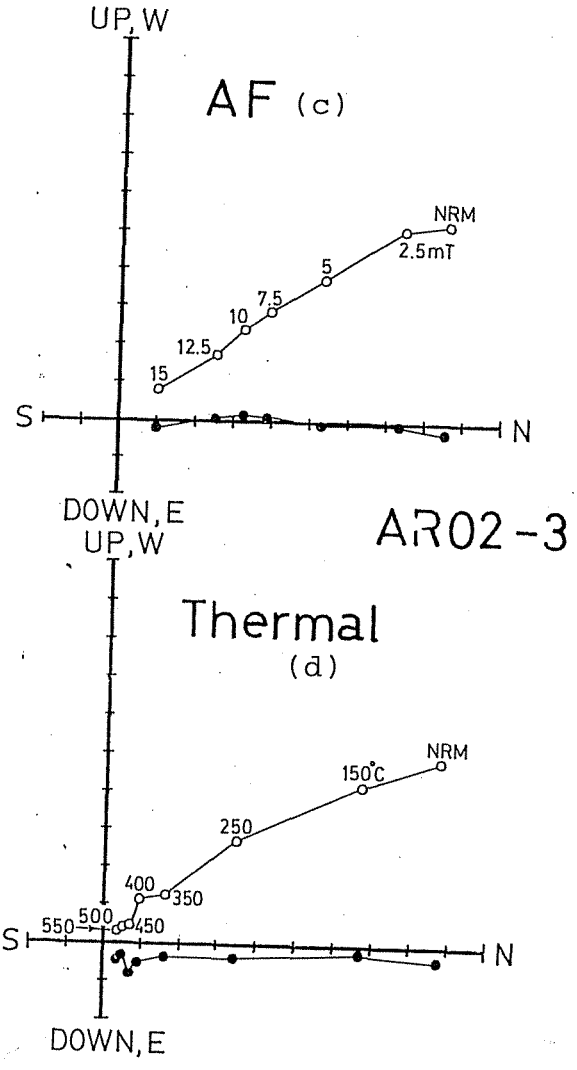

Fig.4c,d Zijderveld diagram of AR02 by AF demagnetization (c) and thermal demagnetization (d).

and paleomagnetic field directions were obtained from 22 specimens in total. All specimens showed normal polarity magnetization with slight counterclockwise declination shift from north. Pillow lava samples (AR02) were also AF demagnetized and measured with a Schonstedt spinner magnetometer (Fig. 4-4c). Thermal demagnetization showed blocking temperature distribution up to 580°C (Fig. 4-4d). Obtained field directions are not well grouped but show slight eastward declination shift which is significantly different from those of shales (Fig.4-5). The bedding corrections are performed on these directions.

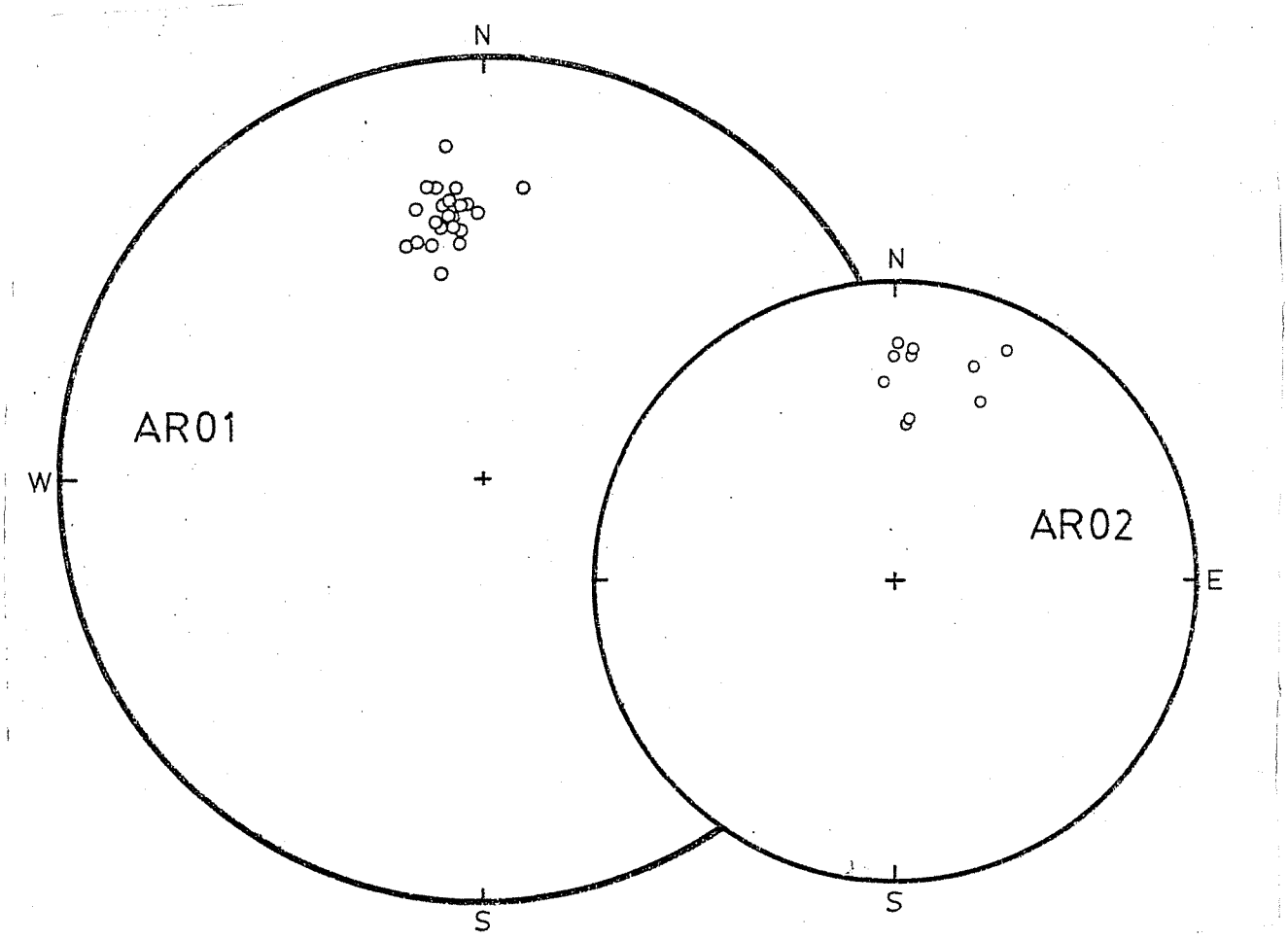

Fig. 4-5 Equal-area projection of field directions of AR01 samples and AR02 samples. All inclinations are negative (upward).

No significant direction and/or intensity differences were observed for four horizon groups (AR01;31-36, 11-15, 22-25, 41-47&51) among which the uppermost horizon (AR01; 41-47&51) is just under the contact between pillow lava and shale. Initial susceptibilities were also measured to obtain Qn ratios but also no significant differences were detected between those of the uppermost contact samples and lower samples (Fig.4-6). Hence, it

Fig.4-6 Initial susceptibilities versus intensities of natural remanent magnetizations and the lines indicating the Königsberger ratio (Qn) of 1 and 0.1. Solid circles indicate specimens of AR01 shales and open circles indicate the specimens just under the contact between AR01 and AR02. Stars indicate AR02 pillow lava specimens.

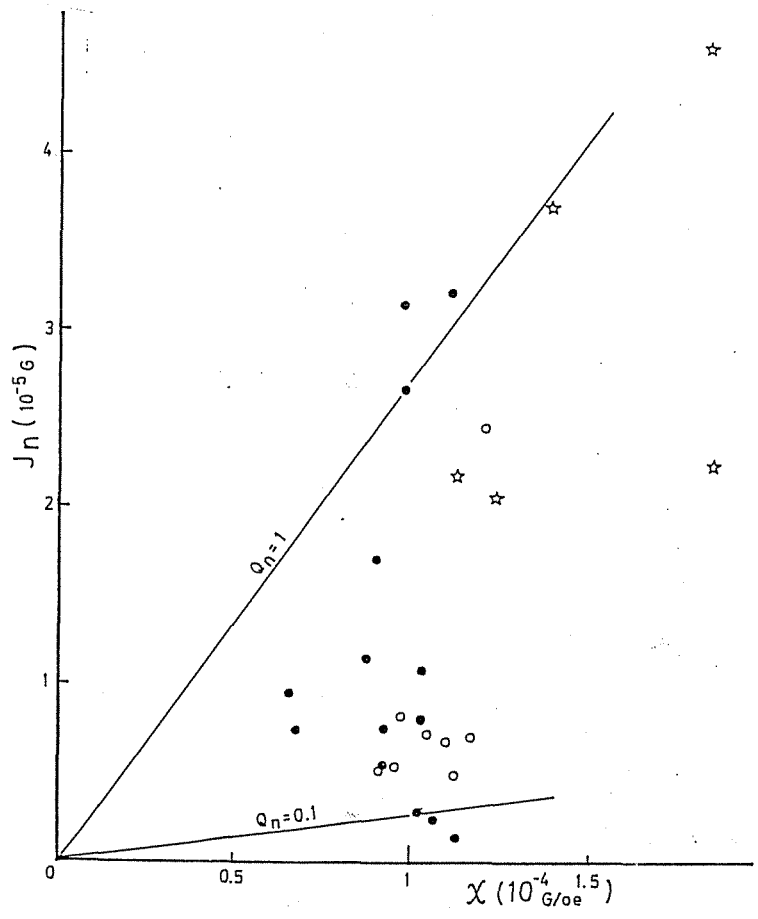

is suggested that shale layers sampled here did not suffer any thermal effect from overlying pillow lava. Significant difference of paleomagnetic field direction of the pillow lava from those of shales support this interpretation. It is therefore envisaged that when AR02 pillow lava flowed out and settled on the AR01 shale, the temperature of the center of each pillow was still higher than its highest blocking temperature but was not so high as to bake underlying AR01 shale strata. Paleomagnetic data are listed in Table 4-1.

Dikes (CY01-27) and their country rocks (CY08,09) NRMs of the country rocks (limestones and calcareous sandstones) were measured using a cryogenic magnetometer in the National Institute of Polar Research and a Schonstedt spinner magnetometer in University of Tokyo. NRM intensity of these rocks varies in two orders of magnitude values in spite of their lithological similarities. As shown in Fig.4-7, NRM intensity is strongly dependent on the distance from the dike contact: NRM intensities of the order of $10^{-5}Am^2/kg$ at the baked part abruptly decrease at the distance of 50-100cm down to the order of $10^{-7}Am^2/kg$ indicating the diminishing thermal effects of the dikes. Samples at farther distances show no more intensity decreases. The NRMs of the baked and unbaked specimens are both of reversed polarity with slight counterclockwise declination shift from today's axial dipole field but inclinations of the baked rocks are significantly deeper than those of unbaked rocks (Fig.4-8). Baked part seems to have acquired thermoremanent magnetization (TRM) at the times of the intrusions of CY08 and CY09 dikes and

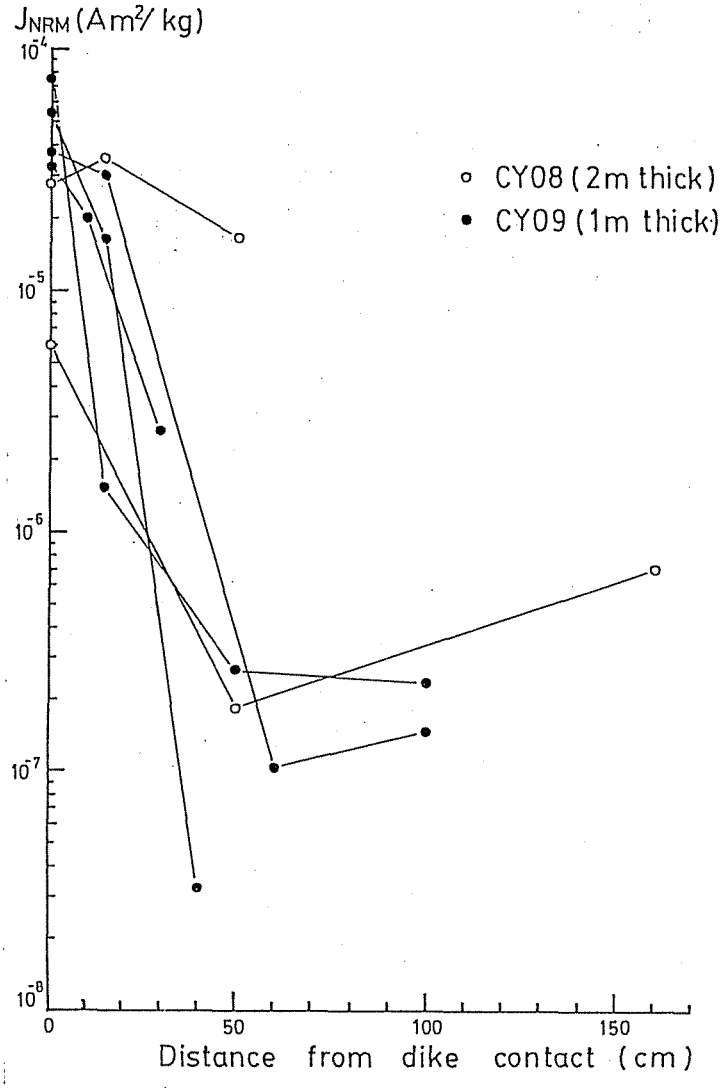

Fig.4-7 NRM intensity versus distance from the dike contact in the baked contact test at CY08 and CY09 dikes.

unbaked part seems to posess pure detrital remanent magnetization (DRM) acquired at or soonly after the time of deposition. Remanent magnetization direction of rocks baked by CY08 dike show good coincidence with CY08 dike samples but concordance at CY09 is not clear because of the large scatter of remanent magnetization directions of CY09 dike rocks probably due to the insufficiency of the removal of the secondary components (see table 4-1). The existence of the unbaked part guarantees that this dike swarm did not suffer wide-region thermal remagnetization and that the TRMs of individual dikes are independent.

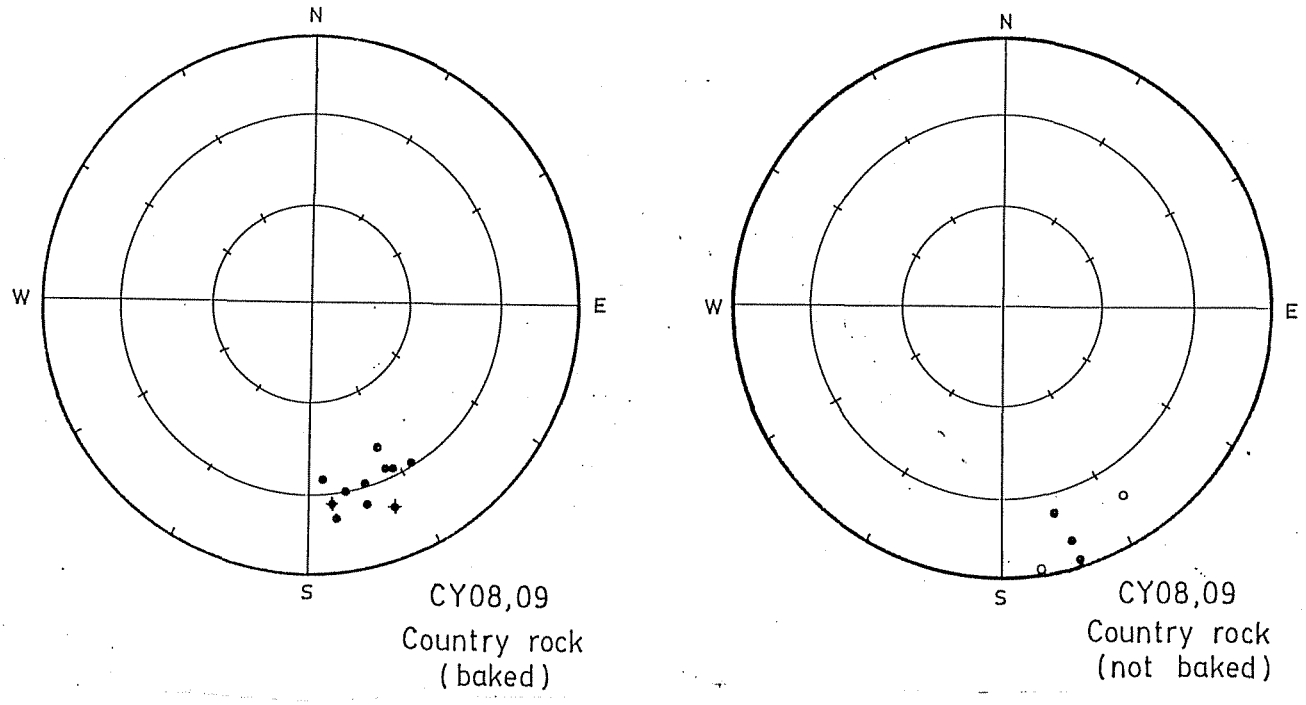

Fig.4-8 Field directions of CY08,09 baked samples (left) and unbaked samples (right). Circles overprinted by crosses in baked rocks indicate CY08 and the others indicate CY09 samples.

NRMs of the dike samples were measured using a Schonstedt spinner magnetometer in University of Tokyo as a bachelor thesis by Nomura and Morikawa (1983) and detailed paleomagnetic and rock magnetic descriptions are available in their thesis. NRM intensities of dikes were small (typically $10^{-5}Am^2/kg$-$10^{-7}Am^2/kg$) in comparison with ordinary igneous rocks and are almost comparable with those of country rocks (CY08,09). On the other hand, initial susceptibilities are not so small making consequent Qn ratios quite small (mostly less than unity). This may be due to some kind of alteration of magnetic minerals such as low temperature oxidation ubiquitously observed in microscopic analyses (Nomura and Morikawa, 1983). Js-T curves measured by a Curie balance often showed the existence of two phases: the lower one around 300-350°C and the higher one almost that of magnetite.

About four fifths of the dikes showed irreversible Js-T characteristics suggesting the existence of low-temperature oxidation. Stepwise AF demagnetization was performed on each specimen. Several specimens showed stable magnetization direction in demagnetization process as shown by Zijderveld diagram (Fig.4-9a,b) but for most specimens, remanent magnetization directions

Fig.4-9a,b Zijderveld diagrams of Cuya dike samples in progressive AF demagnetization after Nomura and Morikawa (1983). Open and solid circles indicate the projections onto vertical and horizontal planes respectively. Steps are 0,2.5, 5, 7.5, 10, 12.5, 15, 20, 25mT for (a) and 0, 2.5, 5, 7.5, 10, 12.5, 15, 20, 25, 30, 40, 50, 60mT for (b). Solid lines indicate the best fit lines by LSF. Inclination and declination are derived as the gradients of these lines.

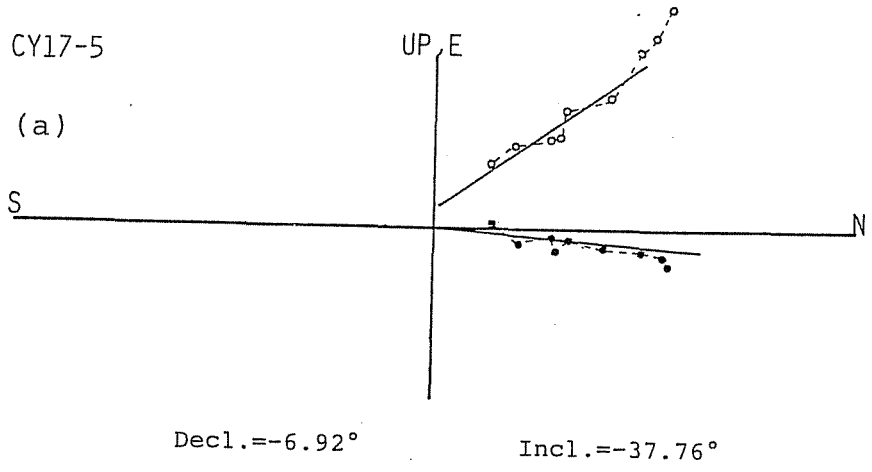

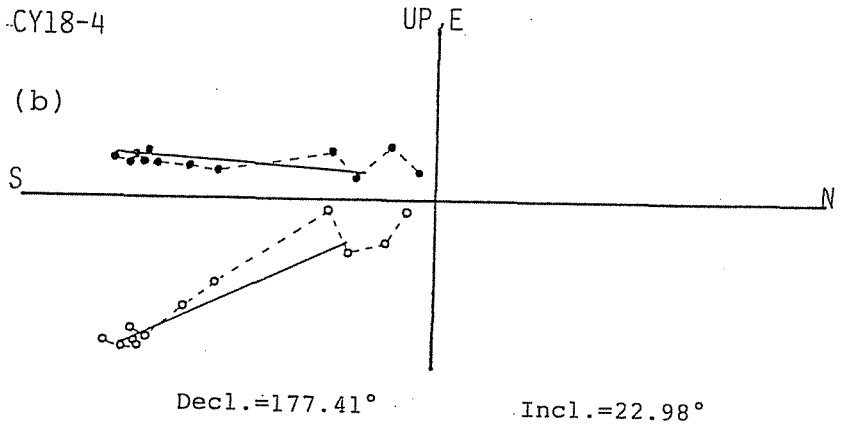

were too unstable to enable LSF to the diagrams. Hence, certain optimum demagnetizing step was determined by the objective criterion of minimum dispersion and remanent magnetization direction at that step were adopted. Several specimens were discarded due to their complete instability against AF demagnetization. MDFs were widely distributed from 10mT to 80mT.

Fig.4-10 Dike-mean field directions and their 95% confidence circles of Cuya dike swarm.

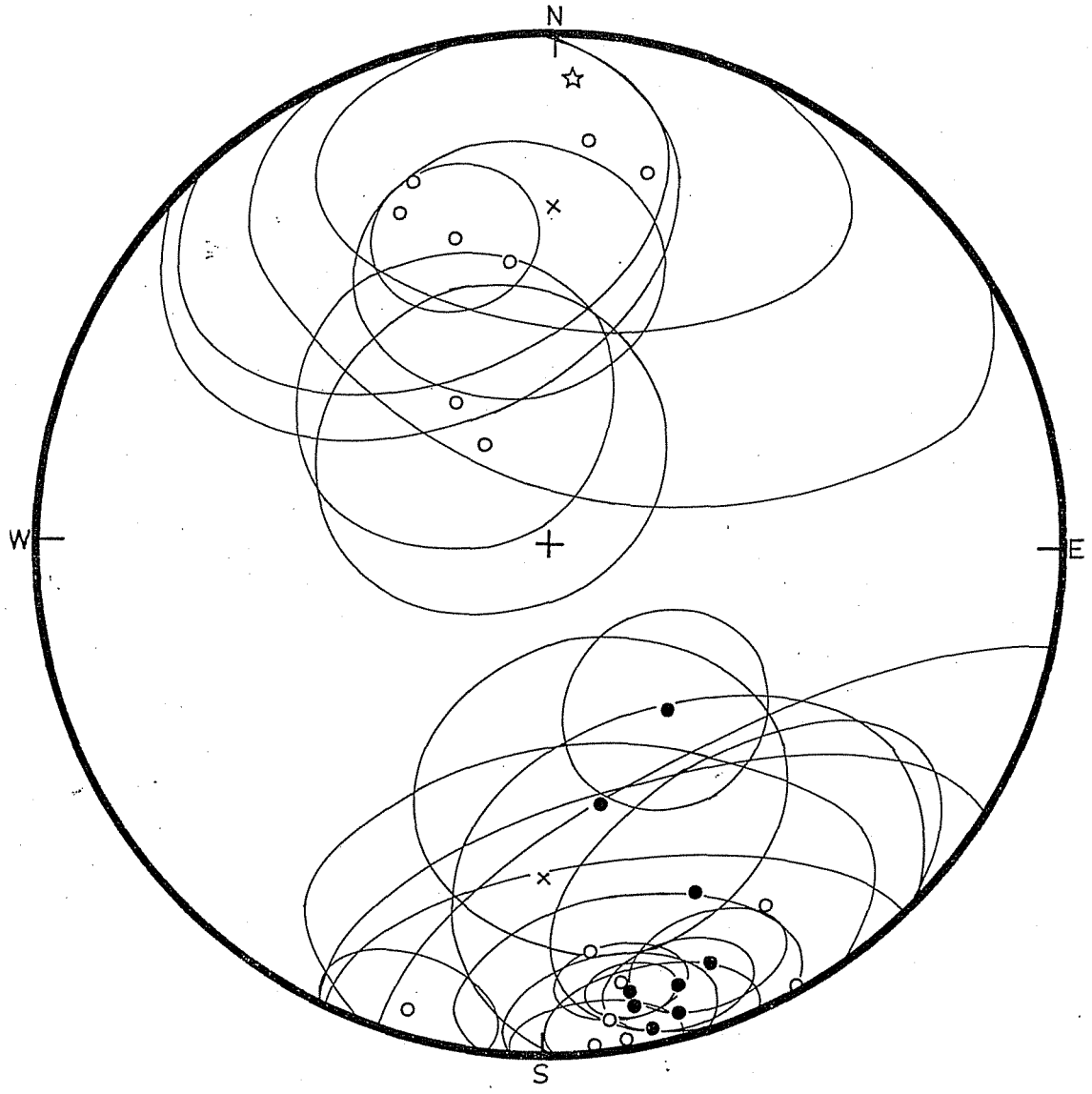

Table 4-1 Paleomagnetic directional data of Chilean Jurassic rocks

Site	N	Incl. (°)	Decl. (°)	R	k	α_{95} (°)	ODF (mT)	Pole Lat. (°N)	Pole Long. (°E)
				(sedimentary rocks)					
AR01									
11-15	4	-34.7	-0.9	3.9853	204	6.4	LSF	89.0	164.6
22-25	4	-40.3	-7.9	3.9860	215	6.3	LSF	81.4	167.1
31-36	6	-39.7	-9.3	5.9927	688	2.6	LSF	80.4	173.2
41-47, 51	8	-35.8	-10.5	7.9055	74	6.5	LSF	80.0	190.4
total	22	-37.6	-7.9	21.8261	121	2.8	LSF	82.1	179.4
AR02	10	-30.4	9.4	9.7351	34	8.4	LSF	80.8	7.7
				(volcanic rocks)					
CY01	4	8.6	168.6	3.8483	20	21.2	30	-71.4	71.6
CY02	4	-1.8	170.2	3.6321	8.2	34.3	40	-67.7	83.2
CY03	6	13.1	158.2	5.8864	44	10.2	30	-65.4	47.6
CY04	6	-71.5	-32.8	5.2570	6.7	27.9	5	45.6	135.4
CY05	4	-26.1	14.5	3.2212	3.9	54.2	0	75.1	0.7
CY06	5	-30.1	-24.6	4.2125	5.1	37.7	0	66.4	-156.7
CY07	6	-37.7	-17.5	5.8298	29	12.6	30	73.5	-166.9
CY08	5	46.8	167.8	4.5341	8.6	27.7	7.5	-75.8	-20.8
CY09	4	-18.3	148.4	3.7440	12	28.0	12.5	-47.7	59.6
CY10	4	-20.8	173.3	3.5543	6.7	38.3	20	-59.3	96.9
CY11	4	5.2	163.7	3.4694	5.7	42.5	15	-67.0	64.0
CY12	4	26.8	156.5	3.6616	8.9	32.7	10	-67.0	28.8
CY13	5	-14.1	169.8	4.9536	86	8.3	20	-61.8	88.0
CY14	6	11.8	168.9	5.9627	134	5.8	30	-72.9	69.1
CY15	4	-22.0	5.1	3.6096	7.7	35.5	0	80.8	-37.1
CY16	5	56.9	143.3	4.8273	23	16.2	10	-53.2	-17.8
CY17	4	-25.4	-21.0	3.6314	8.1	34.3	0	69.0	-147.2
CY18	4	-0.3	149.9	3.3317	4.5	49.0	30	-54.7	49.6
CY20	4	3.3	167.1	3.9439	53	12.7	20	-68.4	72.6
CY21	4	10.8	162.7	3.9673	92	9.7	20	-68.3	56.8
CY22	4	-0.6	173.9	3.9660	88	9.8	60	-69.6	92.1
CY23	5	-5.9	-164.4	4.9210	51	10.9	40	-63.1	146.2
CY24	3	-43.7	-8.3	2.9344	30	22.7	5	80.0	158.7
CY25	3	-63.4	-33.8	2.9188	25	25.4	10	52.0	149.6
CY26	3	-6.6	171.7	2.9786	93	12.8	5	-66.1	89.0
				--country rock--					
Baked (CY08)	2	23.3	164.0	1.9804	51	35.7	LSF	-73.1	42.1
Baked (CY09)	9	31.0	160.6	8.8730	63	6.5	LSF	-71.4	24.4
Unbaked part	5	3.8	161.6	4.7965	20	17.7	LSF	-65.0	61.5

For legends, see Table 3-1.

From 25 dikes, tolerably clustered paleofield directions were obtained. Dike-mean field directions present bimodal and almost antipodal distribution, which are interpreted to represent normal and reversed polarities. Both distributions deviated a little counterclockwisely from present axial dipole field in their declinations. Bedding corrections were made on all these directions according to the structure of the country rocks. There are several dikes whose polarities appear to be intermediate (e.g., CY04) but it is not certain due to their large confidence angles. After all, all directions were classified into normal or reversed polarities by whether VGPs are on the northern hemisphere or on the southern hemisphere and 8 normal and 17 reversed polarity directions were obtained. Paleomagnetic results are listed in Table 4-1 and directions are illustrated in Fig.4-10.

3) Discussion

As for AR01 samples, because no external thermal effects were found in all four layers, paleofield directions of all 22 specimens were averaged irrespective of their horizons and the mean direction was obtained. The corresponding pole is thought to cancel out paleosecular variation and to be a paleomagnetic pole. AR02 direction is considered to be stable TRM also acquired in Middle Jurassic time but this is no more than a "spot-reading" and is not used for the discussions of Jurassic paleomagnetic poles. The averaged direction of many lavas of Camaraca Formation coincide with that of AR01 as shown by Palmer et al. (1980a).

All 25 VGPs showed latitudes higher than 45° and were used for the calculation of the paleomagnetic pole. They were converted to southern hemisphere poles and the paleomagnetic pole was obtained by averaging them. Cuya dike swarm pole, AR01 pole and that derived by Palmer et al. (1980a) on 33 lava flows of Camaraca Formation are listed in Table 4-2.

Arica region paleomagnetic poles were compared with Jurassic platform pole and are illustrated together in Fig. 4-11. Platform poles are roughly coincident with present geographic pole while those of Arica region listed in Table 4-2 show similar but smaller deviations as those of Peruvian poles (chapter 3) suggesting also counterclockwise rotation of this region. Valencio et al. (1983) attributed the Camaraca Formation discordant pole (Palmer et al., 1980a) not to the tectonic

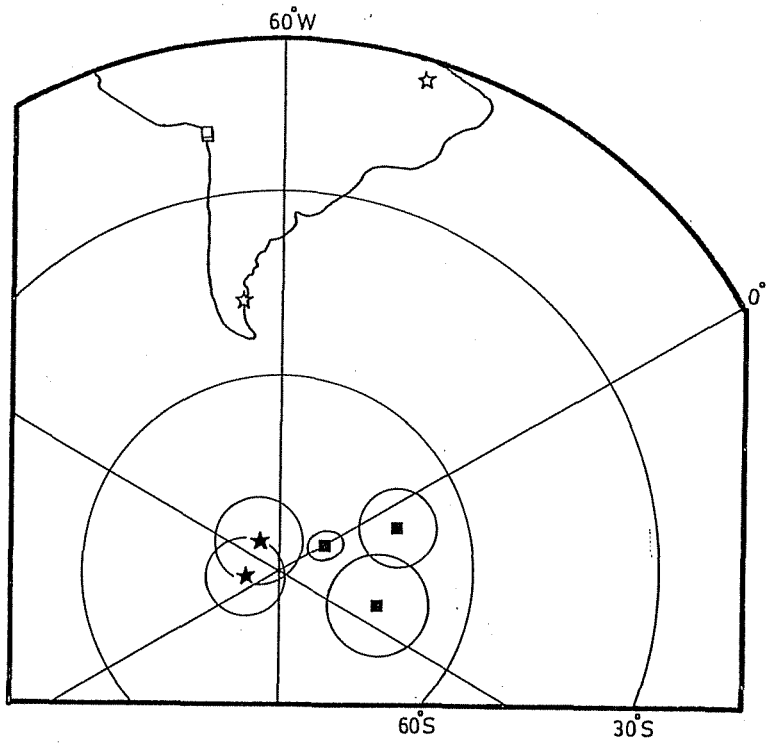

Fig.4-11
Paleomagnetic poles of Jurassic rock units in the Arica region (squares) and in the stable platform (stars). 95% confidence circles/ovals are also illustrated. Corresponding sampling localities are shown as small open symbols in the map.

Table 4-2 Jurassic poles in the northern Chile.

Rock unit	Locality Lat. (°S)	Long. (°W)	Age	Pole Lat. (°S)	Long. (°E)	dp (°)	dm (°)	A_{95} (°)
Camaraca Fm. shale (AR01)	18.6	70.3	Jm	82.1	-0.6	1.9	3.3	
Camaraca Fm. lavas*	18.6	70.3	Jm	71	10			6
Cuya dike swarm (CY01-26)	19.2	70.2	J	74.1	49.1			7.8

For legends, see Table 3-2.

*Palmer et al. (1980a)

movements but to the hairpin motion of the South American paleomagnetic pole from the observation that the distribution of the VGPs contained in individual Jurassic paleomagnetic poles are not circular but are elongated toward the longitude of about 30°E. However, paleomagnetic pole of the Arica region from the Middle Jurassic to the Cretaceous (next section) all deviate in a similar sense and the original interpretation of Palmer et al. (1980a) of tectonic rotation appears more plausible.

c)Cretaceous sedimentary and volcanic rocks in the northern Chile

1) Geology

Jurassic Arica Group is overlain unconformably by Neocomian Vilacollo Group, which consists of two supposedly synchronous formations: Atajaña Formation and Sausine Formation (Salas et al., 1966). The former formation crops out at the Cordillera de la Costa (Coastal Cordillera) and the latter formation is exposed in the deep canyons of the main rivers such as Rio Lluta, Quebrada de Azapa and Rio Camarones at several tens of kilometers upstream from the coast. Both units are composed of andesitic volcanics and continental clastic sediments and are overlain unconformably by Tertiary Azapa and Oxaya Formations.

Atajaña Formation consists of conglomerates, sandstones and andesite lava flows and is first defined by Cecioni and Garcia (1960) for the rocks in Atajaña mountain in the department of Pisagua. In the Coastal Cordillera of Arica department, in the main valleys such as Mal Paso, Ache, and Vitor, lithologically very similar rock sequences overlying Arica Group were found and suggested to correspond to Atajaña Formation by Salas et al. (1966).

Along Quebrada Vitor, some 30km south of the city of Arica, well stratified coase reddish violet sandstones crop out and are considered to correspond to the middle member of Atajaña Formation (Fig.4-1b). 28 hand samples were taken from seven different horizons of very coarse to coarse grained sandstone layer in this exposure (AR24; 61, 51-54, 41-44, 31-35, 21-24, 11-14, 01-04, in ascending order, Fig.4-12). In Quebrada de la Higuera, some 10km

southeast of the city of Arica, a basaltic and andesitic dike swarm was found in the red sandstone and tuff breccia layer of Atajaña Formation (named "Arica dike swarm"; Fig.4-1b). Dikes trend generally east-west which is perpendicular to the general trend of dikes in Cuya dike swarm 50km south of Arica dike swarm. Thicknesses are typically 1-2 m. Six hand samples were taken from each of 19 dikes (AR31-49) along the Panamerican Highway. Country rocks have southward dip of about 15° with strike of N60°E. Six paleomagnetic samples were also taken from red sandstone layer (AR50) at the place far from the adjacent dikes. No thermal effects of dikes are considered to be present for AR50 samples.

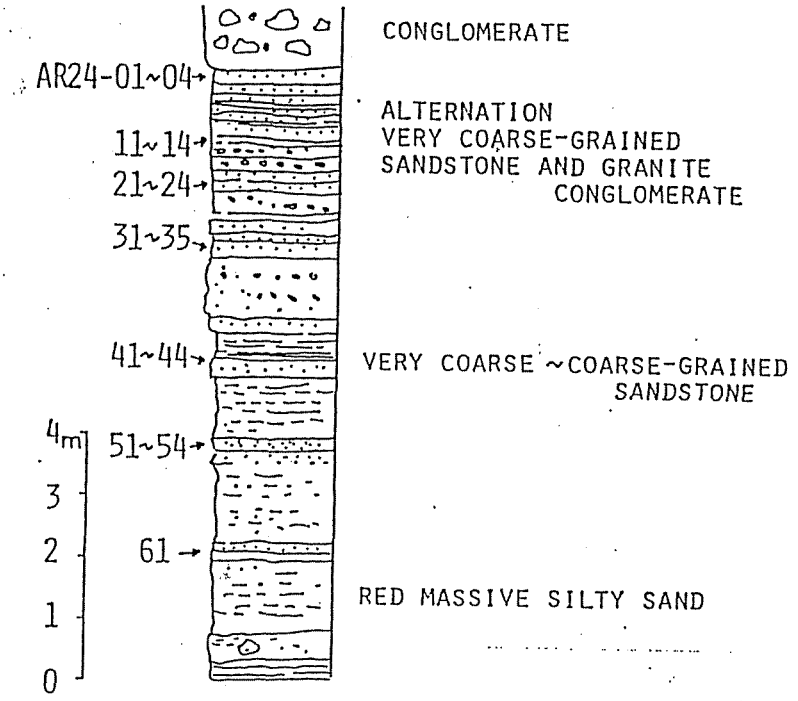

Fig.4-12 Columnar section of the sampling site of the sandstones of Atajaña Formation (AR24). Sample numbers are shown to the left and lithofacies are shown to the right of the column.

2) Experimental procedure and paleomagnetic results

Red sandstone (AR24) Magnetic remanences of AR24 red sandstones were measured using a Schonstedt spinner magnetometer in University of Tokyo. Original NRM intensities are fairly uniform irrespective of their sampling horizons and are typically around 1 x 10^{-5} Am^2/kg. AF demagntization performed up to 200mT reduced only one fourth of the original intensity and was found to be ineffective. Instead of AF, stepwise thermal demagnetizations were performed on all specimens. Blocking temperatures were found to be distributed up to over 650°C suggesting the existence of hematite as the major carrior of the remanences (Fig.4-13). Magnetization directions showed little change after

Fig.4-13 Zijderveld diagram of a specimen of Cretaceous red sandstone (Atajaña Formation, AR24) in stepwise thermal demagnetization.

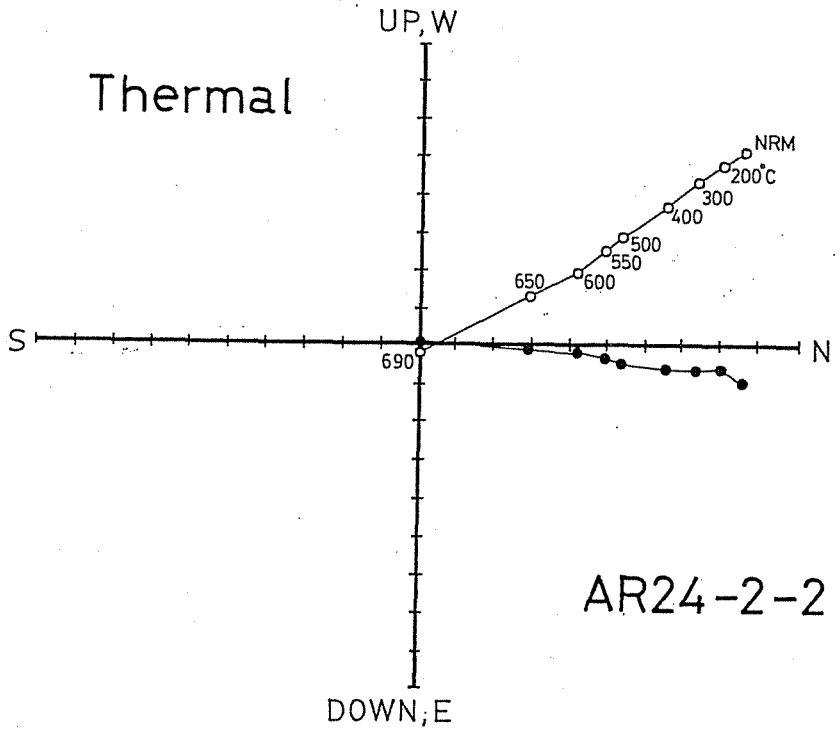

the demagnetization up to 600°C. As paleofield directions, those at 600°C step were taken. Bedding corrections were made on these directions. All specimens showed normal polarity directions with the declination a little counterclockwisely deviated from north. No significant direction/intensity differences were detected among seven horizons. Paleomagnetic results are listed and illustrated in Table 4-3 and Fig.4-14 respectively.

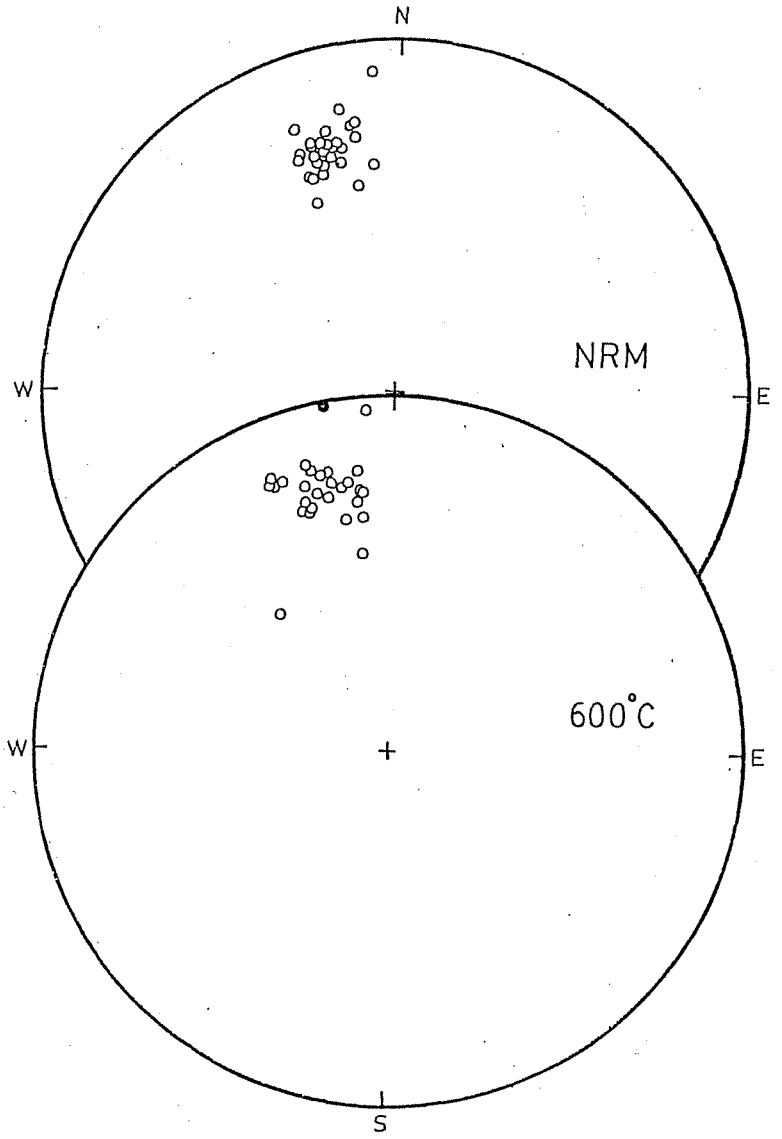

Fig.4-14 Equal-area projection of field directions of the specimens of AR24 at NRM step (above) and after the thermal demagnetization at 600°C.

Dikes (AR31-49) and their country rocks (AR50) Also a spinner magnetometer was used for these rocks. Dikes showed NRM intensities typically of the order of $10^{-5}Am^2/kg$. Each dike specimen was stepwisely demagnetized in AF. MDFs were generally between 10 and 15mT. Several specimens were also thermally demagnetized. Zijderveld diagrams (Fig.4-15a,b) of both kinds of demagnetization demonstrate that NRMs consist of stable single component with minor amount of secondary overprint. Paleofield directions were determined from the gradients of the linear portions of the AF demagnetization diagrams in principle. For several dikes (AR46, 49) which had large secondary magnetization and did not present sufficient length of linear portion, certain optimum demagnetizing steps were selected by minimum dispersion criterion. Blocking temperature distribution (Fig. 4-15b) and Js-T curves (Fig.4-16) derived by Curie balance indicate magnetite as a main carrier of the remanence. No structural corrections were made on field directions because the intrusions are interpreted as post-folding from the plunge of dike contacts. All these directions showed normal polarities and also deviate by 10°-20° from north. Dike mean field directions are illustrated and listed in Fig.4-17 and Table 4-3.

For the host rocks (AR50), AF demagnetization up to 200mT reduced about a half of their original NRM intensities (Fig.4-18a). Direction of remanent magnetization slightly changes its direction after AF demagnetization at 200mT. Stepwise thermal demagnetization was carried out on the specimens after AF demagnetization (Fig.4-18b) and showed that upon further thermal treatment the direction of decreasing remanence remain steady,

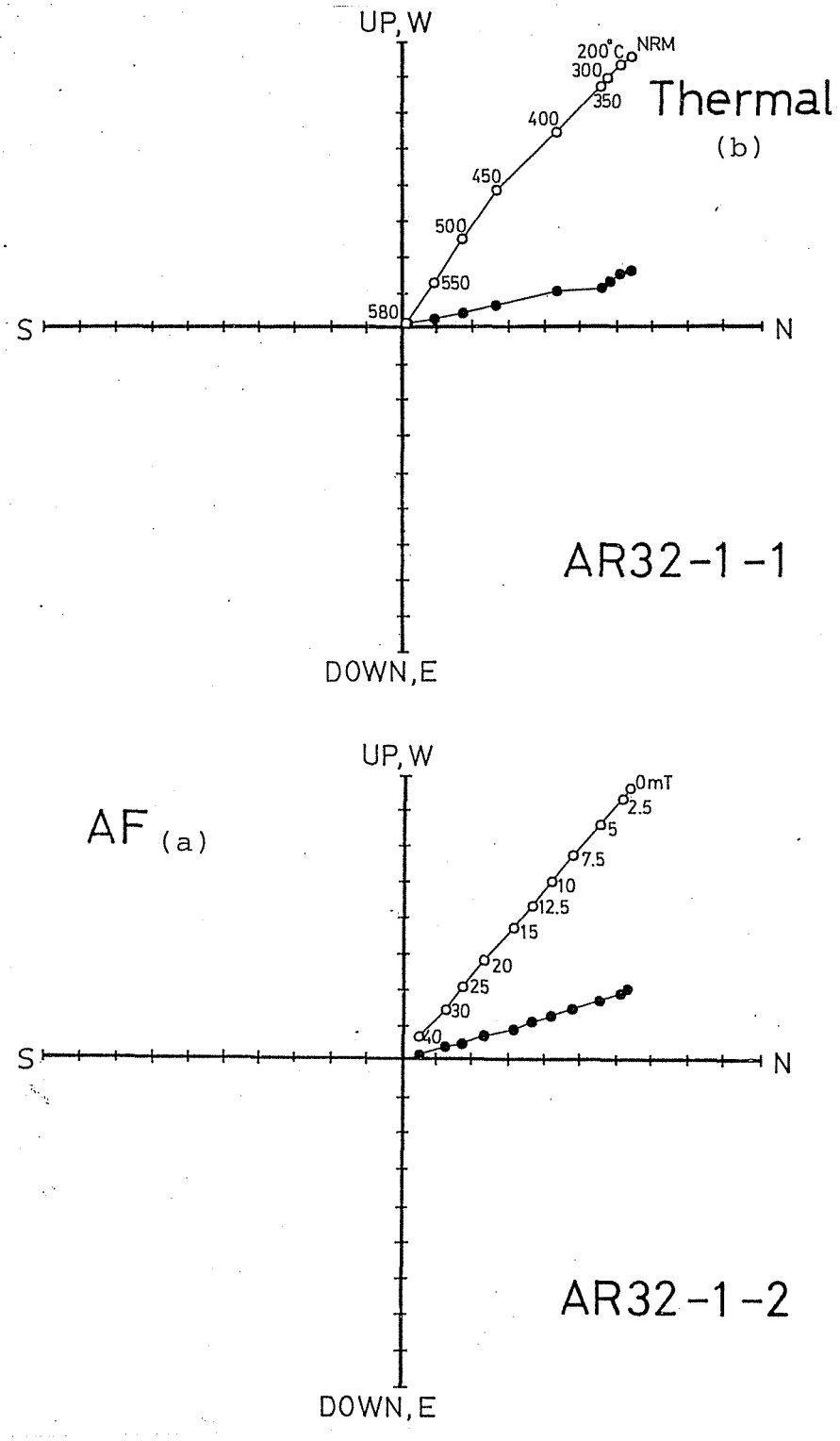

Fig.4-15a,b Zijderveld diagram of the specimens of Arica dike swarm by stepwise AF demagnetization (a) and thermal demagnetization (b).

Fig.4-16 Js-T curves of the samples of Arica dike swarm obtained by an automatic Curie balance.

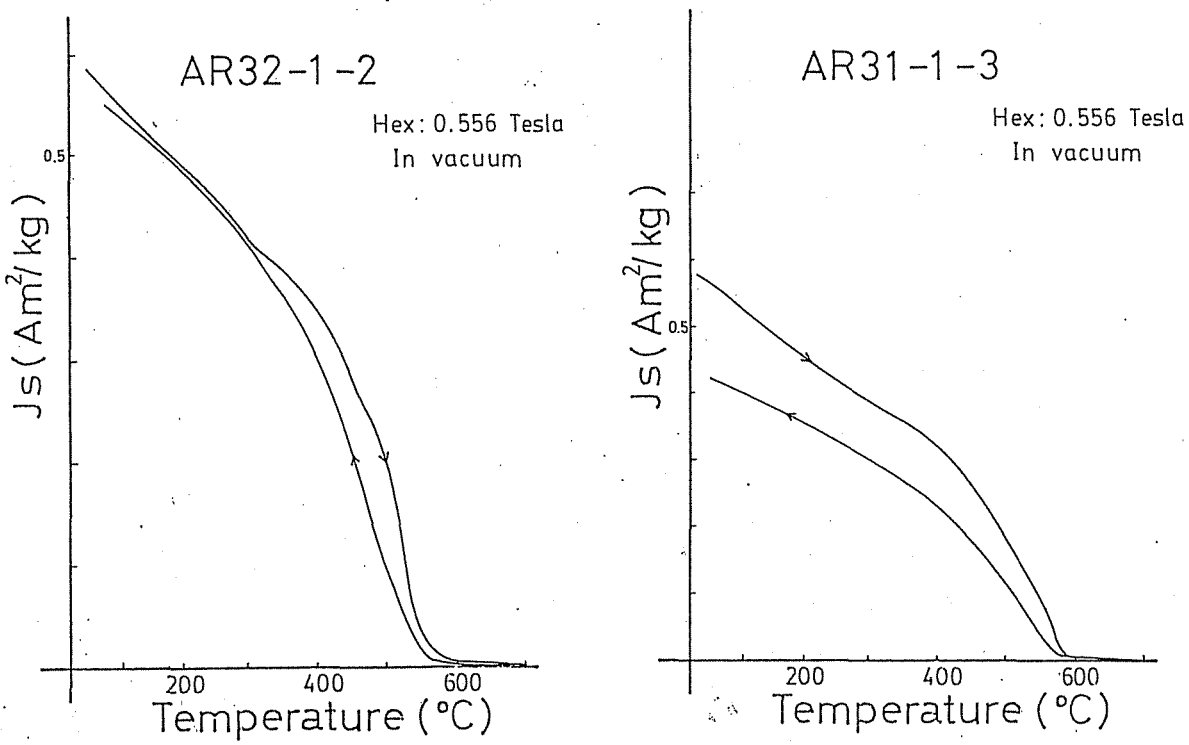

proving only one component was left after AF demagnetization. Slight but significant directional difference (Fig. 4-19) might indicate the time lag of the acquisitions of two magnetization components: component A which was AF demagnetized as far as 200mT and component B which cannot be AF demagnetized under 200mT and only thermally demagnetized. If this idea is true, the two components of magnetization correspond to the depositional remanence carried by magnetic minerals of probably magnetite series (A) and the CRM acquired by the growth of hematitic pigments (B). Field directions of AR50 B-component remanence were compared with that of AR24 red sandstone which was sampled in Quebrada Vitor some 20km south of AR50 and has different bedding plane from AR50. Fold test (Graham, 1949) shows these remanences

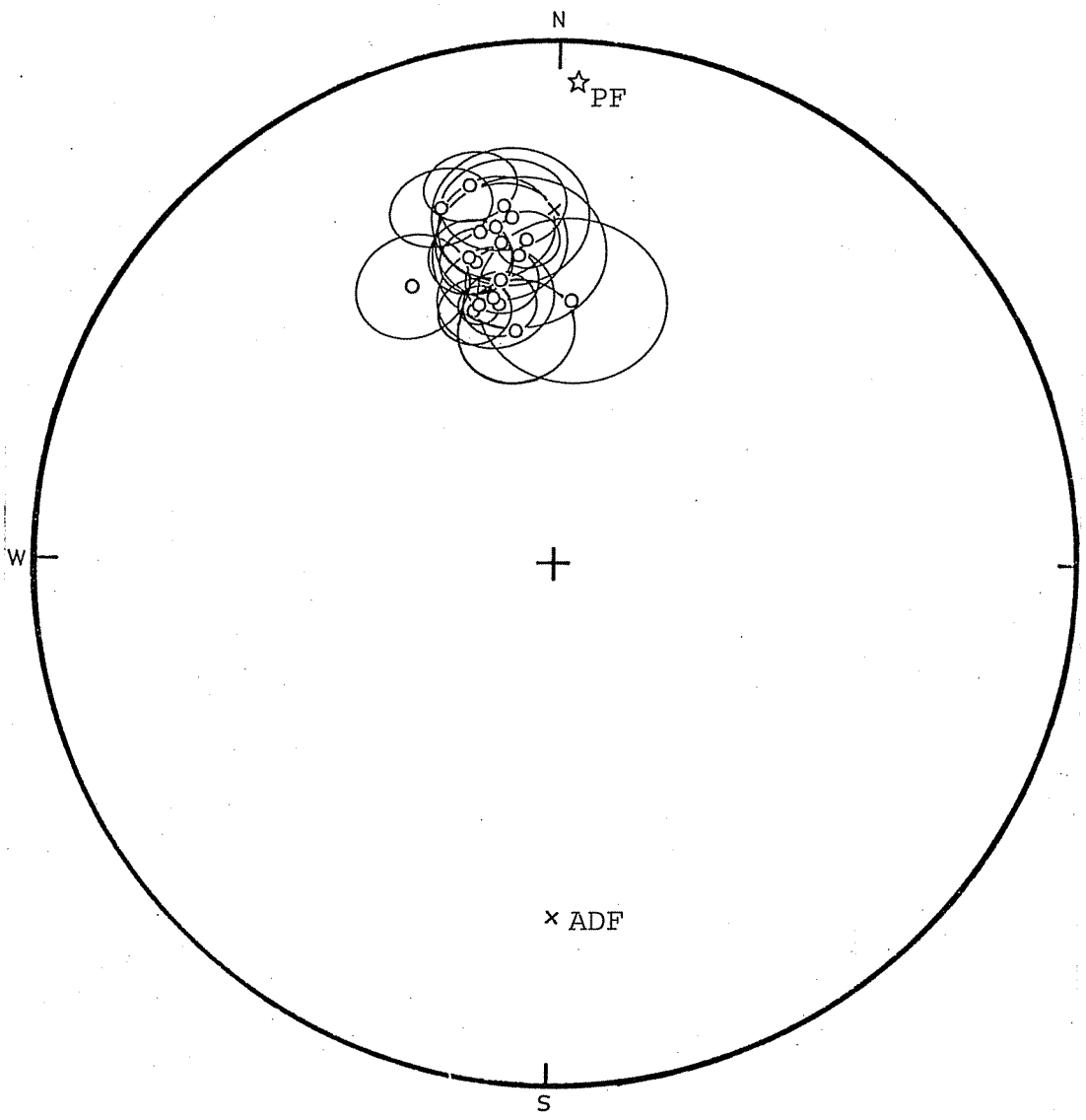

Fig.4-17 Dike-mean field directions and their 95% confidence circles of Arica dike swarm.

are pre-folding (Fig. 4-20) and structural corrections should be made on these directions.

Fig.4-18a,b Zijderveld diagram of AR50 samples by AF demagnetization (a) and of thermal demagnetization (b) performed on the AF-demagnetized samples.

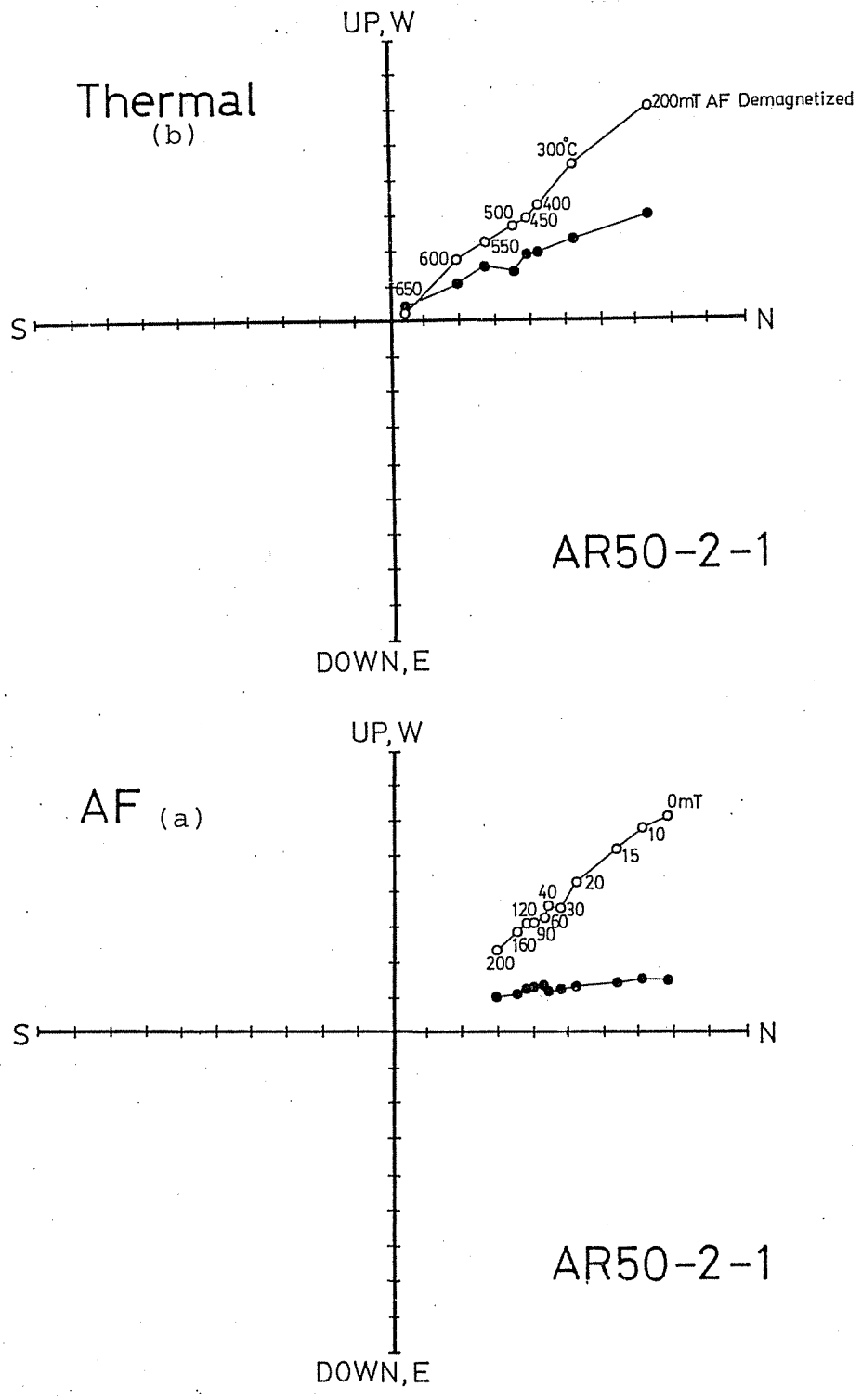

Table 4-3 Paleomagnetic directional data of Cretaceous rocks in the northern Chile

Site	N	Incl. (°)	Decl. (°)	R	k	α_{95} (°)	Step (°C,mT)	Pole Lat. (°N)	Pole Long. (°E)
				(sedimentary rocks)					
AR24									
1-4	4	-27.3	-7.7	3.9859	213	6.3	650	81.5	-132.2
11-14	4	-21.7	-16.4	3.9827	173	7.0	600	72.5	-137.7
21-24	4	-23.2	-11.7	3.9094	33	16.2	600	77.0	-132.0
31-34	4	-25.5	-19.5	3.9775	133	8.0	600	70.6	-147.7
41-44	4	-24.9	-12.8	3.9633	82	10.2	600	76.5	-138.0
51-54	4	-25.5	-13.3	3.8266	17	22.7	600	76.2	-140.2
61-64	4	-30.0	-24.7	3.8876	27	18.1	600	66.3	-158.1
total	28	-25.6	-14.9	27.4089	46	4.1	600	74.7	-142.1
				(volcanic rocks)					
AR31	5	-39.0	-5.3	4.9825	228	5.1	LSF	84.0	164.1
AR32	7	-45.0	-11.6	6.9526	127	5.4	LSF	76.7	160.9
AR33	5	-36.1	-13.8	4.9709	138	6.5	LSF	76.9	191.2
AR34	5	-32.6	-8.8	4.9508	81	8.5	LSF	81.6	-155.8
AR35	6	-41.0	-15.4	5.9646	141	5.7	LSF	74.8	178.2
AR36	3	-48.1	-17.0	2.9986	1388	3.3	LSF	71.3	162.4
AR37	5	-38.7	-10.0	4.9448	73	10.0	LSF	80.1	179.0
AR38	6	-41.0	-28.1	5.9161	60	8.8	LSF	63.4	184.2
AR39	5	-30.4	-18.8	4.9646	113	7.2	LSF	71.9	-156.1
AR40	6	-53.5	-10.2	5.9216	64	8.5	LSF	72.1	138.2
AR41	6	-40.0	-16.1	5.9567	116	6.3	LSF	74.4	181.5
AR42	4	-41.4	-7.1	3.9355	47	13.6	LSF	81.6	160.4
AR43	6	-47.9	-13.6	5.9285	70	8.1	LSF	73.8	157.3
AR44	6	-48.9	-13.2	5.9658	146	5.6	LSF	73.6	154.2
AR45	5	-49.4	3.1	4.8797	33	13.5	LSF	78.0	96.7
AR46	6	-36.1	-10.5	5.9054	53	9.3	10	80.0	189.8
AR47	6	-48.8	-18.2	5.9690	161	5.3	LSF	70.1	162.4
AR48	6	-28.0	-13.4	5.9532	107	6.5	LSF	76.6	-146.2
AR49	5	-34.9	-7.7	4.9180	49	11.1	12.5	82.7	193.5
AR50	6	-30.9	-10.1	5.9811	265	4.1	LSF	80.2	-150.5
AR50	6	-27.9	-23.3	5.9873	395	3.4	200	67.4	-154.2

For legends, see Table 3-1

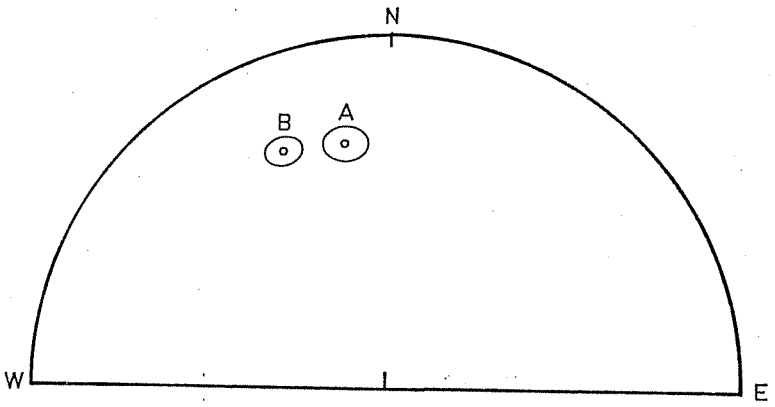

Fig.4-19 Mean field directions of AR50 components A and B (see text) and their 95% confidence circles.

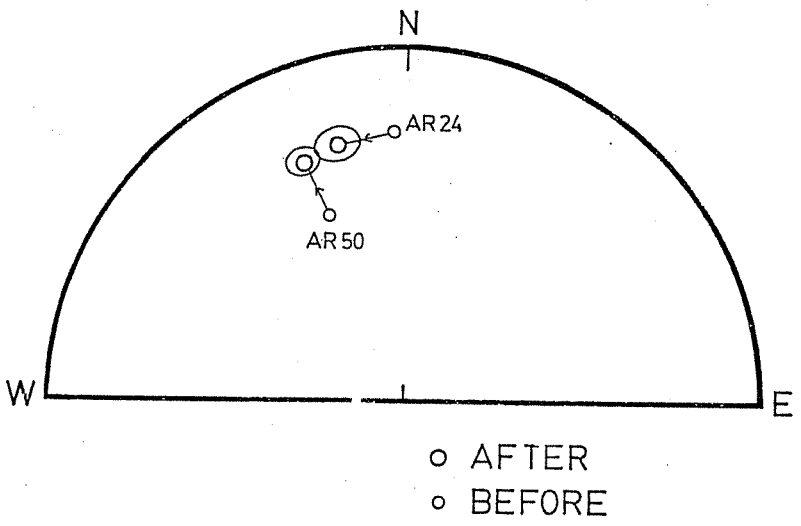

Fig.4-20 Field directions of the red sandstones of Atajaña Formation (AR24&AR50) before and after the bedding correction. 95% confidence circles are shown for the directions after the correction.

3) Discussion

Paleofield directions of 28 specimens in AR24 were averaged and the pole corresponding to this mean direction was calculated. This pole is very similar to the Jurassic poles of this region summarized in Table 4-2.

VGPs from 19 dikes yielded an ASD value of 7.2° with 95% confidence interval of 5.9° and 9.4°. This is considerably smaller than the value expected from Late Cenozoic ASD global trend (McElhinny and Merrill, 1975). Since there are no

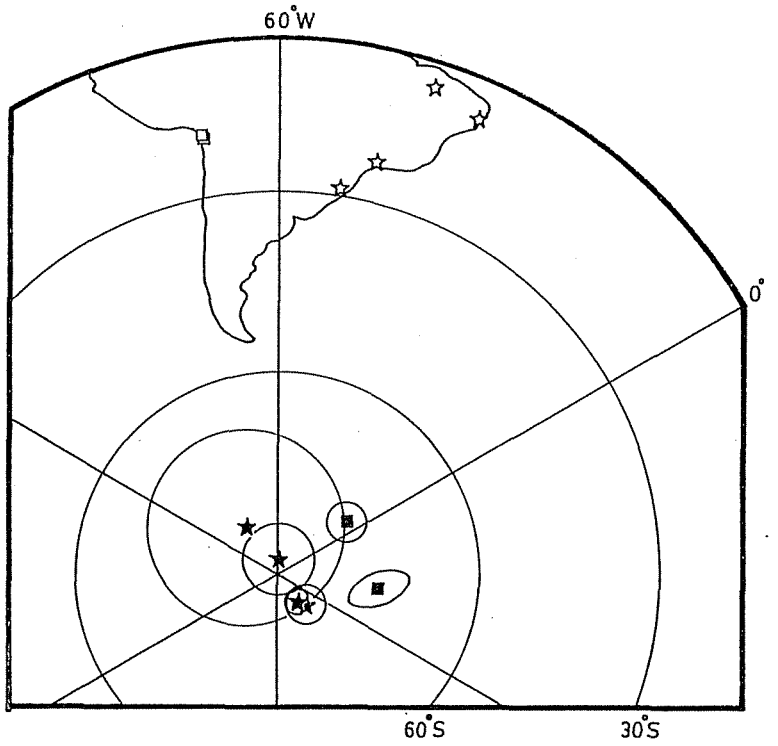

Fig.4-21
Paleomagnetic poles of Cretaceous rock formations in the northernmost Chile (squares) and the stable platform (stars) and their 95% confidence circles/ovals. Corresponding sampling localities are shown as small open symbols in the map.

Table 4-4 Cretaceous poles in the northern Chile.

Rock unit	Locality Lat. (°S)	Locality Long. (°W)	Age	Pole Lat. (°S)	Pole Long. (°E)	dp (°)	dm (°)	A_{95} (°)
Atajaña Formation (AR24)	18.6	70.3	Kl	74.7	37.9	2.4	4.4	
Arica dike swarm (AR31-49)	18.6	70.3	K	77.2	352.4			3.3

For legends, see Table 3-2.

sufficient ASD data of such older ages, only tentative speculations can be made. One possibility is that paleosecular variation in this time is considerably smaller than in Late

Cenozoic time (Irving and Pullaiah, 1976) and another is that these dike intrusions occurred in relatively short time length in comparison with the time span sufficient to average the whole spectrum of paleosecular variation. Cretaceous paleomagnetic poles of Arica region reported here are listed in Table 4-4 and are illustrated in Fig.4-21.

Chapter 5. Summary of paleomagnetic studies in the Central Andes

a) Paleomagnetic poles of the Central Andes

Paleomagnetic poles in the Central Andes are listed in Tables 2-2 (poles by other workers), 3-2 (Peru, Cretaceous), 3-4 (Peru, Neogene), 4-2 (Arica region, Jurassic), 4-4 (Arica region, Cretaceous). Here I divide these poles into three latitudinal groups based on their positions relative to the Arica-Santa Cruz deflection. The northern Central Andes (the Peruvian Andes; 5°S-18°S) and the southern Central Andes (the Chilean and Argentine Andes; 20°S-47°S) correspond to the northern and southern wings of the deflection respectively and are treated as two different groups. The Arica region, or the northernmost Chilean Andes (18°S-20°S) occupies the very point of Arica-Santa Cruz deflection and is discussed separately from other two groups.

Cenozoic rock units, viz., Ocros dike swarm (probably Late Miocene) and Salla Group (early Eocene) by Hayashida et al. (1983) is rather special in that it is considerably younger than other rock units and so are discussed separately. The poles range in their ages from the Jurassic to the Cretaceous but these can be compared together since there are no serious differences in the positions of the reference poles in this period (Table 2-1). These Mesozoic poles are plotted in Fig. 5-1, where circles, squares and triangles denote northern group, central group and southern group poles respectively. It is noted that there are significant differences among these three groups while they are nearly consistent within each group.

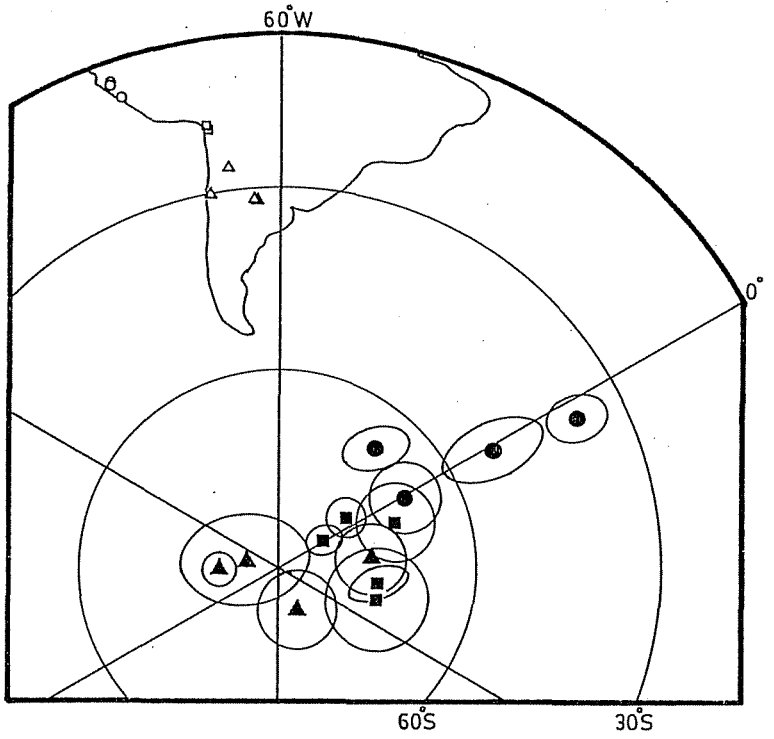

Fig.5-1 Mesozoic paleomagnetic poles of the Central Andes. Circles, squares and triangles denote poles of the Peruvian Andes, the northernmost Chile and the Chilean/Argentine Andes respectively. 95% confidence circles-/ovals are also illustrated. Corresponding sampling localities are shown as small open symbols in the map.

Rotations (R) and flattenings (F) (for definitions, see chapter 2-c and Fig. 2-4) are calculated and listed with their 95% confidence intervals in Table 5-1. They are also plotted in Fig. 5-2 taking R and F as abscissa and ordinate, respectively. Although individual values are a little divergent, no systematic tendencies are found in F suggesting that the deviation of Peruvian and Arica region poles with respect to the references can be solely attributed to the counterclockwise rotations. The amounts of the rotation are 20°-50° for the Peruvian Andes and about 10°-25° for the northernmost Chile.

Rotations are illustrated as angles from the south on the map of the Central Andes in Fig. 5-3. In this figure, it is noticed that the rotated declinations in the Peruvian Andes are

quite coincident with the trend of the coastline, in other words, Peruvian coastline is parallel to the Mesozoic north-south axis. This is quite important to argue the origin of observed counterclockwise rotations as discussed in the next section.

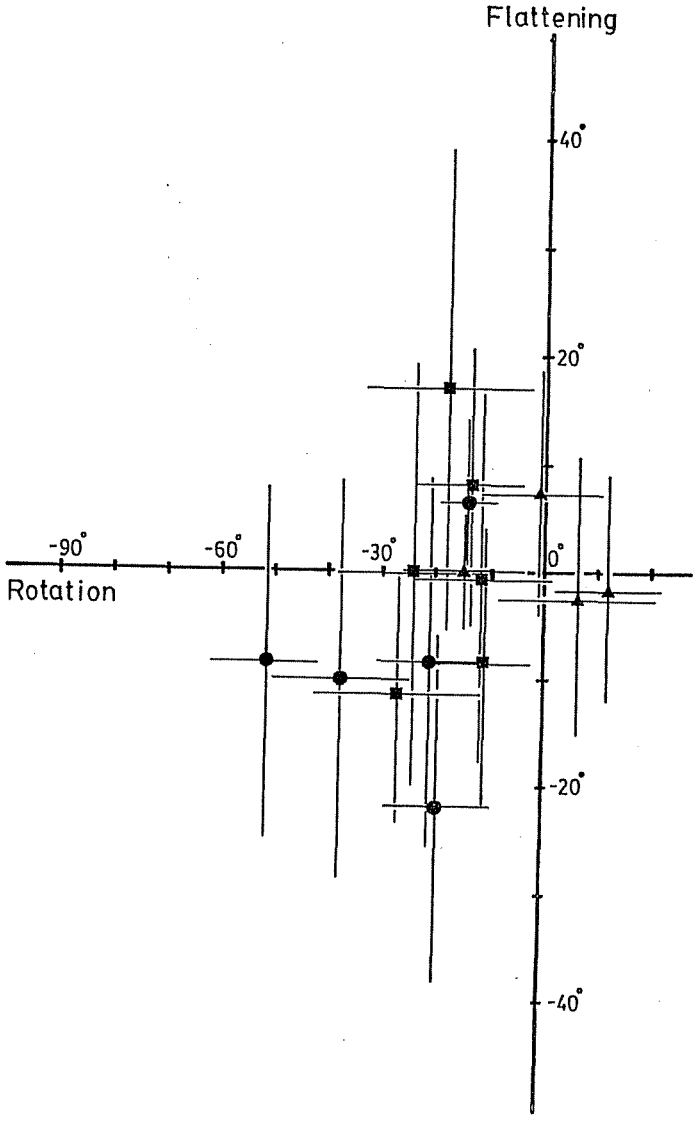

Fig.5-2 Rotation and flattening and their 95% confidence intervals observed in the Central Andes (Table 5-1). Circles, squares and triangles indicate the Peruvian Andes, the southernmost Chile and the Chilean/Argentine Andes respectively.

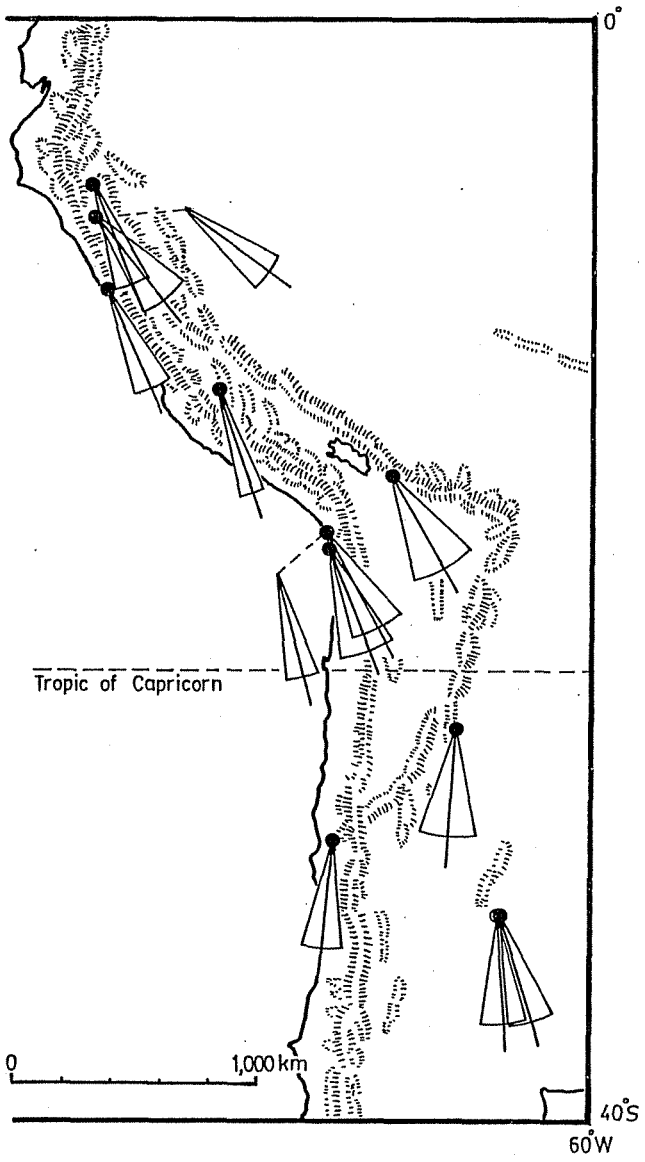

Fig.5-3 Rotations and their 95% confidence limits illustrated as the angles from the south. Rotations for Atajaña Fm. sandstones (AR24) and Camaraca Fm. shales (AR01) are not illustrated in this figure. Red:Jurassic, green: Cretaceous, brown:Tertiary.

From Mesozoic paleomagnetic poles, it may be concluded as follows; 1) the Peruvian Andes underwent over post-Cretaceous counterclockwise rotation of more than 20°, 2) in the northernmost Chile, counterclockwise rotations are a little smaller and is 20° or less, 3) in the southern Central Andes, no systematic rotations seem present, 4) systematic flattenings are not observed in the Central Andes suggesting the absence of substantial latitudinal movements.

Early Eocene Salla Group (Hayashida et al., 1983) shows similar rotation with Mesozoic rock units suggesting that the occurrence of counterclockwise rotation postdates the early Eocene Salla Group. On the other hand, Neogene Ocros dike swarm pole shows only 14.2° counterclockwise rotation (chapter 3-b). This makesus envisage that the counterclockwise rotation of the Peruvian Andes is rather recent and the Ocros dike swarm possibly recorded intermediate point of the rotation of the Peruvian Andes.

b) Origin of the counterclockwise rotation in the Central Andes.

There are several mechanisms other than oroclinal bending to produce systematic rotations in a certain region. Here I argue which mechanism best explains systematic counterclockwise rotations observed by paleomagnetic studies in the Peruvian Andes and the northernmost Chile. Local scale rotations are explained by the mechanisms listed in MacDonald (1980) such as differential folding, fault block or plastic drag in strike-slip faults, and others. MacDonald (1980) also suggested the existence of mechanism giving rise to spurious rotations such as tilting about non-horizontal axes. The diversity of the observed rotation values might possibly be explained either by some small local rotations or by the noise caused by spurious rotations. Nevertheless, large-area systematic rotation found in the whole Peruvian Andes would need much greater scale rotation mechanisms. Such a rotation can be explained by the following two different mechanisms: A) large scale coherent rotation (oroclinal bending of an

orogenic belt), B) individual rotation of small terranes composing the concerned region. Typical example of mechanism B is in the western edge of North America. As mentioned in chapter 1, buoyant unsubductable mass such as oceanic plateaus and aseismic ridges which were carried on subducting oceanic plate reached at the North American continent and are considered to be "plastered" to the western margin of the continent. Presently available geological and paleontological informations suggest the discontinuity between the individual terranes and the allochthonous origin of these terranes. Clockwise rotations are thought to have occurred at the times of or soon after the accretion due to the right-lateral shear rising from the oblique subduction of Kula plate. It may also have occurred relatively recently due to right-lateral transform faulting as represented by today's San Andreas Fault in California (Jones et al., 1982).

Mechanisms A and B can be distinguished paleomagnetically by the uniformity of the rotation and/or flattening within a region. In the case of North America, since the rocks of these terranes were originally formed at ocean closer to the equator or even in southern hemisphere (Alvarez et al., 1980), flattenings as well as rotations are commonly detected (Beck, 1980). Such F and R have notable characteristics that their senses (e.g., whether R is counterclockwise or clockwise) are quite uniform but the amounts are fairly divergent (Beck, 1980). On the other hand, in case of mechanism A, since the concerned region is thought to rotate coherently as a rigid block, it is expected that R is almost uniform within the block and F is, if any, not

so large.

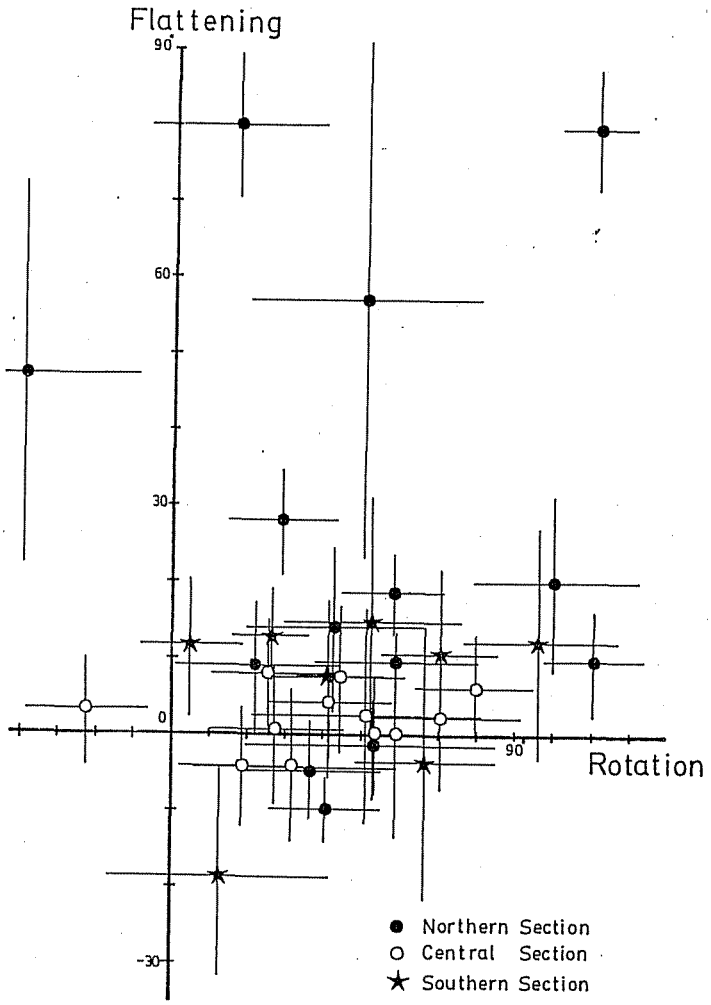

Fig.5-4 Rotation and flattening and their 95% confidence intervals observed in the western edge of North America from Alaska (northern section) to California (southern section) after Beck (1980).

In Fig. 5-4, R and F of North American exotic terranes are plotted on the orthogonal plane in a similar manner as Fig. 5-2. Comparison of Fig. 5-2 and Fig. 5-4 clearly indicates that in North America, not only R but also F are common and both are quite divergent while in the Central Andes, only R is significant and is less divergent. It is also noticed that the rotations have no correlation with the strike of orogenic belt in North America while rotations are closely correlated with structural trend of

the Andes in South America as is evidently observed in Fig. 5-3. This can be statistically tested by the comparison of the dispersion of the poles before and after the Central Andes are unbent so as to make the strike due north-south (Fig.5-5a). Structural trends were obtained from the map of the Central Andes by Mercator projection in Hayes (1974). In Fig. 5-5b, poles before and after unbending of the Central Andes are illustrated. The difference of the angular standard deviations of these two pole groups (17.1° and 11.8°) is significant at 95% confidence level by F-test after Watson (1956).

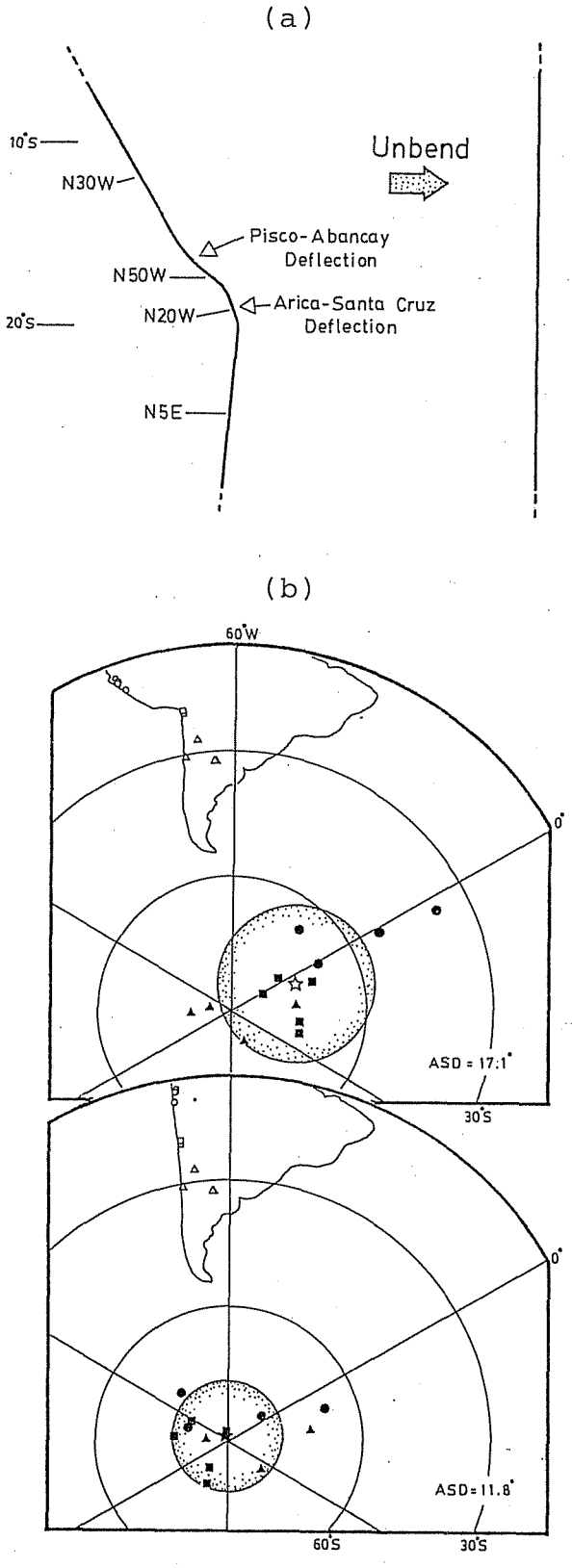

Fig.5-5a,b The Andean structural trend read from the map of the Andes (a) and its unbending. The poles before and after the unbending (b) are illustrated with their ASDs.

Table 5-1 Rotation and flattening derived from paleomagnetic poles of the Central Andes

Rock unit (Ref)	Age	(I_o, D_o)* (°)	(I_x, D_x)* (°)	R (°)	F (°)
		--Peruvian Andes--			
Coastal volcanics	K	(26.7, 157.9)	(18.1, 178.9)	-21.0±9.8	-8.6±17.3
Chulec Fm.	K	(22.6, 141.7)	(12.6, 178.9)	-37.2±13.7	-10.0±18.5
Paria -tambo Fm.	K	(21.1, 127.5)	(12.6, 178.9)	-51.4±10.0	-8.5±16.3
Yumagual Fm.	K	(32.2, 159.4)	(10.3, 178.9)	-19.5±10.0	-21.9±16.4
Ocros dike swarm	Tm-p	(31.8, 165.8)	(25.5, 180.0)	-14.2±5.5	-6.3±8.4
		--Northernmost Chile (partly Bolivia)--			
Camaraca Fm. shale	J	(37.6, 172.1)	(37.1, 183.9)	-11.8±13.3	-0.5±17.5
Camaraca Fm. lava(1)	J	(37.1, 159.9)	(37.1, 183.9)	-24.0±14.2	0.0±19.4
Cuya dike swarm	J	(21.1, 165.9)	(37.9, 183.9)	-18.0±15.1	16.8±22.2
Atajaña Fm. redbed	K	(25.6, 165.1)	(33.5, 178.7)	-13.6±9.5	7.9±13.0
Arica dike swarm	K	(41.7, 167.6)	(33.2, 178.7)	-11.1±9.0	-8.5±13.2
Salla G. (2)	Te	(42.9, 152.8)	(31.4, 180.0)	-27.2±16.5	-11.5±12.1
		--Chilean and Argentine Andes--			
Pirgua Subgroup(3)	K	(45.7, 185.4)	(43.4, 178.6)	6.8±14.4	-2.3±13.0
Central Chile(4)	K	(50.2, 190.4)	(48.4, 178.6)	11.8±10.5	-1.8±10.5
Vulcanitas Cerro Rumipalla Fm. (5)	K	(43.8, 177.2)	(51.1, 178.5)	-1.3±11.4	7.3±11.6
Vulcanitas Cerro Colorado Fm. and Almafuerte lava flows(6,7,8)	K	(51.1, 163.5)	(51.1, 178.5)	-15.0±11.4	0.0±10.6

References, 1;Palmer et al. (1980a), 2;Hayashida et al. (1983), 3;Valencio et al.(1977), 4;Palmer et al. (1980b), 5;Vilas (1976), 6;Valencio (1972), 7;Mendia (1978), 8;Vilas (1976)

(to be continued)

(continued)

I_o:observed inclination, D_o:observed declination, I_x:expected inclination, D_x:expected declination, R:rotation and its 95% confidence interval, F:flattening and its 95% confidence interval. For the calculation, see Chapter 2-c.

*All directions are expressed as reversed polarity directions irrespective of their actual polarities.

I infer that the large scale counterclockwise rotation of the Peruvian Andes is a consequence of a rotation as a coherent rigid body judging from following two facts: 1) deviations of Mesozoic poles in Peru and the northernmost Chile from the reference are expressed only in terms of uniform counterclockwise rotation of the region, 2) rotation angle is significantly correlated with the Andean structural trend in Peru and Chile. Also there are no positive suggestions from geology and paleontology of the discontinuity in the presently studied region except the Arequipa Massif, at the coast of southern Peru, which is suggested to be allochthonous by several investigators (e.g., Nur and Ben-Avraham, 1978). Arica-Santa Cruz deflection is therefore interpreted as the later feature occurred as a consequence of the oroclinal bending of the Central Andes around some hinge in Arica region. I resurrect the orocline hypothesis by Carey (1955) and hereafter call it as "Bolivian orocline".

Chapter 6. Bolivian orocline and its geodynamic implications

a) Introduction - timing of the oroclinal bending

Present Mesozoic paleomagnetic data only demonstrate that the occurrence of the Bolivian orocline is post-Cretaceous and the scarcity of the data for the younger age makes it still ambiguous when it occurred. Precise determination of the time of the bending needs much more paleomagnetic data covering the whole Tertiary period. Also it is quite problematical whether the actual bending was a steady and continuous process or episodic events as represented by several discrete "pulses" just like the Andean orogenic cycles described in this section.

The only available clue to infer the timing of the bending would be the rotation angle of Ocros dike swarm (chapter 3-b), which is probably of Late Miocene age (6-8Ma) and presents about a half (-14°) of the Cretaceous rotation angle. This implies that there should be 14° counterclockwise rotation at least during the last 6-8Ma and that the minimum rotation rate with an assumption of constant rotation in this period is 2°-2.5° per million years. When we fix the Peru-Chile border as a hinge and rotate the whole Peruvian Andes (5°S-18°S) at the rate of 2°-2.5°/Ma, the velocity of the northernmost of this block exceeds 10cm/yr and is comparable with the absolute velocities of the most rapidly moving plates which are currently known (Minster et al., 1974). If we take larger velocity to be unlikely, it is inferred that this 14° counterclockwise rotation should have occurred steadily by using the most part of the last 6-8Ma, that

is to say, it lasted until quite recent times or even until present time. The timing of the earlier half of the orocline is less definitely known at present. However, if we assume continuous oroclinal bending as a single event and simply extrapolate this rate over older times, the last 12-15Ma (after Middle Miocene) is considered to be plausible as the time of the rotation. Now, I discuss this time in comparison with times of the Andean orogenic cycles (reviewed from Bellido (1979)).

The post-Hercynian Andean orogeny in Peru is composed of three major compressive pulses: Peruvian orogeny, Incaic orogeny and Quechuan orogeny in ascending order (Steinmann, 1929). The first Peruvian pulse occurred between Late Cretaceous and Eocene and made open foldings in the western Peruvian trough (Wilson, 1963). This pulse is synchronous with the uplift of the Peruvian trough from the ocean. Following erosion process deposited great amount of clastic sediments and formed extensive red beds. This pulse was followed by the volcanic activities which made volcanic formations such as Toquepara, Sacsaquero and Calipuy Volcanics. After these effusive volcanisms, the second Incaic stage started in Late Eocene and lasted until Oligocene time (Noble et al., 1979). This phase was much stronger than the previous stage of Peruvian orogenic phase and brought a lot of overturned foldings and overthrusts throughout the Central Andes. The majority of the Andean batholiths were emplaced after this stage. This orogenic stage was followed by vigorous andesitic volcanisms forming Tacaza, Castrovirreyna and Casapalca Groups.

In the last Quechuan orogeny, foldings and normal faults

were also formed. The age of the Quechuan stage is the most ambiguous and is tentatively considered to be Middle to Late Miocene (Bellido, 1979). Farrar and Noble (1976) bracketed the onset of the deformation between 21Ma and 14Ma ago and suggested the age of the termination to be about 10Ma ago. The period after this stage is considered to be rather calm. Continuous erosion over a long time made the so-called Puna surface which was originally at the elevation of 2,000m-2,500m (Bellido, 1979). Afterwards, this surface was uplifted up to the present altitude of 4,200m-4,500m and occupies the considerable part of the present Altiplano. The timing of this huge vertical uplift is investigated by many workers (Hollingworth, 1964; Rutland et al.,

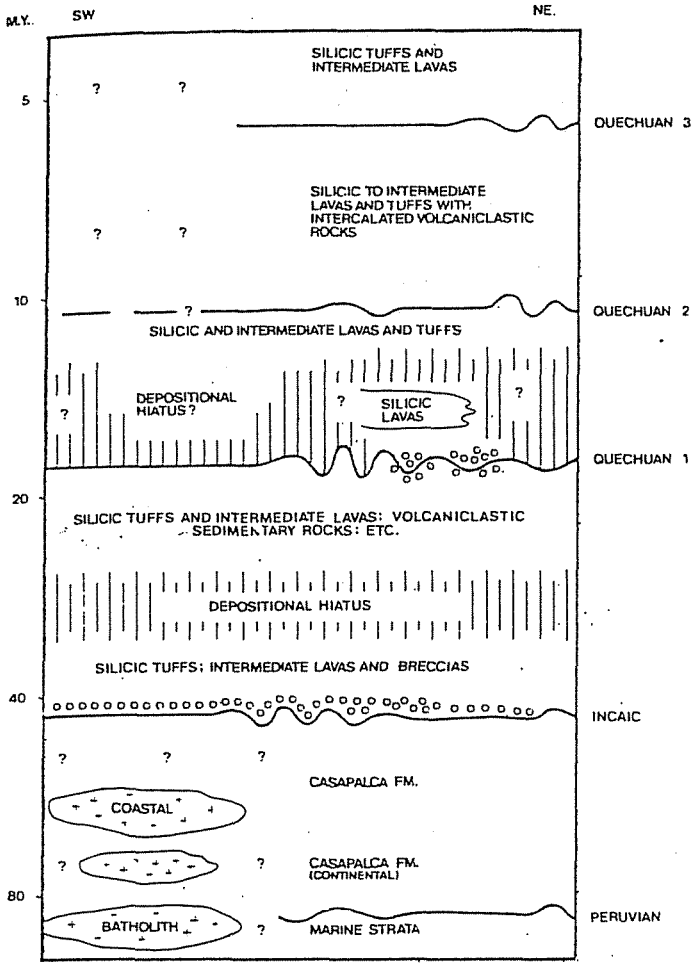

Fig.6-1 Major lithostratigraphic sequences and tectonic pulses in the late Mesozoic and Cenozoic of south-central Peru after McKee and Noble (1982). Relative intensity of compressive deformation is indicated diagrammatically by the form of the heavy horizontal lines. Post-tectonic and syntectonic conglomerate wedges are shown by open circles.

1965) and they consider that this uplift began in the Peistocene (or Pliocene) and is continuing until now.

These events are summarized in Fig. 6-1. At least the latter half and possibly the entire period of the formation of Bolivian orocline appears to be synchronous with the Quechuan orogeny and the last vertical uplift. This is compatible with the observation of fold axis in the Peruvian Andes which are nearly parallel to the trench axis and oblique to the present direction of convergence. If the orocline predated major folding events, fold axis would not be parallel to the trench axis but form en-echelon pattern to some extent as described in Japan by Kaizuka (1973).

b) Constraints for the deformation of South American continent

Once a huge mountain chain such as the Andes is oroclinally bent, it should give rise to a great amount of distortion in the surrounding area (that is, the plate to which the mountain chain belongs). As for the bending of island arcs such as Japanese Islands (Kawai et al., 1961) and Mariana Islands (Larson et al., 1975), their back-arc regions consist of oceanic plates and the distortion can be easily compensated by the production and/or the consumption of the oceanic plates. The production corresponds to the crustal accretion in the mid-oceanic ridge and the consumption is executed as the subduction of an oceanic plate at a trench. For example, the distortion caused by the bending of Japanese Islands is considered to have been compensated by the formation of Japan Sea as the opening of a back-arc basin and the

bending of Mariana arc is similarly thought to be compensated by the currently spreading Mariana Trough.

On the contrary, the Central Andes do not have oceanic region behind them at present, nor are there evidences that there used to be the region of oceanic affinity. As a natural consequence, the distortion behind the Central Andes is considered to be absorbed by the continental lithosphere of the South American plate. There is serious differences between an oceanic plate and a continental plate that the former can be created and consumed while the latter cannot be subducted due to its buoyancy and also cannot be created in mid-oceanic ridges. Hence the conpensation of the distortion should have occurred as a plastic deformation of the continental plate. This conflicts with the classical view of plate tectonics that plates are rigid spherical blocks. Of course the developers of plate tectonics is admitting that if the continents were really rigid blocks, there would be no need to study structural geology. For example, Cox (1973) slightly modifies this basic assumption as follows: "most" large-scale deformation occurs in narrow zones between plates that are "nearly" rigid. Here I review the constraints for the deformation of South American continent and discuss "how" rigid South America has been.

There are several constraints which inhibit deformations within a continent. The most important one would be the coherency of the coastline configurations in paleoreconstruction with other continents. The shape of the South American continent between the mouth of the Amazon and Tierra del Fuego fits well with the

western side of Africa as indicated by classical computational fit of Bullard et al.(1965). This implies that at least the coastal zone (Fig. 6-2) should have been intact since the Early Cretaceous break-up of the Western Gondwana. However, this constraint does not extend to the interiors of the continent nor to the western and northern sides of the continent.

The second constraint is from paleomagnetism. The coincidence of contemporaneous paleomagnetic poles within some region may bear a rough evidence that the region is undeformed. However, paleomagnetic data give only paleolatitude and orientation with respect to the meridian, and do not constrain longitudinal movements. This uncertainty is avoided if apparent polar wonder paths of finite length are available in multiple sites. The complete coincidence of apparent polar wonder paths of different places indicates that the relative position of two points have been stationary. In case of South America, paleomagnetic data older than Carboniferous age is too sparse to establish apparent polar wonder path even of the whole South America (see Chapter 2-b) and the data covering widely distributed sampling sites in South America are only post-Permian. Yet paleomagnetic poles after Permian time is almost stationary in the vicinity of the present pole (Chapter 2-b), and we can argue the existence of the deformation using this essentially single pole position. After all, the concordance of paleomagnetic poles of these post-Permian ages proves the inexistence of rotation and latitudinal movements but do not constrain the movements along the present latitude lines. In Fig. 6-2, the area marked as "paleomagnetism" shows the region where post-Permian poles coincide with each

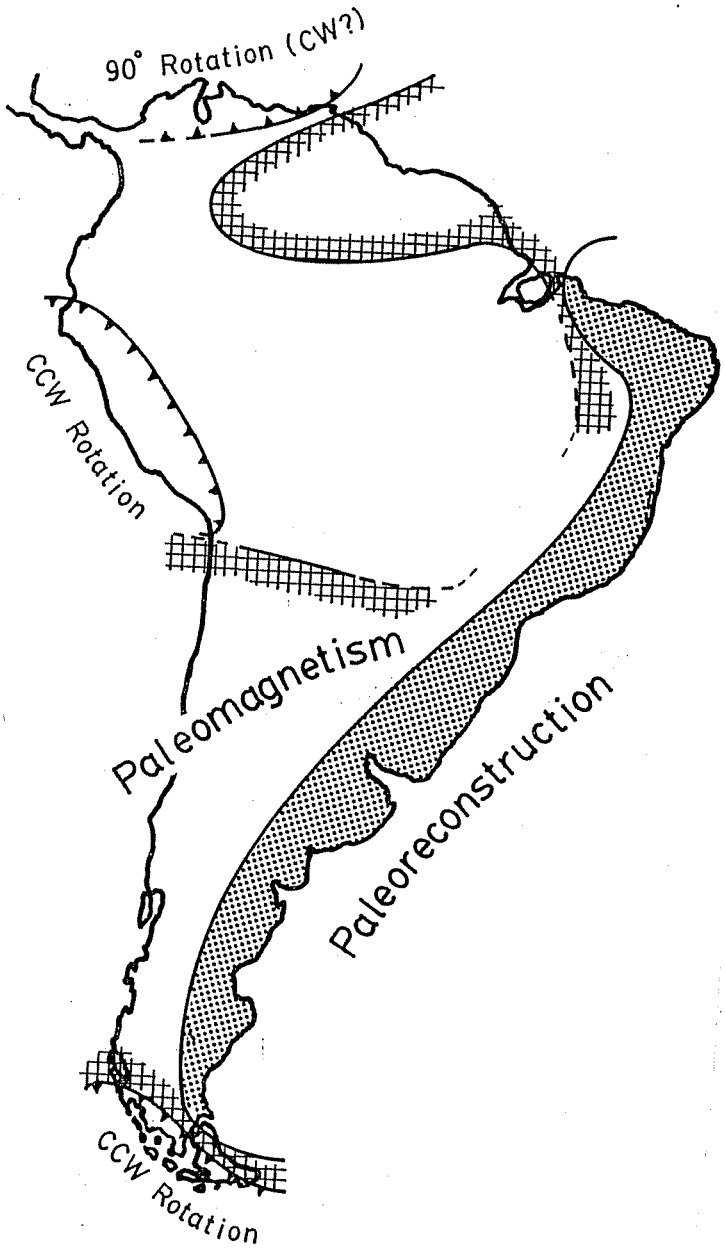

Fig.6-2 Constraints for the deformation of South American continent. See text.

other. This is the region where neither rotations nor latitudinal movements took place after Permian time but it is unknown whether or not this region underwent differential longitudinal movements. It is inferred that Guiana shield and the whole Chilean and Argentine region (except the southernmost Andes) are included in this region.

The region within the Andes where anomalous paleomagnetic poles are known such as Caribbean Andes and Patagonian Andes (see

chapter 2-c) are also indicated with their rotation senses in Fig. 6-2. The Peruvian Andes where counterclockwise rotation was demonstrated in the present work are also indicated in this figure. The region not covered by any items are the region where no or little informations are available. For example, the Amazon basin is entirely unknown about its deformation due to the lack of constraints of paleomagnetism nor paleoreconstruction. There are other important constraints from the evidences of structural geology but, for the time being, I neglect it since geological structures in this continent are not thought to be so well investigated as to give objective conclusions about the large-scale deformations.

c) Possible tectonic consequences of Bolivian orocline

- Orocline tectonics in western South America -

1) South American foreland

As discussed in the previous section, distortion caused by Bolivian orocline should have been absorbed by the deformation in the continental lithosphere of South American plate. Two kinds of constraints for the deformation of the continent were also mentioned. Bearing these constraints in mind, a model of deformation is constructed by considering following two extremes (Fig.6-3): A) the region to the south of Bolivian orocline retreat landward (,or eastward) along the latitude and the Peruvian Andes rotate about the fixed vertical axis at the Peru-Ecuador border, B) Peruvian Andes is pushed out differentially toward the Pacific

ocean with a fixed hinge at the Peru-Chile border. These two mechanisms both satisfy the constraints of deformation but postulate different type of deformations behind the Central Andes, that is, the mechanism A necessitates uniform amount of east-west shortening behind the Chilean and Argentine Andes and the mechanism B needs differential stretching behind the Peruvian Andes. The actual model of the deformation would be explained by the combination of these two different mechanisms and geological and geophysical observation of the foreland should clarify which mechanism was the predominant.

There are regions with structures demonstrating crustal shortening such as low-angle reverse faults behind the whole Central Andes. Allmendinger et al. (1983) investigated the structural geology of the Subandean belt in the northwestern Argentine Andes (about 22°S-28°S) and by restoring listric thrusts and folds they estimated the shortening to be about (or a little more than) 60km (33% of the original palinspastically restored section). On the other hand, the east-west shortening to acount for Bolivian orocline with the mechanism A amounts to nearly 1,000km in this region for which there is no supporting evidence. Consequently, the actual mechanism is considered to be closer to mechanism B rather than A.

Mechanism B attributes the deformation to the differential east-west stretching behind the Peruvian Andes, that is, the westernmost part of Amazon Basin. The amount of the stretching is 1,000km at maximum (northernmost portion) and zero behind the Peru-Chile border (see Fig. 6-3). Continental stretching and

subsequent formation of sedimentary basin is known in several localities such as North Sea (e.g., Leeder, 1983; Sclater and Christie, 1980) and Intra-Carpathian basin (Sclater et al., 1980). The largest Tertiary extension of continental region is presently known in the Basin and Range province in North America (about 100km or as large as 300km; Miyashiro, 1979) and Aegean Sea (200km; McKenzie, 1978a) but these extensions are still smaller than the extension expected in the Amazon Basin by mechanism B orocline. As a consequence of the continental stretching

Fig.6-3 Two mechanisms accounting for the deformation causing Bolivian orocline.

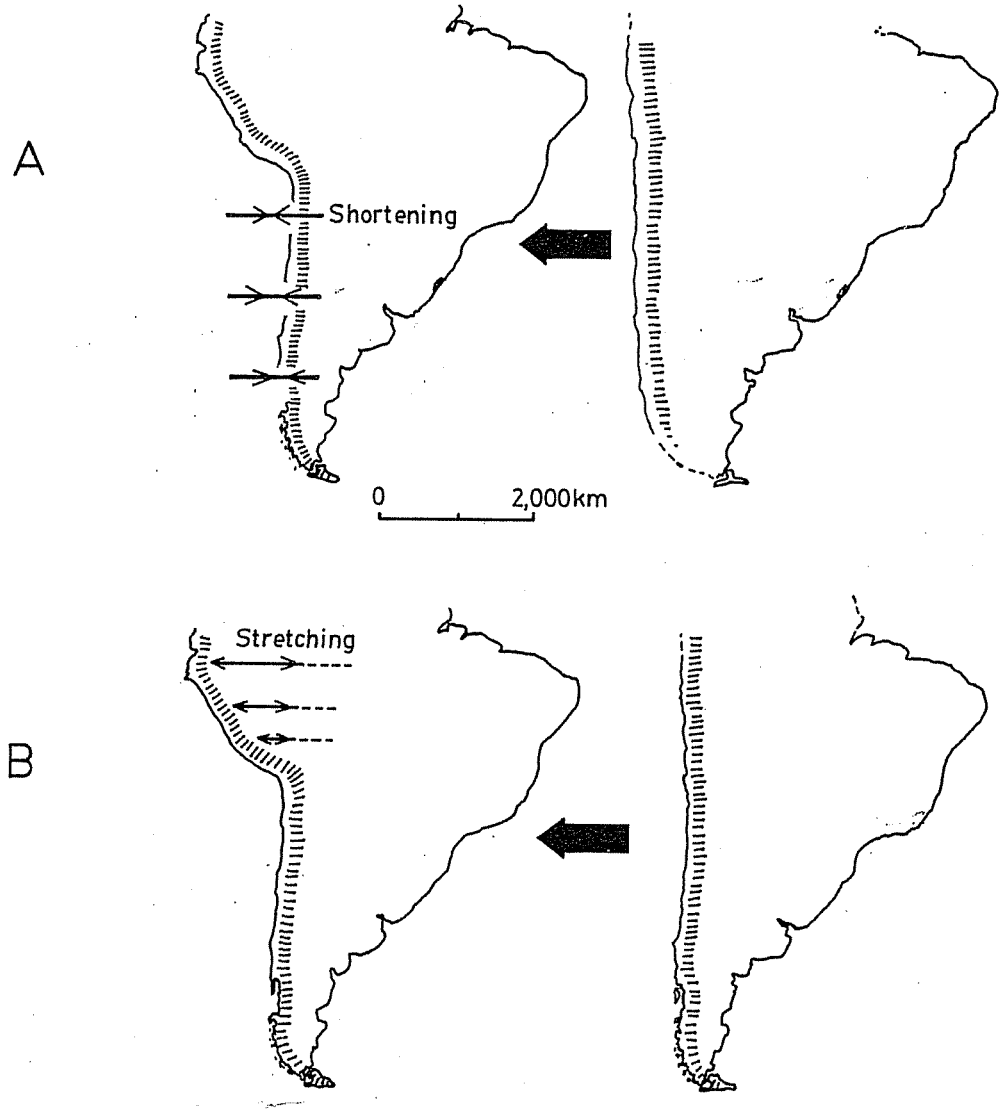

we can expect several surface tectonics such as normal listric faults as a result of crustal thinning. Angelier and Colletta (1983) classified the extensional tectonic features by the ratio of extension. According to them, southern Basin and Range is the typical region of the largest extension (about 200%), where tension fractures are developed and form multiple tilted "packs-of-cards" structure. The ratio of the stretching in the Amazon Basin depends on the assumption of how much part of the basin participated in the stretching and we cannot determine which kind of tectonics should appear in the stretched region behind Peru. These features are, if any, considered to be difficult to observe because of thick Quaternary alluvium and intense vegetation.

The whole lithospheric thinning as well as crustal thinning is expected throughout the stretched region. According to the widely accepted view (McKenzie, 1978b), such continental stretching gives rise to rapid vertical rebound to attain the isostatic equilibrium, high heat flow and very slow thermal subsidence due to the growth of the lithosphere. Among these consequences, high heat flow and isostatic rebound should be observable today. Unfortunately, heat flow is not measured in this region (see Uyeda and Watanabe, 1982). Isostatic rebound can be both positive (subsidence) and negative (uplift) by choosing the initial condition of crustal thickness. This is because the thinning of the crust and the "lid" (mantle portion of the lithosphere) cause vertical isostatic movements in opposite directions, that is, the crustal thinning and lid thinning make the lithosphere subside or uplift respectively. For example, the crust thicker (thinner)

than 18km subsides (is uplifted) after stretching when we assume the uniform stretching of the whole lithosphere of 100km thick (McKenzie, 1978b). Because ordinary continental crust is thicker than 30km, stretched continental lithosphere is considered to subside, which would result in a rapid accumulation of sediments. Geological investigation of Bigarella (1973) which is based mainly on the boreholes for petroleum excavation indicates about 500m thick Tertiary clastic sediments (Alter do Chão Formation) but it is not certain whether this formation is the consequence of the rapid subsidence. Heat flow measurement and the investigation of the upper mantle seismic wave velocity structure will clarify the existence of lithospheric thinning.

2) Subducting oceanic plate

Subduction of an oceanic plate underneath the Andes seems to have been continued at least since early Mesozoic time (James, 1971). Rapid bending of the Central Andes might have influenced the subducting oceanic plate. Detailed seismological studies revealed that currently subducting Nazca plate is divided into five segments in their subduction dip angles, that is, in three portions (5°N-2°S, 16°S-28°S, 33°S-47°S) Nazca plate is subducting at normal dip angles of about 30° and in two portions (2°S-16°S, 28°S-33°S) the plate is subducting at anomalously low angle, say, less than 10° (Isacks and Barazangi, 1977; Barazangi and Isacks, 1979: Fig. 6-4b). There is another notable feature that the portions with steeper dip angles are associated with

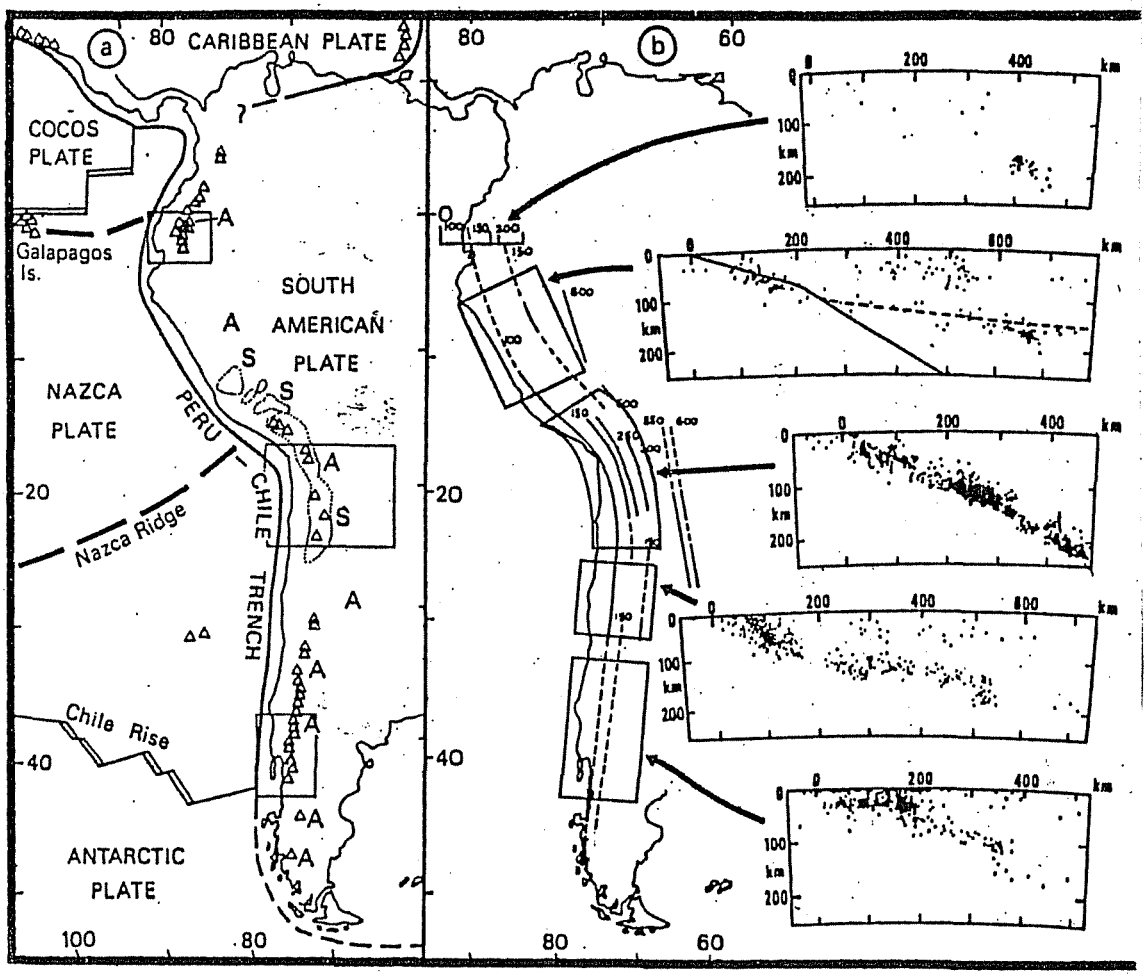

Fig.6-4a,b The distribution of active volcanoes and their relationship to plate tectonics in South America. (a) Active volcanoes (open triangles) in relation to plate tectonics. Solid lines are destructive and thin paired lines are constructive plate boundaries respectively. Thick broken lines are oceanic ridges and/or rises in the Nazca plate. The thin broken line south of 42° is the boundary of the Antarctic and South Amreican plates. The dotted line outlines the ignimbrite province of the Central Andes; S=shoshonitic and A=alkaline volcanic rocks. (b) Seismicity in South America. Profiles showing the distribution of seismicity at different depths and distances from the oceanic trench (0km) are shown for the areas distinguished by Barazangi and Isacks (1976) and the solid line is the Benioff-Wadati zone inferred by James (1978). After Thorpe et al. (1982).

active volcanoes about 200km inland of the trenches while no active/Quaternary volcanoes exist on the other portions (Fig.6-4a). The absence of the intervening asthenosphere between slab and overriding plate is considered to be responsible for such volcanic gaps.

Several models were presented to explain such segmentation of subducting slab. For example, Pilger (1981) proposed the subduction of aseismic ridges having continental crust as a cause of low angle subduction and consequent volcanic gaps. According to him, two aseismic ridges, namely, Nazca ridge and Juan Fernandez ridge have been subducting underneath the northern (Peruvian) and southern (Chilean) volcanic gaps respectively and the buoyancy of these ridges prevents normal angle subduction and formed two flat-lying segments of the subducted Nazca plate. Nur and Ben-Avraham (1981) also consider similar collision of aseismic ridges as a cause of two volcanic gaps. Chinn et al.(1980) suggested from anomalous seismic wave propagation

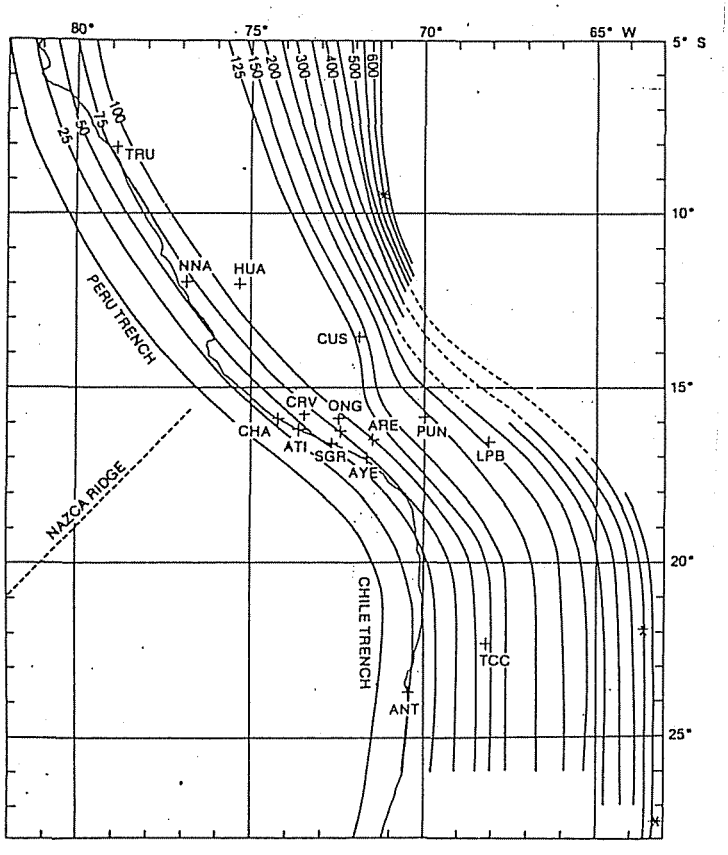

Fig.6-5 Deep-focus earthquake depth contours (unit: kilometers) deduced from seismological studies by Hasegawa and Sacks (1981). Broken lines indicate that the data are ambiguous.

across the transition zone that Nazca plate is "teared" between flat lying slab and the normally subducting slab. Hasegawa and Sacks (1981), however, pointed out from fine structures of Wadati-Benioff zone around the transition zone in southern Peru that the segmentation of the slab is rather gradual and continuous (Fig. 6-5).

Fig.6-6 Cenozoic volcanic activity and tectonic events after Drake (1976) in the Central Andes. Open circles and triangles indicate the intrusive and extrusive volcanic activities. Solid triangles indicate those west of today's Cordillera. Dotted line indicates the last transgressive event and dashed line indicates the time of the last compressive deformation.

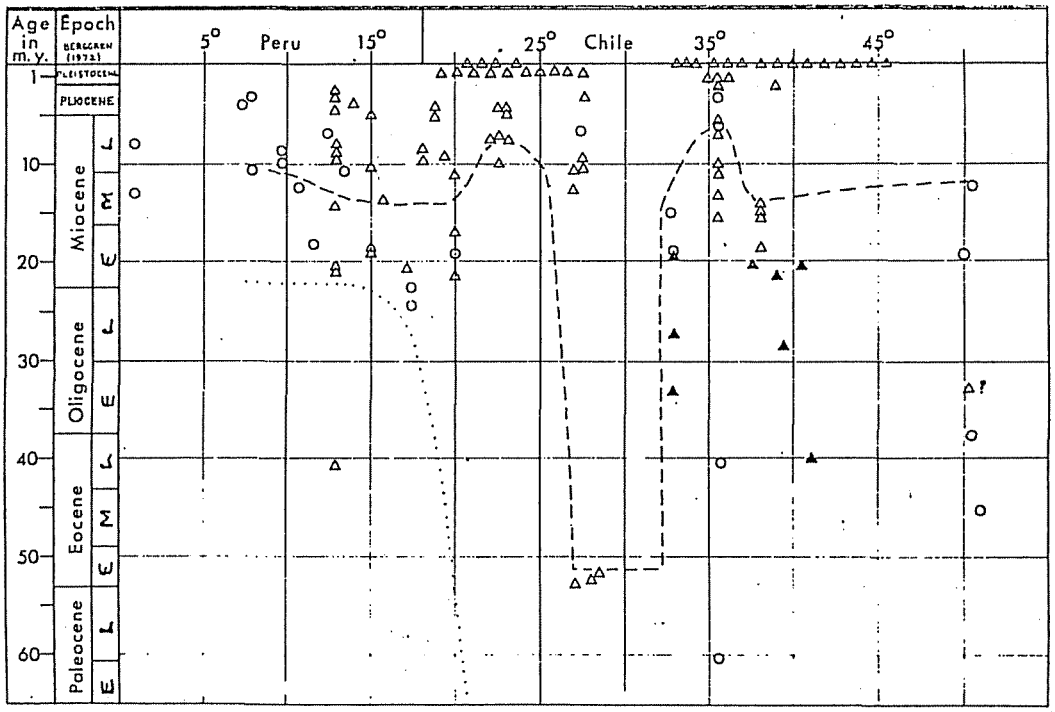

Radiometric age determinations of the Cenozoic volcanics demonstrate that there had been active volcanism in today's Peruvian volcanic gap zone until Late Miocene or even Pliocene (Drake, 1976: Fig. 6-6). This implies that vigorous volcanism disappeared rather abruptly about 5-10Ma ago in this zone. On the other hand, in Chilean volcanic gap (28°S-33°S), no Neogene

volcanisms are known (Fig. 6-6). If the lack of asthenospheric substances is responsible for the present absence of volcanism in the Peruvian volcanic gap, the dip angle of the slab during the Neogene period must have been much greater than it is now (James, 1977), which implies that the slab have undergone considerable upward movement from 30° dip to 10° dip in a very short period, say, the last 5-10Ma.

The subduction geometry is thought to be controlled by several factors such as the age of subducting oceanic plate, convergence rate, the absolute velocity of the overriding plate, the existence of subducting aseismic ridges or seamounts, duration of subduction (age of volcanic arc), and others (Cross and Pilger, 1982). Among these factors, the influence of oroclinal bending will appear in the convergence rate and the absolute velocity of the landward plate. Uyeda and Kanamori (1979) proposed "anchored slab" model in which the downgoing slab is anchored to the mantle, so that the position of a trench is also fixed with respect to the mantle. According to this model, the motion in the mantle is slow in comparison with that of surface plate and the motion of the landward plate controls the subducting slab angles and the opening and nonopening of back-arcs. Present South American plate is advancing oceanward at a rate between 1.5-1.8cm/yr at the Central Andes (Minster et al., 1974). This absolute motion together with high convergence rate (more than 10cm/yr) makes the slab angle the lowest in the world representing one end member of the comparative subductology as "Chilean" type subduction (Uyeda, 1982).

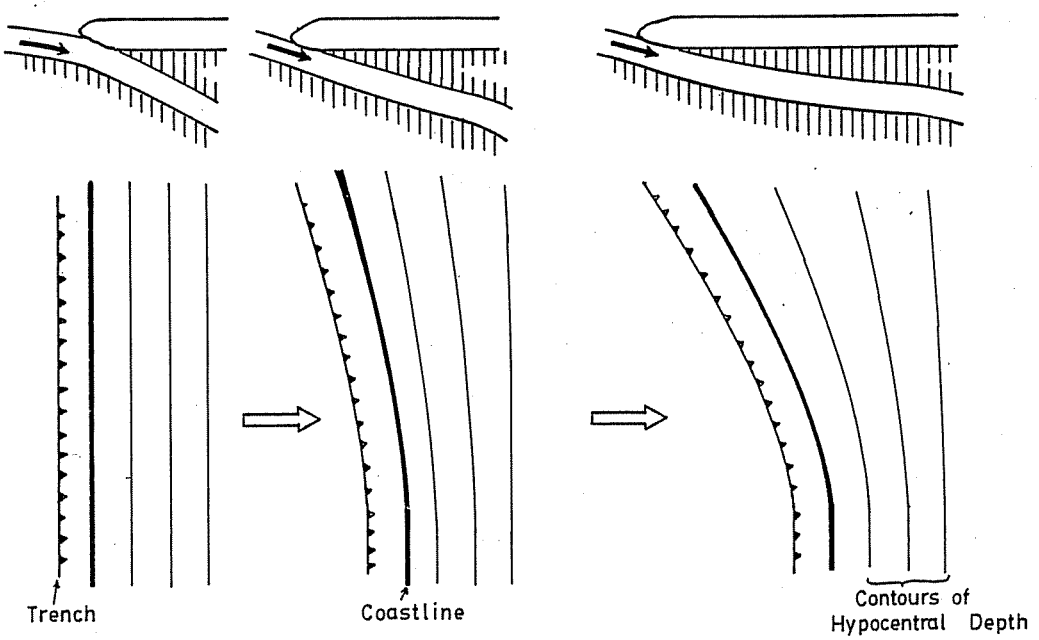

Fig.6-7 A model to explain the shallow dip angle of the subducting slab and the disappearence of the volcanism in the Peruvian Andes north of 13°S.

In Fig. 6-5, it is also noticed that the depth contours of deep focus earthquakes after Hasegawa and Sacks (1981) are not parallel to the trench in the 2°S-16°S zone of the Peruvian Andes but tend to become nearer to the north-south axis as the depth increases. The deepest contour (600km deep) strikes at almost north-south. Here I propose the model that post-Miocene rapid rotation of the Peruvian Andes made differential oceanward absolute motion of the continental plate in Peru resulting in that the northern portion of the slab tend to lie in more flat angle than southern portion (Fig. 6-7). This well explains recent upward migration of the subducting slab and consequent disappearence of volcanism in the Peruvian Andes north of 16°S without recourse to subducting aseismic ridges.

3) Deflection zone - Andean Cordillera in southern Peru and northern Bolivia

Rapid bending of a mountain belt of a finite width should give rise to characteristic surface tectonics near the bending axis. The most characteristic crustal deformation is expected to appear as the strain along the curvature of the orocline. In case of Bolivian orocline, such tectonic features are expected in the Andean Cordillera in northern Bolivia and southern Peru. Because Bolivian orocline is concave toward the ocean, the strain is either lengthening or shortening by assuming the axis of bending to be offshore or inland.

Mercier (1981) pointed out that the compressive deformation of the Central Andes (see introduction of this chapter) occurred as several short-lived (less than a few million years) "pulses" with longer extensional regime between the compressive pulses. Recent study of neotectonics and Neogene strain pattern between these pulses in this region (e.g., Soulas, 1978; Lavenu, 1978) revealed that present-day tectonics in the Altiplano of southern Peru and northern Bolivia and surrounding Eastern and Western Cordillera are characterized by approximately north-south extension and consequent lengthening and less amount east-west extension (Fig. 6-8). These are observed as Quaternary normal faults in predominantly east-west direction. This strain pattern is compatible with the east-west δ_{Hmax} direction observed by recent flank crater distribution (Ui et al., 1983) in this region.

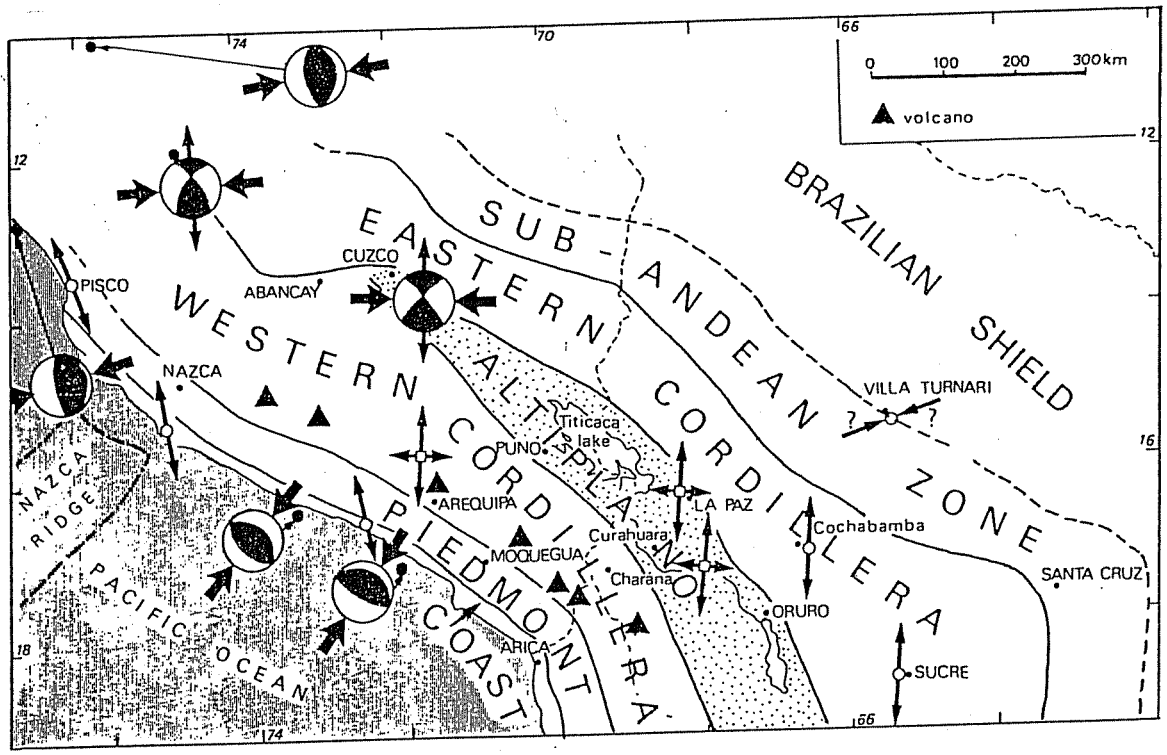

Fig.6-8 Pleistocene-recent strain pattern in south Peru and north Bolivia deduced mainly from neotectonic studies (Mercier, 1981).

Nakamura and Uyeda (1980) showed that in the overriding plate at subduction zones, the stress is, from the plate boundary landward, compressional, shear and tensional even in the region where active back-arc spreading is not taking place. In the region described here, σ_{Hmax} maintain subparallel to that of the convergence just like the situations in the central Europe and central America. This can be explained by the gradual landward decrease of the compressional stress in the direction of convergence. In many cases, σ_{Hmax} direction is changed to become parallel to the arc in the tensional region suggesting the occurrence of largest extension perpendicular to the arc. This often results in the occurrence of the back-arc rifting parallel to the arc. The mechanism of the extension of such a direction is sometimes described such as boundary force by the pulling of

the landward retreat of overriding plate (e.g., Chase, 1978), suction force (e.g., Kanamori, 1971) basal shear force by McKenzie-Sleep-Toksöz type induced flow (e.g., Sleep and Toksöz, 1973). Nevertheless, none of the models proposed so far, seems to explain the observed extensional tectonics parallel to the arc in back arc regions in the Andean Cordillera of southern Peru and northern Bolivia, that is to say, a certain cause apart from the subduction itself is necessary.

Such north-south extension might be explained by the oroclinal bending. If we assume the orocline axis at offshore region of the Peru-Chile border, bending of the whole Central Andes will necessitate north-south lengthening of the hinge region in Andean Cordillera as suggested by neotectonic studies in this region. The studies of ancient strain pattern back to the Neogene time (Mercier, 1981) do not always show north-south extension but sometimes show north-south compression. Detailed chronology of strain pattern will clarify the relationship between the surface deformation and the orocline more fully. It is also interesting that in coastal Ecuador, relatively young graben system with east-west direction is present (Shephard and Moberly, 1981) which appears as current topography of Gulf of Guayaquil. It is tempting to attribute this also to another oroclinal bending which made the feature of Huancabamba deflection.

d) Some speculations on the mechanism of formation of Bolivian orocline

1) Major intraplate features of South America

The largest known intraplate feature behind the Andes would be the Amazon fault running approximately from the mouth of Amazon to the Gulf of Guayaquil in Ecuador (De Loczy, 1970a,b; Gansser, 1973; Shephard and Moberly, 1981; Szatmari, 1983; Grabert, 1983). Its eastern part near the mouth of Amazon, more than 1,300km long is characterized by a zone of positive Bouguer anomalies, 25 to 100 mgal high. Linsser (1958) and Vollbrecht (1963) ascribed this to the rifting and the consequent mantle intrusions, which is also thought as the cause of the subsequent subsidence and sediment accumulation of the basin. Trough-like structures in the Amazon region are considered to have been established in Mesozoic time and Paleozoic sediments are preserved in them. From these points of view, Amazon fault is also called as "Amazon Graben". Great amount of basic and ultrabasic intrusive rocks are known along this fault from bore-hole drilling for oil excavation. For example, 600m thick diabase sill of Jurassic age is known in the central part of the Amazon Basin (Bigarella, 1973).

There have also been many suggestions that the Amazon Graben exhibits dislocation by a transcurrent fault system such that the northern block (Guiana shield) is transported considerably to the west when compared with the southern block (Brazilian shield). Amazon Graben is therefore called "Amazonas Megashear", "Amazon shearing system", etc. (Szatmari, 1983; Grabert, 1983). Grabert (1983) estimates this transportation from the structure and age

differences of two shields to be several hundred kilometers.

If we assume viscous coupling between continental lithosphere and lower mantle convective movement as the main driving force of South American plate following the modern view of plate driving forces (Alvarez, 1982), differential westward drag force is envisaged as a cause of such shearing system such that stronger drag works under Guiana shield and weaker one under Brazilian shield. One possibility is that the Tertiary rejuvenation of this left-lateral system across the South American continent caused the counterclockwise rotation of Peruvian block and formed coupled orocline at around 5°S (Huancabamba deflection) and at 20°S (Arica-Santa Cruz deflection). This idea is similar to those of Tethyan Megashear by Carey (1976) and Persian Megashear by Neev and Hall (1982) that global megashear system formed many large-scale tectonic features including Bolivian orocline.

2) Possibilities of collided terranes at the orocline axis

Vogt (1973) and Vogt et al. (1976) suggested that subduction of an aseismic ridge underneath the island arc prevents normal subduction process and consequent back-arc spreading and then forms the bending axis of the arc making a cusp feature in island arcs. For example, such cusps are ubiquitously found in Western Pacific island arcs such as between Aleutian and Kurile-Kamchatka arcs, between Izu-Ogasawara and Mariana arc, between Mariana and Yap arc where aseismic ridges are subducting, namely, Emperor seamounts, Marcus Necker ridge and Caroline ridge respectively.

The direct application of this concept over the bending of the Central Andes is rather difficult because it assumes the formation of marginal seas behind the arc. However, there are some possibilities that collision of certain unsubductable mass is related to the formation of the bending axis in the Central Andes. Since South American plate has westward absolute velocity (Minster et al., 1974), Peru-Chile trench is also thought to be moving westward. When buoyant mass of continental affinity such as aseismic ridges or oceanic plateaus arrives at a trench, mechanical coupling between two plates is enhanced at this place and might stop the receding oceanic trench at that place and so form the axis of bending of this arc-trench system.

Precambrian metamorphic massif is known in the coast from southern Peru possibly to northern Chile (Isaacson, 1975; Lehmann, 1978) as the Arequipa Massif which is commonly interpreted as the trans-Andean extension of Brazilian shield (Shakleton et al., 1979; Cobbing and Pitcher, 1972). There is also another interpretation that Arequipa Massif is a remnant of collided and accreted allochthon (Nur and Ben-Avraham, 1978; 1982). If the latter interpretation is correct, this massif might have played an above mentioned role and have determined the axis of bending. Paleomagnetic study of the massif is in progress by several workers (Langridge, R., written communication) and would to some extent elucidate this problem.

References

Allmendinger, R. W., V. A. Ramos, T. E. Jordan, M. Palma and B. L. Isacks, Paleogeography and Andean structural geometry, Northwest Argentina, Tectonics, 1, 1-16, 1983.

Alvarez, W., Geological evidence for the geographical pattern of mantle return flow and the driving mechanism of plate tectonics, J. Geophys. Res., 87, 6697-6710, 1982.

Alvarez, W., D. V. Kent, I. P. Silva, R. A. Schweikert and R. A. Larson, Franciscan Complex limestone deposited at 17° south paleolatitude, Geol. Soc. Am. Bull., 91, 476-484, 1980.

Angelier, J. and B. Colletta, Tension fractures and extensional tectonics, Nature, 301, 49-51, 1983.

Barazangi, M. and B. L. Isacks, Spatial distribution of earthquakes and subduction of the Nazca plate below South America, Geology, 4, 686-692, 1976.

Barazangi, M. and B. L. Isacks, Subduction of the Nazca plate beneath Peru: evidence from spatial distribution of earthquakes, Geophys. J. R. astr. Soc., 57, 537-555, 1979.

Beck, M. E., Jr., Paleomagnetism of a thick Tertiary volcanic sequence in northern California, Rep. AFCRL 62-821, pp.45, U. S. Air Force Cambridge Res. Lab., 1962.

Beck, M. E., Jr., Paleomagnetic record of plate-margin tectonic processes along the western edge of North America, J. Geophys. Res., 85, 7115-7131, 1980.

Bellido, B. E., Sinopsis de la geologia del Peru, Instituto Geologico Minero y Metalurgico Bol. 22, pp.54, 1979.

Bigarella, J. J., Geology of the Amazon and Parnaiba Basins, in The Ocean Basins and Margins, 1, edited by Nairn, A. E. M. and

F. G. Stehli, 25-86, Plenum, New York, 1973.

Bullard, E., J. E. Everett and A. G. Smith, The fit of the continents around the Atlantic, Phil. Trans. R. Soc., A258, 41-51, 1965.

Burns, K. L., M. L. Rickard, L. Belbin and F. Chamalaun, Further paleomagnetic confirmation of the Magellanes orocline, Tectonophys., 63, 75-90, 1980.

Carey, S. W., The orocline concept in geotectonics, Proc. R. Soc. Tasmania, 89, 255-288, 1955.

Carey, S. W., A tectonic approach to continental drift, in Symposium on Continental Drift, pp.177-355, Univ. of Tasmania, Hobart, 1958.

Carey, S. W., The Expanding Earth, Elsevier, pp488, 1976.

Cecioni, G. and F. Garcia, Observaciones geologicas in la Cordillera de la Costa de Tarapaca, Instituto de Investigaciones Geologicas, Chile, Boletin, 6, pp28, 1960.

Channel, J. E. T. and D. H. Tarling, Paleomagnetism and the rotation of Italy, Earth Planet. Sci. Lett., 25, 177-188, 1975.

Channel, J. E. T., W. Lowrie, F. Medizza and W. Alvarez, Paleomagnetism and tectonics in Umbria, Italy, Earth Planet. Sci. Lett., 39, 199-210, 1978.

Channel, J. E. T., R. Catalano and B. D'Argenio, Paleomagnetism and the deformation of the Mesozoic continental margin in Sicily, Tectonophys., 61, 391-407, 1980.

Channel, J. E. T., R. Freeman, F. Heller and W. Lowrie, Timing of diagenetic haematite growth in red pelagic limestones from Gubbio (Italy), Earth Planet. Sci. Lett., 58, 189-201, 1982.

Chase, C., Extension behind island arcs and motions relative to hot spots, J. Geophys. Res., 83, 5385-5387, 1978.

Chinn, D. S., B. L. Isacks and M. Barazangi, High-frequency seismic wave propagation in western South America along the continental margin, in the Nazca plate and across the Altiplano, Geophys. J. R. astr. Soc., 60, 209-244, 1980.

Cobbing, E. J., The geosynclinal pair at the continental margin of Peru, Tectonophys., 36, 157-165, 1976.

Cobbing, E. J. and W. S. Pitcher, Plate tectonics and the Peruvian Andes, Nature Phys. Sci., 240, 51-53, 1972.

Coupland, D. H. and R. Van der Voo, Long-term nondipole components in the geomagnetic field during the last 130 M.Y., J. Geophys. Res., 85, 3529-3548, 1980.

Cox, A., Remanent magnetism of lower to middle Eocene basalt flows from Oregon, Nature, 179, 685-686, 1957.

Cox, A., Analysis of present geomagnetic field for comparison with paleomagnetic results, J. Geomag. Geoelectr., 13, 101-112, 1962.

Cox, A., Confidence limits for the precision parameter k, Geophys. J. R. astr. Soc., 18, 545-549, 1969.

Cox, A., Latitude dependence of the angular dispersion of the geomagnetic field, Geophys. J. R. astr. Soc., 20, 253-269, 1970.

Cox, A., Plate Tectonics and Geomagnetic Reversals, pp670, Freeman, 1973.

Creer, K. M., Palaeomagnetism of the Serra Geral Formation, Geophys. J. R. astr. Soc., 7, 1-22, 1962a.

Creer, K. M., The dispersion of the geomagnetic field due to

secular variation and its determination for remote times from paleomagnetic data, J. Geophys. Res, 67, 3461-3476, 1962b.

Creer, K. M., A palaeomagnetic survey of South American rock formations, Phil. Trans. R. Soc., A267, 457-558, 1970.

Creer, K. M. and D. A. Valencio, Palaeomagnetic and rock magnetic studies on Cenozoic basalts from Western Argentina, Geophys. J. R. astr. Soc., 19, 113-146, 1969.

Creer, K. M., J. G. Mitchell and J. Abou Deeb, Palaeomagnetism and radiometric age of the Jurassic Chon Aike formations from Santa Cruz province, Argentina, Earth Planet. Sci. Lett., 14, 131-138, 1972.

Creer, K. M., D. A. Valencio, A. M. Sinito, P. Tucholka and J. F. A. Vilas, Geomagnetic secular variation 0-14,000 yr BP as recorded by lake sediments from Argentina, Geophys. J. R. astr. Soc., 74, 159-221, 1983.

Cross, T. A. and R. H. Pilger, Jr., Controls of subduction geometry, location of magmatic arcs, and tectonics of arc and back-arc regions, Geol. Soc. Am. Bull., 93, 545-562, 1982.

Dalziel, I. W. D. and D. H. Elliot, The Scotia Arc and Antarctic margin, in Ocean Basins and Margins, vol.1, The South Atlantic, edited by A. E. M. Nairn and F. G. Stehli, pp.171-245, Plenum, New York, 1973.

Dalziel, I. W. D., R. Kligfield, W. Lowrie and N. D. Opdyke, Paleomagnetic data from the southernmost Andes and the Antarctandes, in Implications of Continental Drift to the Earth Sciences, edited by D. H. Tarling and S. K. Runcorn, vol.1, pp.87-101, Academic, New York, 1973.

De Loczy, L., Tectonismo transversal na América do Sul e suas relaçõ̃es genéticas com as zonas das cadeias meio-oceânicas, An. Acad. brasil. Ciênc., 42, 185-205, 1970a.

De Loczy, L., Role of transcurrent faulting in South American tectonic framework, Am. Assoc. Petrol. Geol. Bull., 54, 2111-2119, 1970b.

Deuser, W. G., Hypothesis of the formation of the Scotia and Caribbean Sea, Tectonophys., 10, 391-402, 1970.

Drake, R. E., Chronology of Cenozoic igneous and tectonic events in the Central Chilean Andes - latitudes 35° 30' to 36° S, J. Volcan. Geotherm. Res., 1, 265-284, 1976.

Duncan, R. A., Hotspots in the southern oceans - an absolute frame of reference for motion of the Gondwana continents, Tectonophys., 74, 29-42, 1981.

Farrar, E. and D. C. Noble, Timing of late Tertiary deformation in the Andes of Peru, Geol. Soc. Am. Bull., 87, 1247-1250, 1976.

Feraud, G. and R. Campredon, Geochronological and structural study of Tertiary and Quaternary dikes in southern France and Sardinia: an example of the utilization of dike swarms as paleostress indicators, Tectonophys., 98, 297-325, 1983.

Fisher, R. A., Dispersion on a sphere, Proc. R. Soc. A217, 295-305, 1953.

Gansser, A., Facts and theories on the Andes, J. Geol. Soc. Lond., 129, 93-131, 1973.

Grabert, H., The Amazon shearing system, Tectonophys., 95, 329-336, 1983.

Graham, J. W., The stability and significance of magnetism in

sedimentary rocks, J. Geophys. Res., 54, 131-167, 1949.

Gunn, N. M. and A. S. Murray, Geomagnetic field magnitude variations in Peru derived from arghaeological ceramics dated by thermoluminescence, Geophys. J. R. astr. Soc., 62, 345-366, 1980.

Hargraves, R. B. and R. Shagam, Paleomagnetic study of La Quinta Formation, Venezuela, Am. Assoc. Petrol. Geol. Bull., 53, 537-552, 1969.

Harrington, H. J., Paleogeographic development of South America, Am. Assoc. Petrol. Geol. Bull., 46, 1773-1814, 1962.

Hasegawa, A. and I. S. Sacks, Subduction of the Nazca plate beneath Peru as determined from seismic observations, J. Geophys. Res., 86, 4971-4981, 1981.

Hattori, I. and K. Hirooka, Paleomagnetic results from Permian greenstones in Central Japan and their geological significance, Tectonophys., 57, 211-235, 1979.

Hayashida, A., Colombia, Bolivia no Daisankiso no Kochijiki, in the program of the 74th meeting of the Society of Terrestrial Magnetism and Electricity of Japan, p163, 1983.

Hayashida, A., Y. Nogami, L. A. Rodrigo and A. Saavedra, Fission track dating and paleomagnetic study of the Cenozoic continental deposits at Salla, Bolivian Andes, in Kyoto University Overseas Research Report of New World Monkeys, Kyoto University Primate Research Institute, in press, 1983.

Hayes, D. E., Continental margin of western South America, in The Geology of Continental Margins, edited by Burk, C. A. and C. L. Drake, 581-590, Springer-Verlag, 1974.

Heki, K., Paleomagnetic study of the Higashi-Izu monogenetic volcano group and pyroclastic flow deposits in Kagoshima Prefecture: paleosecular variation during the last 40,000 years in Japan, J. Geomag. Geoelectr., 35, in press, 1983.

Heki, K. and H. Tsunakawa, Paleomagnetism of the Shimokura dike swarm, Northeast Japan - an estimation of the activity duration of a dike swarm -, Rock Mag. Paleogeophys., 8, 17-21, 1981.

Heki, K. and H. Tsunakawa, Paleomagnetism of the Shimokura dike swarm: post-Miocene tectonic rotation, submitted to J. Geomag. Geoelectr., 1983.

Hess, H. H., History of ocean basins, in Petrologic Studies: a volume to Honor A. F. Buddington, edited by Engel, A. E. J., H. L. James and B. F. Leonard, 599-620, Geol. Soc. Amer., 1962.

Hollingworth, S. E., Dating the uplift of the Andes of Northern Chile, Nature, 201, 17-20, 1964.

Instituto de Geologia y Mineria, Mapa Geologico del Peru, Escala 1:1,000,000, 1975.

Irving, E., Paleomagnetism and its application to geological and geophysical problems, Wiley, New York, 1964.

Irving, E., Drift of the major continental blocks since the Devonian, Nature, 270, 304-309, 1977.

Irving, E., Paleopoles and paleolatitudes of North America and speculations about displaced terranes, Can. J. Earth Sci., 16, 669-694, 1979.

Irving, E. and N. D. Opdyke, The paleomagnetism of the Bloomsburg redbeds and its possible application to the tectonic history of the Appalachians, Geophys. J. R. astr. Soc., 9, 153-167, 1965.

Irving, E. and G. Pullaiah, Reversals of the geomagnetic field,

magnetostratigraphy, and relative magnitude of paleosecular variation in the Phanerozoic, Earth Sci. Rev., 12, 35-64, 1976.

Isaacson, P. E., Evidence for a western extracontinental land source during the Devonian period in the Central Andes, Geol. Soc. Am. Bull., 86, 39-46, 1975.

Isacks, B. and M. Barazangi, Geometry of Benioff zones: lateral segmentation and downwards bending of the subducted lithosphere, in Island Arcs, Deep Sea Trenches and Back Arc Basins, edited by Talwani, M. and W. Pitman, pp99-114, American Geophysical Union, Ewing Series 1, 1977.

Ito, H. and K. Tokieda, Tilting of Hokkaido island and Kitakami mountains deduced from the NRM of Cretaceous granitic rocks, Rock Mag. Paleogeophys., 2, 54-58, 1974.

James, D. E., Plate tectonic model for the evolution of the Central Andes, Geol. Soc. Am. Bull., 82, 3325-3346, 1971.

James, D. E., Magmatic and seismic evidence for subduction of the Nazca Plate beneath Central Peru, Carnegie Inst. Wash. Year Book, 76, 830-840, 1977.

James, D. E., Subduction of the Nazca plate beneath central Peru, Geology, 6, 174-178, 1978.

Jenks, W. F., Minami America no chishitsu, in Sekai no Chishitsu, Iwanami Chikyu Kagaku Koza, edited by A. Miyashiro, translated by Y. Katsui, 16, Iwanami, 1979. (in Japanese)

Jones, D. J., A. Cox, P. Coney and M. Beck, The growth of western North America, Sci. Amer., 247, 50-64, 1982.

Kaizuka, S., Tokokei no daichikei to plate tectonics, in Sekai no hendotai, edited by Uyeda S. and A. Sugimura, 297-305, Iwanami,

1973. (in Japanese)

Kanamori, H., Great earthquakes at island arcs and the lithosphere, Tectonophys., 12, 187-198, 1971.

Kaneoka, I. and C. Guevara, K-Ar age determination of Upper Tertiary and Quaternary Andean volcanic rocks, southern Peru, submitted to Geochem. J., 1983.

Kawai, N., H. Ito and S. Kume, Deformation of the Japanese islands as inferred from rock magnetism, Geophys. J. R. astr. Soc., 6, 124-130, 1961.

Kawai, N., T. Nakajima and K. Hirooka, The evolution of the island arc of Japan and the formation of granites in the Circum-Pacific belt, J. Geomag. Geoelectr., 23, 267-293, 1971.

Kellogg, K. S. and R. L. Reynolds, Paleomagnetic results from the Lassier coast, Antarctica, and a test for oroclinal bending of the Antarctic Peninsula, J. Geophys. Res., 83, 2293-2299, 1978.

Kodama, K., A. Taira, M. Okamura and Y. Saito, Paleomagnetism of the Shimanto Belt in Shikoku, Southwest Japan, in Accretion Tectonics in the Circum-Pacific Regions, edited by M. Hashimoto and S. Uyeda, pp231-241, Terra Scientific Publishing Company, Tokyo, 1983.

Ladd, J. W., Relative motion of South America with respect to North America and Caribbean tectonics, Geol. Soc. Am. Bull., 87, 969-976, 1976.

Larson, E. E., R. L. Reynolds, M. Ozima, Y. Aoki, H. Kinoshita, S. Zashu, N. Kawai, T. Nakajima, K. Hirooka, R. Merrill and S. Levi, Paleomagnetism of Miocene volcanic rocks of Guam and the curvature of the southern Mariana island arc, Geol. Soc. Am. Bull., 86, 346-350, 1975.

Larson, R. L. and J. W. Ladd, Evidence of the opening of the South Atlantic in the early Cretaceous, Nature, 246, 209-212, 1973.

Lavenu, A., Cah. O. R. S. T. O. M. Sér. Géol., 10, 115-126, 1978.

Leeder, M. R., Lithospheric stretching and North Sea Jurassic clastic sourcelands, Nature, 305, 510-514, 1983.

Lehmann, B., A Precambrian core sample from the Altiplano/Bolivia, Geol. Rund., 67, 270-278, 1978.

Le Pichon, X., Sea-floor spreading and continental drift, J. Geophys. Res., 73, 3661-3697, 1968.

Linares, E. and D. A. Valencio, Paleomagnetism and K-Ar ages of some trachybasaltic dikes from Rio de Los Molinos, Province of Cordoba, Republic of Argentina, J. Geophys. Res., 80, 3315-3321, 1975.

Linsser, M., Interpretation of the regional gravity anomalies in the Amazon area, PETROBRAS report, 8p, 1958.(republished in Portuguese, Boletin Tecnico da PETROBRAS, 17, 3-15, 1975.)

Lowrie, W. and F. Heller, Magnetic properties of marine limestones, Rev. Geophys. Space Phys., 20, 171-192, 1982.

MacDonald, W. D., Net tectonic rotation, apparent tectonic rotation and the structural tilt correction in paleomagnetic studies, J. Geophys. Res., 85, 3659-3669, 1980.

MacDonald, W. D. and N. D. Opdyke, Tectonic rotation suggested by paleomagnetic results from northern Colombia, South America, J. Geophys. Res., 77, 5720-5730, 1972.

MacDonald, W. D. and N. D. Opdyke, Triassic paleomagnetism of northern South America, Am. Assoc. Petrol. Geol. Bull., 58,

208-215, 1974.

Malfait, B. T. and M. G. Dinkelman, Circum-Caribbean tectonic and igneous activity and the evolution of the Caribbean plate, Geol. Soc. Am. Bull., 83, 251-272, 1972.

Matsuda, T., K. Nakamura and A. Sugimura, Katsudanso to neotectonics, in Hendo suru Chikyu I, Iwanami Chikyu Kagaku Koza, edited by Kasahara, K. and A. Sugimura, 10, 1979. (in Japanese)

McElhinny, M. W., Palaeomagnetism and Plate Tectonics, Cambridge Earth Science Series, pp.358, Cambridge University Press, London, 1973.

McElhinny, M. W. and R. T. Merrill, Geomagnetic secular vatiation over the past 5m.y., Rev. Geophys. Space Phys., 13, 687-701, 1975.

McKenzie, D. P. and R. L. Parker, The North Pacific: an example of tectonics on a sphere, Nature, 216, 1276-1280, 1967.

McKenzie, D., Active tectonics of the Alpine-Himalayan belt: the Aegean Sea and surrounding regions, Geophys. J. R. astr. Soc., 55, 217-254, 1978a.

McKenzie, D., Some remarks on the development of sedimentary basins, Earth Planet. Sci. Lett., 40, 25-32, 1978b.

Megard, F. and H. Philip, Plio-Quaternary tectono-magmatic zonation and plate tectonics in the Central Andes, Earth Planet. Sci. Lett., 33, 231-238, 1976.

Mendia, J. E., Palaeomagnetism of alkaline lava flows from El Salto - Almafuerte, Cordoba Province, Argentina, Geophys. J. R. astr. Soc., 54, 539-546, 1978.

Mercier, J. L., Extensional-compressional tectonics associated

with the Aegean Arc: comparison with the Andean Cordillera of south Peru - north Bolivia, Phil. Trans. R. Soc. Lond., A300, 337-355, 1981.

Minster, J. B., T. H. Jordan, P. Molnar and E. Haines, Numerical modelling of instantaneous plate tectonics, Geophys. J. R. astr. Soc., 36, 541-576, 1974.

Miyashiro, A., Kita America no chishitsu, in Sekai no chishitsu, Iwanami Chikyu Kagaku Koza, edited by A. Miyashiro, 16,1979. (in Japanese)

Morgan, W. J., Rises, trenches, great faults, and crustal blocks, J. Geophys. Res., 73, 1959-1982, 1968.

Myers, J. S., Cretaceous stratigraphy and structure, western Andes of Peru between latitudes 10°-10°30'., Am. Assoc. Petrol. Geol. Bull., 58, 474-487, 1974.

Nakamura, K. and S. Uyeda, Stress gradient in arc-back arc regions and plate subduction, J. Geophys. Res., 85, 6419-6428, 1980.

Neev, D. and J. K. Hall, A global system of spiraling geosutures, J. Geophys. Res., 87, 10689-10708, 1982.

Noble, D. C., E. H. McKee and F. Megard, Early Tertiary "Incaic" tectonism, uplift, and volcanic activity, Andes of central Peru, Geol. Soc. Am. Bull., 90, 903-907, 1979.

Nomura, K. and N. Morikawa, Palaeomagnetic study on Jurassic and Cretaceous dike swarms near Cuya, northern Chile, Bachelor Thesis, Faculty of Science, Chiba University, 1983. (in Japanese)

Nur, A. and Z. Ben-Avraham, Speculations on mountain building and

the lost Pacifica continent, J. Phys. Earth, 26, Suppl., S21-S37, 1978.

Nur, A. and Z. Ben-Avraham, Volcanic gaps and the consumption of aseismic ridges in South America, Geol. Soc. Am. Mem., 154, 729-740, 1981.

Nur, A. and Z. Ben-Avraham, Oceanic plateaus, the fragmentation of continents, and mountain building, J. Geophys. Res., 87, 3644-3661, 1982.

Opdyke, N. D. and W. D. MacDonald, Paleomagnetism of Late Cretaceous Pocos de Caldas alkaline complex, southern Brazil, Earth Planet. Sci. Lett., 18, 37-44, 1973.

Otofuji, Y. and T. Matsuda, Paleomagnetic evidence for the clockwise rotation of Southwest Japan, Earth Planet. Sci. Lett., 62, 349-359, 1983.

Pacca, I. G. and F. Y. Hiodo, Palaeomagnetic analysis of Mesozoic Serra Geral basaltic lava flows in southern Brazil, An. Acad. bras. Ciênc., 48(suplem.), 207-214, 1976.

Palmer, H. C., A. Hayatsu and W. D. MacDonald, The Middle Jurassic Camaraca Formation, Arica, Chile: paleomagnetism, K-Ar age dating and tectonic implications, Geophys. J. R. astr. Soc., 62, 155-172, 1980a.

Palmer, H. C., A. Hayatsu and W. D. MacDonald, Paleomagnetic and K-Ar age studies of a 6km-thick Cretaceous section from the Chilean Andes, Geophys. J. R. astr. Soc., 62, 133-153, 1980b.

Pilger, Jr., R. H., Plate reconstructions, aseismic ridges, and low-angle subduction beneath the Andes, Geol. Soc. Am. Bull., 92, 448-456, 1981.

Prince, R. A., Bathymetry of the Peru-Chile continental margin

and trench, Part 1: Geological Society of America Map and Chart Series MC-34, scale 1:1,000,000, 1980.

Rankin, D. W., Appalachian salients and recesses: Late Precambrian continental breakup and the opening of the Iapetus Ocean, J. Geophys. Res., 81, 5605-5619, 1976.

Reyes, R. L., Geologia de los cuadrangulos de Cajamarca, San Marcos y Cajabamba, Instituto Geologico Minero y Metallurgico, pp.67, 1979.

Roy, J. L., N. D. Opdyke and E. Irving, Further paleomagnetic results from the Bloomsburg Formation, J. Geophys. Res., 72, 5075-5086, 1967.

Rutland, R. W. R., J. E. Guest and R. L. Grasty, Isotopic ages and Andean uplift, Nature, 208, 677-678, 1965.

Salas, R., R. Kast, I. Montecinos and I. Salas, Geologia y recursos minerales del Departamento de Arica, Provincia de Tarapaca, Instituto de Investigaciones Geologicas, Chile, Boletin, 21, ppl13, 1966.

Schult, A. and S. D. C. Guerreiro, Palaeomagnetism of Mesozoic igneous rocks from the Maranhâo Basin, Brazil, and the time of opening of the South Atlantic, Earth Planet. Sci. Lett., 42, 427-436, 1979.

Schult, A. and S. D. C. Guerreiro, Paleomagnetism of Upper Cretaceous volcanic rocks from Cabo de Sto. Agostinho, Brazil, Earth Planet. Sci. Lett., 50, 311-315, 1980.

Schwartz, S. Y. and R. Van der Voo, Paleomagnetic evaluation of the orocline hypothesis in the Central and Southern Appalachians, Geophys. Res. Lett., 10, 505-508, 1983.

Sclater, J. G. and P. A. F. Christie, Continental stretching: an explanation of the post-Mid-Cretaceous subsidence of the Central North Sea Basin, J. Geophys. Res., 85, 3711-3739, 1980.

Sclater, J. G., L. Royden, F. Horvath, B. C. Burchfiel, S. Semken and L. Stegena, The formation of the Intra-Carpathian basins as determined from subsidence data, Earth Planet. Sci. Lett., 51, 139-162, 1980.

Shackleton, R. M., A. C. Ries, M. P. Coward and P. R. Cobbold, Structure, metamorphism and geochronology of the Arequipa Massif of coastal Peru, J. Geol. Soc. Lond., 136, 195-214, 1979.

Shagam, R. and R. B. Hargraves, Geologic and paleomagnetic study of Permo-Carboniferous redbeds (Sabaneta and Merida facies), Venezuelan Andes, Am. Assoc. Petrol. Geol. Bull., 54, 2336-2348, 1970.

Shepherd, G. L. and R. Moberly, Coastal structure of the continental margin, northwest Peru and southwest Ecuador, Geol. Soc. Am. Mem., 154, 351-391, 1981.

Shibuya, H., S. Sasajima and S. Yoshikura, Study on the Silurian acidic tuffs in the Yokokurayama lenticular body of the Kurosegawa tectonic zone, Kochi Prefecture, Japan, J. Geol. Soc. Japan, 89, 307-309, 1983. (in Japanese with English abstract)

Skerlec, G. M. and R. B. Hargraves, Tectonic significance of paleomagnetic data from Northern Venezuela, J. Geophys. Res., 85, 5303-5315, 1980.

Sleep, N. and M. N. Toksöz, Evolution of marginal basins, Nature, 233, 548-550, 1973.

Smith, A. G. and A. Hallam, The fit of the southern continents, Nature, 225, 139-144, 1970.

Soulas, J. -P., Revue Géogr. phys. Géol. dyn., 20, 399-414, 1978.

Steinmann, G., Geologie von Peru, pp488, Carl Winters Universitäts-buchhandlung, Heiderberg, 1929.

Sterns, C., F. J. Mauk and R. Van der Voo, Late Cretaceous-Early Tertiary paleomagnetism of Aruba and Bonaire (Netherlands Leeward Antilles), J. Geophys. Res., 87, 1127-1141, 1982.

Sykes, L. R., W. R. McCann and A. L. Kafka, Motion of Caribbean plate during last 7 million years and implications for ealier Cenozoic movements, J. Geophys. Res., 87, 10656-10676, 1982.

Szatmari, P., Amazon rift and Pisco-Jurua fault: Their relation to the separation of North America from Gondwana, Geology, 11, 300-304, 1983.

Taira, A., A preliminary note of the Cretaceous stratigraphy of northern Peru, in Andes Science 2 - report of the geophysical studies of the Central Andes, edited by Kono, M., 20-34, Tokyo Institute of Technology, 1983.

Thomas, W. A., Continental margins, orogenic belts, and intracratonic structures, Geology, 11, 270-272, 1983.

Thorpe, R. S., P. W. Francis, M. Hammill and M. C. W. Baker, Regional distribution and character of active andesite volcanism: the Andes, in Andesites: orogenic andesites and related rocks, edited by R. S. Thorpe, pp187-205, John Wiley & Sons, 1982.

Tosha, T., Paleomagnetism of Northeast Japan, Doctoral Thesis, Faculty of Science, University of Tokyo, 1983.

Trottereau, G. and G. Ortiz, Geologia de los cuadrangulos de Chimbote y Casma: Lima, Peru, Servicio Geologia y Mineria Bol., 1963.

Ui, T., M. Kono, Y. Hamano and F. Monge, Paleovolcanology of Ocros dike swarm, Central Andes, submitted to J. Volcanol. Soc. Japan, 1983.

Uyeda, S., Subduction zones: an introduction to comparative subductology, Tectonophys., 81, 133-159, 1982.

Uyeda, S. and H. Kanamori, Back-arc opening and the mode of subduction, J. Geophys. Res., 84, 1049-1061, 1979.

Uyeda, S. and A. Miyashiro, Plate tectonics and the Japanese islands: A synthesis, Geol. Soc. Am. Bull., 85, 1159-1170, 1974.

Uyeda, S. and T. Watanabe, Terrestrial heat flow in western South America, Tectonophys., 83, 63-70, 1982.

Valencio, D. A., Palaeomagnetism of the Lower Cretaceous Vulcanitas Cerro Colorado Formation of the Sierra de Los Condores group province of Cordoba, Argentina, Earth Planet. Sci. Lett., 16, 370-378, 1972.

Valencio, D. A. and J. F. Vilas, Paleomagnetism of some Middle Jurassic lavas from south-east Argentina, Nature, 225, 262-264, 1970.

Valencio, D. A. and J. F. Vilas, Sequence of the continental movement occurred prior to and after the formation of the South Atlantic, An. Acad. brasil. Ciênc., 47(suplem.), 377-386, 1976.

Valencio, D. A., J. F. Vilas and J. E. Mendia, Palaeomagnetism of Quaternary rocks from South America, An. Acad. brasil. Ciênc., 47(Suplem.), 21-32, 1975.

Valencio, D. A., E. Mendia, A. Giudici and J. O. Gascon, Palaeomagnetism of the Cretaceous Pirgua Subgroup (Argentina) and the age of the opening of the South Atlantic, Geophys. J. R. astr. Soc., 51, 47-58, 1977.

Valencio, D. A., A. M. Sinito and J. F. Vilas, Palaeomagnetism of Upper Precambrian rocks of the La Tinta formation, Argentina, Geophys. J. R. astr. Soc., 62, 563-575, 1980.

Valencio, D. A., J. F. Vilas and I. G. Pacca, The significance of the palaeomagnetism of Jurassic-Cretaceous rocks from South America: predrift movements, hairpins and magnetostratigraphy, Geophys. J. R. astr. Soc., 73, 135-151, 1983.

Van der Voo, R. and J. E. T. Channel, Paleomagnetism in orogenic belts, Rev. Geophys. Space Phys., 18, 455-481, 1980.

Van der Voo, R. and R. B. French, Paleomagnetism of the Late Ordovician Juniata Formation and the remagnetization hypothesis, J. Geophys. Res., 82, 5796-5802, 1977.

Vilas, J. F. A., Palaeomagnetism of some igneous rocks of the Middle Jurassic Chon Aike Formation from Estancia La Reconquista, Province of Santa Cruz, Argentina, Geophys. J. R. astr. Soc., 39, 511-522, 1974.

Vilas, J. F. A., Palaeomagnetism of the Lower Cretaceous Sierra de Los Condores Group, Cordoba province, Argentina, Geophys. J. R. astr. Soc., 46, 295-305, 1976.

Vilas, J. F. A., Palaeomagnetism of South American rocks and the dynamic process related with the fragmentation of Western Gondwana, in Paleoreconstruction of the Continents, edited by M. W. McElhinny and D. A. Valencio, 115-128, American

Geophysical Union, Washington, 1981.

Vincenz, S. A. and S. N. Dasgupta, Paleomagnetic study of some Cretaceous and Tertiary rocks on Hispaniola, Pure Appl. Geophys., 116, 1200-1210, 1978.

Vine, F. J. and D. H. Matthews, Magnetic anomalies over oceanic ridges, Nature, 199, 947-949, 1963.

Vogt, P. R., Subduction and aseismic ridges, Nature, 241, 189-191, 1973.

Vogt, P. R., A. Lowrie, D. R. Bracey and R. N. Hey, Subduction of asiesmic oceanic ridges: effects on shape, seismicity, and other characteristics of consuming plate boundaries, Geol. Soc. Am. Special Paper, 172, pp59, 1976.

Vollbrecht, K., Die Diabasvorkommen des Amazonasgebietes und das Problem des Intrusions-mechanismus, Geol. Rundsch., 53, 686-786, 1963.

Watson, G. S., Analysis of dispersion on a sphere, Mon. Not. R. astr. Soc. Geophys. Suppl., 7, 153-159, 1956.

Wilson, J. J., Cretaceous stratigraphy of Central Andes of Peru, Am. Assoc. Petrol. Geol. Bull., 47, 1-34, 1963.

Wilson, J. T., A new class of faults and their bearing on continental drift, Nature, 207, 343-347, 1965.

Wilson, R. L., Dipole offset - the time-averaged palaeomagnetic field over the past 25 million years, Geophys. J. R. astr. Soc., 22, 491-504, 1971.

Zeil, W., The Andes - A Geological Review, Beitr. Region. Geol. Erde, 13, pp260, 1979.

Zijderveld, J. D. A., A. C. demagnetization of rocks: Analysis of results, in Methods of Paleomagnetism, edited by D. W.

Collinson, K. M. Creer and S. K. Runcorn, pp.254-286, Elsevier, New York, 1967.

Supplement

Bellon, H. and Lefèvre, C., Données géochronometriques sur le volcanisme andin dans le sud du Perou, Implications Volcano tectoniques, Compt. Rend. Acad. Sci. Paris, D283,1-4, 1976.

Appendix.A List of sampling sites and data for dike swarms

Table A-1. Full list of the samples

Site ID	Fm.or G.	Long. (°W)	Lat. (°S)	rock type	Age	Bedding (dike contact)
			(Huarmey volcanics)			
HM01	Casma G.	78°02.6'	10°19.0'	andesite	K	-[1]
HM02	"	78°02.5'	10°19.1'	andisite dike	K	- (?)
HM03	"	78°01.0'	10°21.0'	basalt pil-low lava	K	-
HM04	"	78°01.0'	10°21.0'	basalt dike	K	- (?)
HM05	"	78°00.4'	10°22.3'	basalt	K	-
			(Ancon dikes)			
AC02	"	77°10.8'	11°46.4'	pyx.andesite lava	K	-
AC10	"	77°10.8'	11°46.4'	andesite dike	K	- (N10W 75E)
AC11	"	77°10.8'	11°46.4'	andesite dike	K	- (N10W 86E)
AC12	"	77°10.8'	11°46.4'	andesite dike	K	- (N10W 85E)
AC13	"	77°10.8'	11°46.4'	andesite dike	K	- (N5W 88E)
AC14	"	77°10.8'	11°46.4'	andesite dike	K	- (N10W 80E)
			(other Cretaceous volcanics)			
CM20	?[2]	79°06.7'	7°15.0'	andesite dike	K	N80W 20N (N20E 85W)
NZ01	Casma G.	75°13.8'	14°30.6'	pyx.andesite dike	K	N20E 14S (N40W 80E)
			(Cretaceous sediments in Peru)			
CM10	Pariatambo Fm.	78°20.2'	7°04.5'	limestone	Al.	N40W 50N
CM12	Yumagual Fm.	78°18.5'	7°03.1'	limestone	Cen.	N66E 48S
CM13	Chulec Fm.	78°16.3'	7°02.5'	limestone	Al.	N75E 25S
BG01	Yumagual Fm.	78°09.0'	5°54.0'	limestone	Cen.	N65E 18N
BG02	"	78°09.0'	5°54.0'	limestone	Cen.	N65E 18N

(to be continued)

(continued)

			(Ocros dike swarm, see also Table A-2)			
OC01 -29	Barroso G.	73°56.8'	13°24.0'	basalt -andesite	6-8Ma?	-
			(other Tertiary volcanics)			
CA034		77°38.1'	9°32.9'	pyx. andesite	Tertiary	-
CA035		77°37.9'	9°32.9'	pyx. andesite	Tertiary	-
CA042		70°16.2'	18°00.1'	welded tuff	Neogene	-
CA048		70°06.6'	17°23.8'	bt.rhyorite welded tuff	Neogene	-
AY01		74°16.2'	13°12.3'	aphy. ol. basalt	Miocene	-
			(Jurassic rocks in northern Chile; for Cuya dike swarm, see Table A-2)			
AR01	Camaraca Fm.	70°20'	18°28'	shale	Jm	EW 8S
AR02	"	70°20'	18°28'	aug.hyp.basalt pillow lava	Jm	EW 8S
CY01- 26	Cuya dike swarm	70°09'	19°11'	andesite- basalt	?[3]	
			(Cretaceous rocks in northern Chile; for Arica dike swarm, see Table A-2)			
AR24	Atajaña Fm.	70°15.5'	18°46,5'	red bed	Neocomian	N10W 25E
AR31 -49	Arica dike swarm	70°16'	18°34'	andesite- basalt	?[4]	-
AR50	Atajaña Fm.	70°16'	18°34'	red sandstone	Neocomian	N60E 15E
			(Plio-Quaternary volcanic rocks)			
CA040	Mt. Chachani	71°31.3'	16°18.0'	Hyp.hb andesite	Active volcano	-
CA051	unnamed	71°22.3'	14°05.0'	Bt. rhyorite	Holocene volcano	-
CA058	Barosso G.	73°56.8'	13°22.8'	Bt.hyp.hb. trachyandesite	Q	-
CA059	Barosso G.	73°56.5'	13°22.5'	Hb.bt. trachyandesite	Q	-

(to be continued)

(continued)

AR60	Oxaya Fm.	70°14'	18°46'	Welded tuff	Tm-p	-
AR61	Oxaya Fm.	70°14'	18°46'	Welded tuff	Tm-p	-
GT01	Guallatiri volcano	69°07'	18°27'	Bt.hb.dacite	Active volcano	-
GT02	Guallatiri volcano	69°09'	18°27'	Aug.hyp. dacite	Active volcano	-
CG01	Caldera Ajoya	69°09'	18°17'	Welded tuff	Tp-Q	-
CA043	Caldera Ajoya	69°12'	18°13'	Hyp.hb. andesite lava	Tp-Q	-
CA045	Caldera Ajoya?	69°11'	18°15'	Welded tuff	Tp-Q	-
CA047	Caldera Ajoya	69°14'	18°13'	Hyp.hb. andesite	Tp-Q	-

Abbreviations; hyp.:hypersthene, aug.:augite, hb.:hornblende, bt.:biotite, ol.:olivine, porp.:porphyritic, aphy.:aphyric, pyx.:pyroxene, Jm:Middle Jurassic, K:Cretaceous, Al.:Albian, Cen.:Cenomanian, T(m,p):Tertiary(Miocene, Pliocene), Q:Quaternary.

1.Bedding plane is horizontal or is considered to be nearly horizontal.

2.Intruding into Cretaceous sedimentary formation.

3.Intruding into Jurassic Arica Group.

4.Intruding into Lower Cretaceous Vilacollo Group.

Fig.A-1a,b,c,d (next page) Rose diagrams showing the distributions of the strikes of dikes (a:Ancon dikes, b:Ocros dike swarm, c:Cuya dike swarm, d:Arica dike swarm).

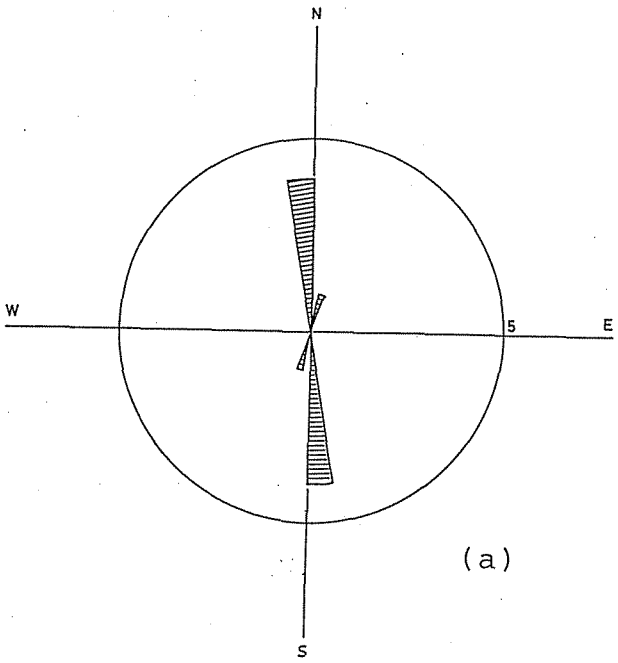

(a)

ANCON DIKES

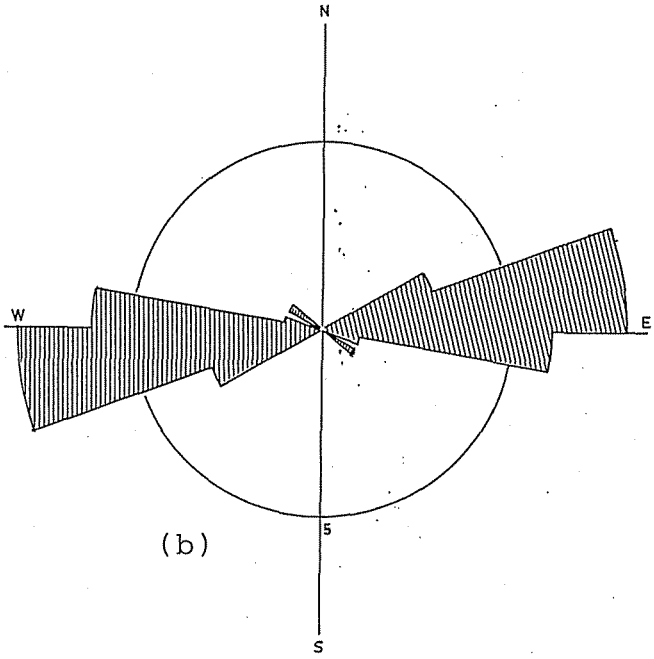

(b)

OCROS DIKE SWARM

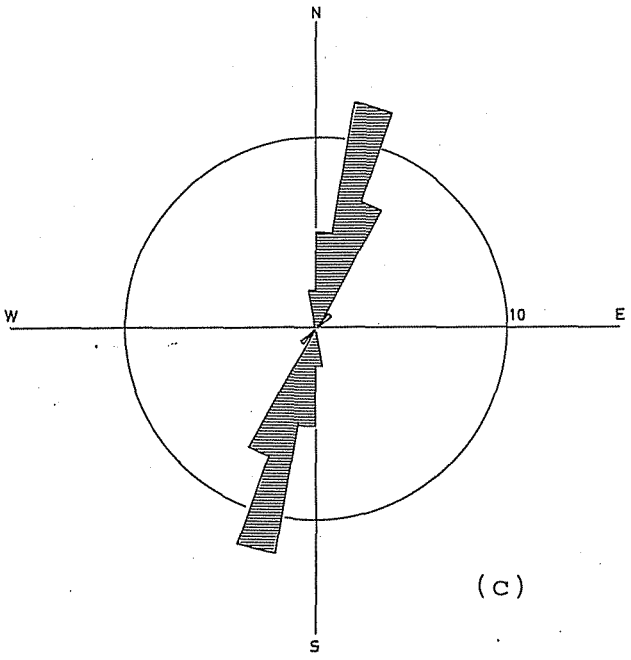

(c)

CUYA DIKE SWARM

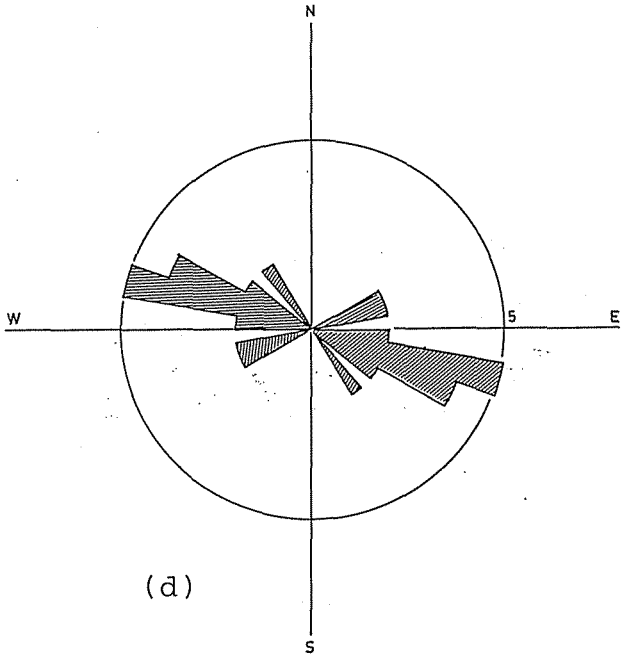

(d)

ARICA DIKE SWARM

Table A-2 Data for dike swarms.

DATA LIST FOR DIKE SWARMS

Sample number	Rock name	Strike	Dip	Lineation	Thickness (m)	Distance along route (m)	Number of magnetic samples	Remarks
Ocros dike swarm								
OC01	Ol.aug.andesite	N85W	85N	10W	6.5	353	6	5,6=contact
OC02	Ol.aug.andesite	N75W(apx)	Vertical	35E	3	399	6	1,6=contact
OC03	Bt.hb.andesite	N80E	Vertical	30E	20	622	6	(1-6)
							6	lava flow (11-16)
OC04	Aug.ol.basalt	N70E	80N		3	675	6	
OC05	Aphy.andesite	EW	80S	45W	5	938	6	(1-6)
							6	S side lava flow (11-16)
							6	N side lava flow (21-26)
OC06	Bt.hb.andesite	EW(apx)	Vertical (apx)	30W	8.5	1098	6	(1-6)
							6	lava flow(21-26)
OC07	Bt.hb.andesite	N60E	Vertical	80E	35(apx)	1258	6	
OC08	Bt.hb.trachyte	N75E	Vertical		6	1739	6	
OC09	Bt.hb.andesite	N70E	80N	5W	60(apx)	1779	6	
OC10	Bt.hb.andesite	N65E	Vertical		20	1896	6	
OC11	Bt.hb.andesite	EW(apx)	Vertical		18	1979	7	
OC12	Hb.bt.andesite	N80E	70N	90	10	2112	6	
OC13	Bt.trachyte	EW	80N	40E	14	2163	6	
OC14	Aug.ol.andesite	N80E	80S	70E	3	2163	6	Intruded into OC13
OC15	Bt.andesite	N75E	70N	90(apx)	3	2220	7	5=country rock
OC16	Hb.ol.aug.andesite	N75E	85N	80E	4.5	2230	6	
OC17	Hb.bt.trachyte	N80E	Vertical	80E	16	2262	6	
OC18	Aug.hb.andesite	N80E	Vertical	80E	25	2461	7	7=country rock
OC19	Aug.ol.basalt	N80E	85N	80E	3	2461	4	Intruded into OC18
OC20	Aug.ol.andesite	N75E	80N	50E	3.5	2865	6	
OC21	Aug.ol.andesite	N70E	Vertical	20E	3	2869	5	
OC22	Hyp.hb.andesite	N70E	80N	10W	6	2899	6	
OC23	Bt.hb.andesite	N80E	80N	25E	10	3372	6	
OC24	Hb.andesite	N85W	85N	20W	1.5	3578	6	
OC25	Hyp.hb.andesite				1.5	3614	6	
OC26	Bt.trachyte	N50W	80S		2	3877	6	
OC27	Aug.ol.andesite	N85E	80N	45W	6	4210	6	
OC28	Bt.hb.andesite	N65W	80S	75E	16	4466	7	
OC29	Hb.andesite	N60E	Vertical		12	4542	6	
Arica dike swarm								
AR31	Aug.hyp.andesite	N70E	80S		1.5		5	
AR32	Aug.ol.basalt	EW	85N		2		7	
AR33	Aug.ol.basalt	N65E	85S		0.6		5	
AR34	Aphy.ol.basalt	N65E	85S		1.5		6	
AR35	Aphy.aug.ol.basalt	N60W(apx)	40E(apx)		2		6	
AR36	Aphy.ol.basalt	N80W	70N		5		6	
AR37	Aphy.basalt	N75W	70N		10		6	
AR38	Ol.aug.andesite	N75W	85N		2.5		5	
AR39	Ol.aug.andesite	N60W	60N		3		6	
AR40	Aphy.ol.basalt	N75E	Vertical		2		6	
AR41	Ol.hyp.aug.andesite	N70W	85N		3.5		6	
AR42	Ol.aug.andesite	N40W	80S		0.2		4	
AR43	Ol.aug.andesite	N40W	80N		1.5		6	
AR44	Aug.ol.andesite	N65W	60S		0.45		6	
AR45	Aug.ol.basalt	N65W	80S		2		5	
AR46	Ol.aug.andesite	N65W	70S		1.2		6	
AR47	Aug.hyp.andesite	N75W	Vertical		2		6	
AR48	Aphy.basalt	N80W	Vertical		0.4		6	
AR49	Aphy.basalt	N75W	Vertical		3.5		6	

(General strike and dip of country rocks N60°E, 15°E)

(to be continued)

(continued)

Sample number	Rock name	Strike	Dip	Lineation	Thickness (m)	Distance along route (m)	Number of magnetic samples	Remarks
Cuya dike swarm								
CY01	Porp.andesite	N10E			7	0	6	
		N65W	35N					sandstone around CY01
CY02	Porp.andesite	N15E			3	11	6	
CY03	Porp.andesite	N20E			>1.5	23	6	
CY04	Porp.andesite	N15E			>4	35	6	
CY05	Porp.andesite	N20E			>3.5 <7	385	6	
		N65W	55N					sandstone around CY05
CY06	Aphy.basalt	N10E	Vertical		1.5	406	6	
CY07	Aphy.basalt	N15E	Vertical		7	454	6	
CY08	Pyx.andesite	N5E	85E		2	499	6	(1-6)
CY08	Calcareous sandstone	N50W	20N					(11-13,21-23)
CY09	Pyx.andesite	N20E	85E		1	594	6	(1-6)
CY09	Limestone	N55W	30N					(11-17,21-27)
CY10	Pyx.andesite	N30E	75E		1.5	626	6	
CY11	Porp.andesite	N15E	85E		1.5	674	6	
CY12	Porp.andesite	N15E	85E		1.6	677	6	
CY13	Porp.andesite	NS	80E		>5	772	6	
CY14	Porp.andesite	N10E	80E		0.4	772	6	Intruded into CY13
CY15	Aphy.basalt	N25E	Vertical		1	828	6	
CY16	Pyx.andesite	N20E	85W		0.7	833	6	
CY17	Aphy.basalt	N25E			0.5	878	6	
CY18a	Andesite	N20E	85W		0.6	913	3	(1-3),intruded into CY18b
CY18b	Porp.andesite	N20E	85W		4	913	3	(4-6)
CY19	Aphy.basalt	NS	Vertical		1.2	928	6	
CY20	Porp.andesite	N20E			2	963	6	
CY21	Porp.andesite	N25E			5	1013	6	
CY22	Porp.andesite	N30E			4	1033	6	
CY23	Porp.andesite	N20E	Vertical		2	1098	6	
CY24	Porp.andesite	N45E	Vertical			1133	6	
CY25	Porp.andesite	N25E			1	1203	6	
CY26	Porp.andesite	N25E			1.5	1233	6	

Abbreviations
Hyp:hypersthene, aug:augite, hb:hornblende, bt:biotite, ol:olivine, porp:porphyritic, aphy:aphyric, pyx:pyroxene, apx:approximately

Appendix.B Paleomagnetic results for Plio-Quaternary rocks

Site	N	Incl. (°)	Decl. (°)	R	k	α_{95} (°)	ODF (mT)	VGP Lat. (°N)	VGP Long. (°E)
CA040	4	6.2	-7.9	3.8610	22	20.2	LSF	69.1	-94.1
CA051	2	-11.8	10.7	1.9999	-	2.8	LSF	76.7	-18.0
CA058	4	-36.4	32.6	3.9709	103	9.1	LSF	58.1	32.9
CA059	3	-44.9	-1.6	2.9820	111	11.8	15	76.8	112.3
AR60	8	-25.1	5.5	7.9492	138	4.7	LSF	82.3	-26.1
AR61	7	-25.8	18.3	6.9790	286	3.6	LSF	71.7	6.0
GT01	6	-43.6	-16.8	5.9431	88	7.2	LSF	72.9	173.7
GT02	6	-37.2	1.7	5.8578	35	11.5	LSF	87.2	76.7
CG01	6	-37.6	1.9	5.9569	116	6.2	LSF	86.7	78.2
CA043	3	47.3	174.6	2.9813	107	12.0	40	-78.6	-44.4
CA045	4	-21.7	6.8	3.9652	86	10.0	15	80.4	-25.3
CA047	5	-39.3	-0.4	4.9447	72	9.1	LSF	85.9	116.0

For legends, see Table 3-1.

Fig.A-2 a,b,c,d (next page) Paleomagnetic field directions of Plio-Quaternary rocks (a:Peruvian rocks, b:Oxaya Formation, northernmost Chile, c:Caldera Ajoya, Chilean Altiplano, d:Guallatiri volcano, Chilean Altiplano). Open and solid symbols indicate negative (upward) and positive (downward) inclinations respectively. 95% confidence circles are also indicated.

PERUVIAN QUATERNARY VOLCANICS

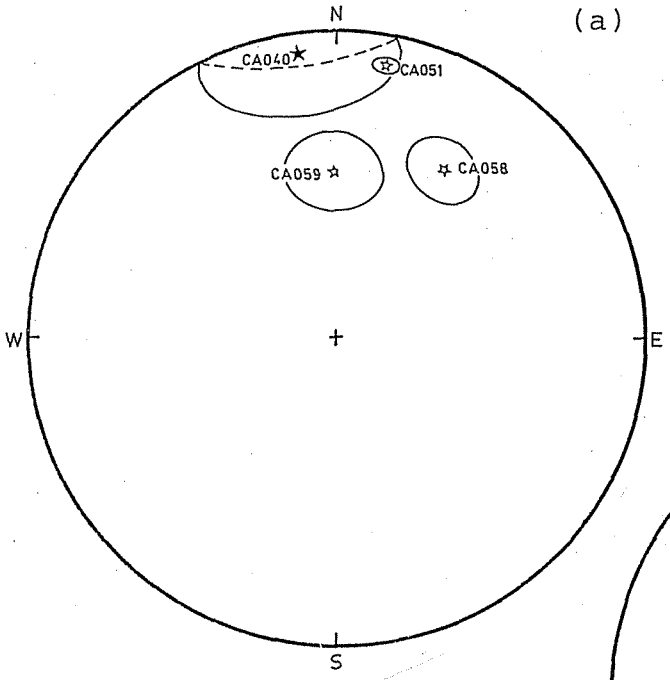

Oxaya FORMATION
IGNIMBRITE

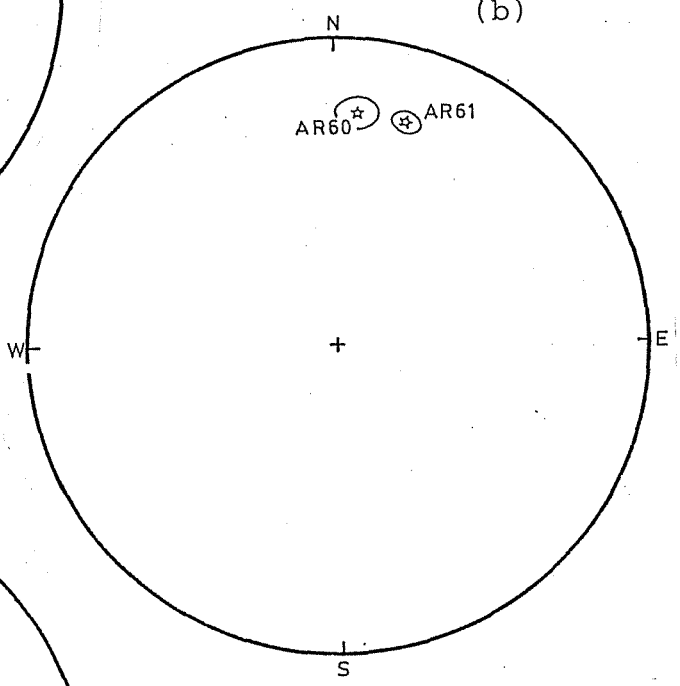

CALDERA AJOYA

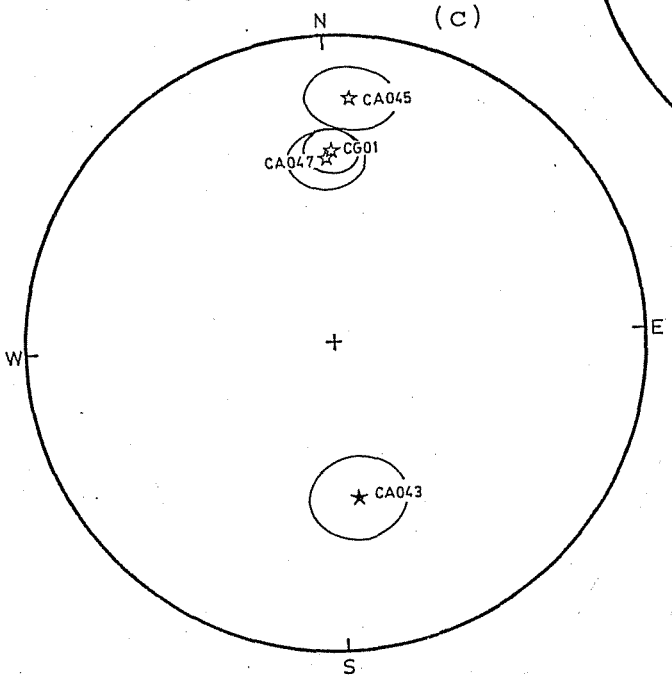

GUALLATIRI VOLCANO